

Joint  
Transportation  
Research  
Program

J T R P

FHWA/IN/JTRP-97/10

Final Report

**INTEGRATION OF REAL-TIME AIR POLLUTION  
PARAMETERS INTO THE DECISION MAKING  
PROCESS REGARDING HIGHWAY  
CONSTRUCTION WORK ZONE TRAFFIC FLOW**

Outtara Fatagoma  
Todd Premo  
Robert Jacko

May 15, 1998

Indiana  
Department  
of Transportation

Purdue  
University



**Final Report**

**FHWA/IN/JHRP-97/10**

**Integration of Real-Time Air Pollution Parameters Into the Decision Making Process  
Regarding Highway Construction Work Zone Traffic Flow Improvements**

**By**

**Ouattara Fatogoma, Ph.D.  
Post-Doctoral Research Associate**

**Todd Premo  
Graduate Research Assistant**

**and**

**Robert B. Jacko, Ph.D., P.E.  
Professor**

**Environmental Engineering  
School of Civil Engineering  
Purdue University**

**Joint Transportation Research Program**

**Project No. C-36-71I  
File No. 8-9-9**

**Prepared in Cooperation with the  
Indiana Department of Transportation  
and the U.S. Department of Transportation  
Federal Highway Administration**

The contents of this report reflect the views of the authors who are responsible for the facts and the accuracy of the data presented herein. The contents do not necessarily reflect the official views or policies of the Federal Highway Administration and the Indiana Department of Transportation. This report does not constitute a standard, specification or regulation.

**Purdue University  
West Lafayette, IN 47907  
May 15, 1998**

Digitized by the Internet Archive  
in 2011 with funding from

LYRASIS members and Sloan Foundation; Indiana Department of Transportation

|  |  |   |           |
|--|--|---|-----------|
| 1. Report No.<br>FHWA/IN/JTRP-97/10  | 2. Government Accession No.                          | 3. Recipient's Catalog No.  |           |
| 4. Title and Subtitle<br>Integration of Real-Time Air Pollution Parameters Into the Decision Making Process Regarding Highway Construction Work Zone Traffic Flow Improvements   |  | 5. Report Date<br>May 15, 1998  |           |
| 7. Author(s)<br>Outtara Fatagoma, Todd Premo, and Robert B. Jacko  |  | 6. Performing Organization Code   |           |
| 9. Performing Organization Name and Address<br>Joint Transportation Research Program<br>1284 Civil Engineering Building<br>Purdue University<br>West Lafayette, Indiana 47907-1284   |  | 8. Performing Organization Report No.<br>FHWA/IN/JTRP-97/10   |           |
|  |  | 10. Work Unit No.   |           |
|  |  | 11. Contract or Grant No.<br>SPR-2176   |           |
| 12. Sponsoring Agency Name and Address<br>Indiana Department of Transportation<br>State Office Building<br>100 North Senate Avenue<br>Indianapolis, IN 46204   |  | 13. Type of Report and Period Covered<br>Final Report   |           |
|  |  | 14. Sponsoring Agency Code  |           |
| 15. Supplementary Notes<br>Prepared in cooperation with the Indiana Department of Transportation and Federal Highway Administration.   |  |   |           |
| <b>16. Abstract</b>  |  |   |           |
| <p>The Midas Fourier Transform Infrared air monitoring system was used to measure real-time vehicular exhaust emission concentrations of carbon monoxide (CO) and hydrocarbons (HCs) during the Purdue Vehicle Emission Monitoring and Modeling Project (PVEMP) conducted in spring and summer 1997. The experiments took place on the Borman Expressway, in Gary, Indiana and on I-65, south of Lafayette, Indiana. Concurrently, two speed-readings were acquired from the passing vehicles in the vicinity of the air monitoring system using a hand-held laser gun. The speeds were integrated to determine the speeds and accelerations of the passing vehicles at the spectrometer. An 8-mm camcorder was used to videotape the passing vehicles in order to determine the vehicle types. Three vehicle types were determined: type I represented all the automobiles, Type II represented all the medium-duty vehicles including light and medium duty trucks, pick-ups, and vans, and type III represented all the heavy-duty vehicle mainly semi-trailers. Meteorological data were also recorded from the nearest surface weather stations. Overall, 16,870 vehicles were monitored. 8,478 were type I vehicles, 4,829 were type II vehicles, and 3,563 were type III vehicles. The flow rates in count per minute were 8.92, for type I, 5.08 for type II, 3.75 for type III, and 17.75 for the combined fleet. However, 4,413 vehicles were retained for data analysis. These included 2,848 (65%) type I vehicles and 1,565 (35%) type II vehicles. Type III vehicles were not included in the analysis because their exhaust emission concentrations were not measured. However, their counts and frequencies were determined.</p> <p>The analysis of the PVEMP database showed that the exhaust emission concentrations were very variable with a logarithmic distribution. On average, type I vehicles exhaust emission concentrations were 1.10 % CO and 0.23 % HC while that of type II vehicles were 1.16 % CO and 0.24 % HCs. They were 1.12 % CO and 0.23 % HCs for the combined fleet. The recorded vehicle speeds varied from 34.5 mph to 83.5 mph with a mean of 56.56 mph. Accelerations varied from -4.5 mph/sec to +4 mph/sec with a mean of 0.17 mph/sec. With a high emitter cut-point set at 4.0 % CO and 0.2 % HCs, 5.7% and 49.2% of the combined vehicle fleet were CO and HC high emitters respectively. The instantaneous values of the exhaust CO and HCs emission concentrations exhibited a non-linear relationship with vehicle speeds and accelerations.</p> <p>Using the PVEMP database, a real-time modal exhaust emission concentration model was developed. The model was based on the non-linear multivariate regression of the speed-acceleration matrix for modal-average CO and HCs exhaust emission concentrations aggregated by vehicle type. This model, the Purdue Vehicle Exhaust Emission Model, the Borman Expressway Application (PVEM-BEA), requires input of vehicle speeds and vehicle type for each passing vehicle at a given location within a short time interval. Then, it calculates the accelerations, the mode-average CO and HCs exhaust emission concentrations for each passing-vehicle, and the average values by class of vehicle within the time interval. It also calculates the vehicle flow rates, and makes decisions about the exhaust emission concentration levels by comparing the flow-average emission rates to designed threshold values.</p> <p>The implementation of PVEM-BEA requires the use of advanced traffic monitoring systems such as the Autoscope™ for the acquisition of real-time traffic parameters. PVEM-BEA may be used as a stand-alone model running on a laptop PC or as integrated in the Borman Expressway traffic management center. The current version of PVEM-BEA requires a FORTRAN compiler.</p> |  |   |           |
| 17. Key Words<br>exhaust emissions monitoring, exhaust emissions modeling, FTIR air monitoring system, construction zone safety.   |  | 18. Distribution Statement<br>No restrictions. This document is available to the public through the National Technical Information Service, Springfield, VA 22161 |           |
| 19. Security Classif. (of this report)<br>Unclassified   | 20. Security Classif. (of this page)<br>Unclassified | 21. No. of Pages<br>110   | 22. Price |



## TABLE OF CONTENTS

|  | <b>Page</b> |
|--|-------------|
| <b>LIST OF TABLES.</b>   | iv          |
| <b>LIST OF FIGURES.</b>  | v           |
| <b>1. INTRODUCTION.</b>  | 1           |
| 1.1. Background.   | 1           |
| 1.2. Objectives.   | 3           |
| <b>2. FTIR REMOTE SENSING TECHNOLOGY.</b>  | 6           |
| <b>3. FIELD EXPERIMENTS.</b>   | 11          |
| 3.1. Preliminary Study.  | 11          |
| 3.2. Borman Expressway Field Experiments..   | 15          |
| <b>4. DATA REDUCTION AND ANALYSIS.</b>   | 19          |
| 4.1. Data Reduction.   | 19          |
| 4.2. Descriptive Statistics.   | 21          |
| 4.2.1. CO and HCs Exhaust Emission Concentrations.   | 21          |
| 4.2.2. Vehicle Speed and Acceleration/Deceleration..   | 26          |
| 4.2.3. Meteorology.  | 30          |
| 4.3. Observed Emission-Speed-Acceleration Correlations.  | 31          |
| 4.4. High Emitters.  | 35          |
| <b>5. REAL-TIME MODAL MODEL DEVELOPMENT.</b>   | 37          |
| 5.1. Modeling Overview.  | 37          |
| 5.2. Model Development.  | 38          |
| 5.2.1. Description of the current model.   | 38          |
| 5.2.2. Analytical Background of PVEM-BEA.  | 39          |
| 5.2.3. Limitations and Extrapolations of PVEM-BEA.   | 48          |
| 5.2.4. Design of Concentration Thresholds for Decision-making.                                 | 49          |
| 5.2.5. Computer Algorithm of PVEM-BEA.   | 50          |
| <b>6. IMPLEMENTATION SUGGESTIONS.</b>  | 54          |
| <b>7. CONCLUSION.</b>  | 57          |
| <b>REFERENCE..</b>   | 59          |
| <b>APPENDIX A: A Portion of the Integrated PVEMP Database.</b>                                 | 60          |
| <b>APPENDIX B: Graphical Representations for Data<br/>Pertaining to the Two Vehicle Types.</b> | 62          |



|  |    |
|--|----|
| APPENDIX C: Graphical Representations of the Regression Data<br>for the Two Vehicle Types. . . . . | 75 |
| APPENDIX D: PVEM-BEA Source Code. . . . .  | 88 |



## LIST OF TABLES



## LIST OF FIGURES

|   | Page |
|---|------|
| Figure 1.1. Local area map showing the Borman Expressway<br>(source: INDOT web page).   | 5    |
| Figure 2.1. Basic schematic of an open-path FTIR system<br>(Source EPA, 92).            | 7    |
| Figure 2.2. Midac Corporation open-path FTIR spectrometer<br>(Source: Midac Web page).  | 7    |
| Figure 2.3. Components of a Plane Mirror Michelson spectrometer<br>(Source: EPA, 92).   | 8    |
| Figure 2.4. Path difference fundamental diagram (Source: EPA, 92).                      | 8    |
| Figure 2.5. The software function diagram (source: EPA 92).                             | 10   |
| Figure 3.1. Preliminary laboratory setup with hexane bottle in place.                   | 11   |
| Figure 3.2. A stationary trial run using a 1991 Suzuki Sidekick.                        | 12   |
| Figure 3.3. HCs Exhaust emission concentrations recorded during a stationary trial run. | 13   |
| Figure 3.4: Four-lane dynamic trial run with a video camera set up..                    | 14   |
| Figure 3.5. CO Exhaust emission concentrations recorded during a dynamic trial run.     | 14   |
| Figure 3.6. Aerodynamic study of the mixing volume behind a moving van.                 | 15   |
| Figure 3.7. Sampling site looking east at I-65 on-ramp to the Borman Expressway.        | 16   |
| Figure 3.8. Equipment setup at the Borman Expressway sampling site.                     | 17   |
| Figure 3.9. Monitoring at I-65 sampling site..  | 17   |
| Figure 4.1.1. Total number of vehicles monitored during PVEMP.                          | 19   |
| Figure 4.1.2. Average vehicle flow rate recorded during PVEMP.                          | 20   |



|  |     |
|--|-----|
| Figure 4.1.3. Total number of vehicles included in the data analysis.  | .20 |
| Figure 4.2.1. Mean and median CO and HCs exhaust emission concentrations for type I and type II vehicles, and the combined fleet.            | .21 |
| Figure 4.2.2. Minimum and maximum CO and HCs exhaust emission concentrations for type I and type II vehicles, and the combined fleet.        | .21 |
| Figure 4.2.3. Histogram of the CO exhaust emission concentration distribution for the combined fleet.  | .22 |
| Figure 4.2.4. Logarithmic distribution of CO exhaust emission concentration for the combined vehicle fleet monitored.                        | .22 |
| Figure 4.2.5. Histogram of the HCs exhaust emission concentration distribution for the combined fleet.                                       | .23 |
| Figure 4.2.6. Logarithmic distribution of HCs exhaust emission concentration for the combined vehicle fleet monitored.                       | .24 |
| Figure 4.2.7. Mean CO concentrations for type I vehicles, type II vehicles, and the combined fleet recorded during each monitoring session.  | .25 |
| Figure 4.2.8. Mean HCs concentrations for type I vehicles, type II vehicles, and the combined fleet recorded during each monitoring session. | .25 |
| Figure 4.2.9. CO and HCs exhaust emission concentration percentiles for the combined fleet.  | .26 |
| Figure 4.2.10. Mean, median, maximum, and minimum speeds for type I and type II vehicles, and the combined fleet.                            | .26 |
| Figure 4.2.11. Mean speeds for type I and type II vehicles, and the combined fleet recorded during each monitoring session.                  | .27 |
| Figure 4.2.12. Variation of mean CO and HCs exhaust emission concentration with mean vehicle speed for the combined vehicle fleet.           | .28 |
| Figure 4.2.13. Mean, median, maximum, and minimum acceleration for type I and type II vehicles and the combined fleet.                       | .28 |
| Figure 4.2.14. Mean accelerations for type I and type II vehicles, and the combined fleet recorded during each monitoring session.           | .29 |
| Figure 4.2.15. Variation of the mean CO and HCs concentrations with the mean vehicle acceleration for the combined vehicle fleet.            | .29 |



|  |     |
|--|-----|
| Figure 4.2.16. Mean meteorological data recorded during each monitoring session.   | .30 |
| Figure 4.3.1. Variation of instantaneous CO exhaust emission concentrations with vehicle speed for the combined vehicle fleet.                             | .32 |
| Figure 4.3.2. Variation of instantaneous CO exhaust emission concentrations with vehicle acceleration for the combined vehicle fleet.                      | .32 |
| Figure 4.3.3. Variation of instantaneous HCs exhaust emission concentrations with vehicle speed for the combined vehicle fleet.                            | .33 |
| Figure 4.3.4. Variation of instantaneous HCs exhaust emission concentrations with vehicle acceleration for the combined vehicle fleet.                     | .33 |
| Figure 4.3.5. Three-dimensional plot for the triple correlation of CO exhaust emission concentration, speed, and acceleration for the combined fleet.      | .34 |
| Figure 4.3.6. Three-dimensional plot for the triple correlation of HCs exhaust emission concentration, speed, and acceleration for the combined fleet.     | .35 |
| Figure 4.4.1. Fractions of CO high emitters and total CO exhaust emission concentrations for the combined vehicle fleet.                                   | .36 |
| Figure 4.4.2. Fractions of HCs high emitters and total HCs exhaust emission concentrations for the combined vehicle fleet.                                 | .36 |
| Figure 5.2.1. Bin-average CO exhaust emission concentration versus speed midpoints.  | .40 |
| Figure 5.2.2. Bin-average HCs exhaust emission concentration versus speed midpoints.   | .40 |
| Figure 5.2.3. Bin-average CO exhaust emission concentration versus acceleration midpoints.   | .41 |
| Figure 5.2.4. Bin-average HCs exhaust emission concentration versus acceleration midpoints.  | .41 |
| Figure 5.2.5. Speed-acceleration matrix for $E_{ij}$ ( $E_{ij}$ = mode-average exhaust emission concentration at speed $i$ and acceleration $j$ ).         | .42 |
| Figure 5.2.6. Three-dimensional plot of the mode-average exhaust CO emission concentration versus speed and acceleration midpoints for the combined fleet. | .43 |



|   |     |
|---|-----|
| Figure 5.2.7. Three-dimensional plot of the mode-average exhaust HCs emission concentration versus speed and acceleration midpoints for the combined fleet.     | .44 |
| Figure 5.2.8. Three-dimensional plot of the mode-average CO exhaust emission concentration obtained from the mathematical relationship for the combined fleet.  | .47 |
| Figure 5.2.9. Three-dimensional plot of the mode-average HCs exhaust emission concentration obtained from the mathematical relationship for the combined fleet. | .48 |
| Figure 5.2.10. Top-down flow chart of the PVEM-BEA subroutines.   | .52 |
| Figure 5.2.11. Sample Output of PVEM-BEA.   | .53 |
| Figure 6.1. The Autoscope™ Video Detection Processor Unit.  | .55 |
| Figure 6.2. Schematic of Video Detection.   | .55 |



## 1. INTRODUCTION

### 1.1. Background

Motor vehicle pollution comes from the by-products of the imperfect fuel combustion process (exhaust) in the engine and from the evaporation of the fuel itself. The main pollutants are hydrocarbons (HCs), nitrogen oxides ( $\text{NO}_x$ ), and carbon monoxide (CO). HCs exhaust emissions result when fuel molecules in the engine do not burn or burn partially. HCs also escape into the air through fuel evaporation that occurs in several ways. The diurnal evaporation resulting from the fuel tank heating as the temperature rises during the day, the running losses of the hot engine and exhaust system, the hot soak after the vehicle is turned off, and the refueling losses.  $\text{NO}_x$  exhaust emissions are formed under high pressure and temperature in the engine when nitrogen (N) and oxygen (O) atoms in the air react to form various  $\text{NO}_x$ . CO is a product of the incomplete combustion that occurs when carbon in the fuel is partially oxidized rather than fully oxidized to carbon dioxide ( $\text{CO}_2$ ). The chemistry of the formation of these chemicals is simplistically represented as follows:  $\text{Fuel (HCs)} + \text{Air (O}_2, \text{N}_2) \rightarrow \text{Unburned HC} + \text{CO} + \text{NO}_x + \text{CO}_2 + \text{H}_2\text{O}$ .  $\text{O}_2$ ,  $\text{N}_2$ , and  $\text{H}_2\text{O}$  represent the molecules of oxygen, nitrogen, and water respectively. In this research project, the exhaust CO and HCs emissions are the main focus. Substantial amounts of CO are produced whenever a rich mixture is used. Spark-ignition engines employ rich mixtures during startup to prevent stalling and at wide-open throttle conditions (hard acceleration) to provide maximum power. For stoichiometric and lean mixtures, CO is produced in large quantity at typical combustion temperature as a result of the dissociation of  $\text{CO}_2$ . Partial oxidation of oil, and deposit layers of unburned fuel is another major source of CO, especially in lean operation. Unburned HCs may result from the flame quenching process which leaves thin layers of unburned fuel-air mixture at the cylinder walls and at the entrance to crevices such as piston top lands and ring packs. Adsorption and desorption of fuel into oil layers in the cylinder walls are also great contributors to unburned HCs. For lean and/or dilute mixtures approaching the flammability limits, unburned HCs may result from incomplete flame propagation in the bulk of the charge (Turns, 1996). The effects of CO and HCs on the environment and human health are well documented. They alter



the properties of the atmosphere and precipitation, harm vegetation, deteriorate materials, and increase morbidity and mortality in humans (Seinfeld, 1986). For example, HCs react in the presence of  $\text{NO}_x$  and sunlight to form ground-level ozone ( $\text{O}_3$ ).  $\text{O}_3$  irritates the eyes, damages the lungs, and aggravates respiratory problems. Moreover, many exhaust hydrocarbons are carcinogens. CO is a colorless and odorless chemical known to reduce the flow of oxygen in the bloodstream.

Construction work zones greatly affect highway traffic patterns and vehicular exhaust emissions. As a matter of fact, the reduction in the number of driving lanes causes heavy congestions and long delays. Because of the unstable stop-and-go effect of traffic flow, the high density of vehicles, and the variable fleet mix, very large amount of exhaust emissions are generated; sometimes exceeding the national standard levels. The current federal standards for 1994 models and later expressed in gram per mile (g/mile) for exhaust emission from cars are 0.25 HCs, 0.4  $\text{NO}_x$ , and 3.4 CO. Despite the implementation of the standards and the development of efficient exhaust emission control technologies, the improvement of air quality has not been great. This is due to three important factors. First, the slow introduction of new, cleaner cars due to the increase of the average age of the vehicle fleet. Second, the offset of the emissions gains by the growth of vehicle miles travelled (VMT) which is doubling every twenty years. Third, and perhaps the most important is the inadequate understanding of real-world emissions. This results in emission test procedures and standards that do not represent the actual source of emissions.

Current mobile source emission estimation is the product of two steps. The determination of a set of emission factors, and the estimation of vehicle activity. The emission factors are produced based on average driving characteristics of the federal test procedure (FTP) which has a specified driving trace of speed versus time intended to reflect actual driving conditions on both arterial and highway. Emissions of CO, HCs, and  $\text{NO}_x$ , are collected for three cycles (cold start, hot stabilized, and hot soak) and are used as base emission rates. Then correction factors are applied to adjust the basic emission rates to reflect the observed differences between different modes of operation. Temperature and speed correction factors are also used to adjust the emission rates of non-FTP cycles; speed greater than 57 mph, and acceleration greater than 3.3 mph/s.



Vehicle activity including VMT, speed distribution, number of vehicles, number of trips, and vehicle mix are derived from macroscale transportation models. This emission inventory method has several shortcomings including the inaccurate representation of actual driving behavior, and the flaw in the emission factor estimation. Because of the characteristics of this methodology, it cannot be used efficiently to evaluate traffic flow improvements that are microscale in nature.

A Fourier transform infrared (FTIR) air monitoring system can measure real-time on-road exhaust emission concentrations from vehicles operating in various driving modes instantaneously. Such a system consists of an infrared source which transmits a collimated beam that is detected by the spectrometer which contains the interfering optics and the detector. Post-car signals immediately acquired after a vehicle passes through the infrared beam are compared to the background ambient air signal in order to determine the concentration of the pollutant in the exhaust plume. Since the vehicle fuel economy cannot be determined in real-time, the concentration measured by FTIR systems are expressed on a volumetric basis (i.e. ppm, %). The rapid introduction of this monitoring system has prompted some states to develop new set of standards based on FTIR data. For example, The North Carolina current standards for 1981 and later models of light and medium duty vehicles are 12000 ppm CO and 220 ppm HCs. The California HCs standard for 1994 models of light and medium duty vehicles is 200 ppm HCs.

## 1.2. Objectives

The main objective of this research is to develop a real-time modal exhaust emission concentration model for light and medium duty vehicles using real-time emission concentration, traffic, and meteorological data. The data were collected during the Purdue Vehicle Emission Monitoring and Modeling Project (PVEMP) field experiments conducted in the spring and summer 1997 on the Borman Expressway. The Borman Expressway is a multi-lane, 16-mile link of highway I-80/94 located in northwest Indiana (Figure 1.1), a non-attainment area for O<sub>3</sub> and other criteria pollutants. The traffic volume on the Borman Expressway is extremely high and alternative routes are limited. Consequently, transportation-related emissions cause major air quality problems. The implementation of the model and the results of the project will integrate air quality as



another parameter in the traffic flow improvement of the Borman Expressway, especially in construction zones. The operation of the model will require the use of real-time traffic parameter inputs obtainable only from advanced traffic monitoring systems such as the Autoscope™ or similar systems. This paper presents the results of the monitoring program, the data reduction and analysis effort, the development of the real-time modal exhaust emission concentration model, and the implementation suggestions of the research.





Figure 1.1. Local area map showing the Borman Expressway (source: INDOT web page).



## 2. FTIR REMOTE SENSING TECHNOLOGY

The FTIR technology is used for the detection of chemical compounds through a particular medium. An energy source in the form of infrared (IR) radiation is sent through a desired medium. This radiation causes the atoms in a molecule to resonate at a certain frequency specific to the molecules mass and structure. When the particular frequency in the IR band meets a molecule resonating at the same frequency, the IR radiation is absorbed. This causes a reduced energy level at that specific wavelength to be measured by the sensing device. Previous tests have been conducted and reference libraries have been established to aid in determining the wavelength at which the molecules of concern absorb. These libraries are referenced by the computer and matched with the output from the spectrometer to ultimately identify the compound existing in the media being tested.

Often the FTIR spectrometer is found in a single unit on a laboratory bench and includes a closed cell containing the sample to be analyzed. In order to sample vehicle exhaust emission concentrations in real time however, an alternative setup has been designed. Such a setup is referred to as an open-path FTIR sensing device and is identified by the separate IR source and spectrometer modules. The free space between the source and the receiving optics is confined only by the cylindrical wave pattern of the IR source. This system includes the IR source, the transmitting optics, the receiving optics, the interferometer, and the detector. A basic macroscopic schematic is illustrated in Figure 2.1.

The system used for this study is designed by Midac Corporation. The IR source is a silica carbide (SiC) element that glows at a temperature of 1550 °K. The element is mounted at the center of a twenty-inch parabolic reflector that yields a cylindrical IR wave pattern for easier alignment with the spectrometer. Within the spectrometer are housed an interferometer, a beamsplitter, and a detector. A Plane Mirror Michelson Interferometer is used in the Midac spectrometer (Figure 2.2). It consists of two perpendicular mirrors and a zinc selenium (ZnSe) beamsplitter.



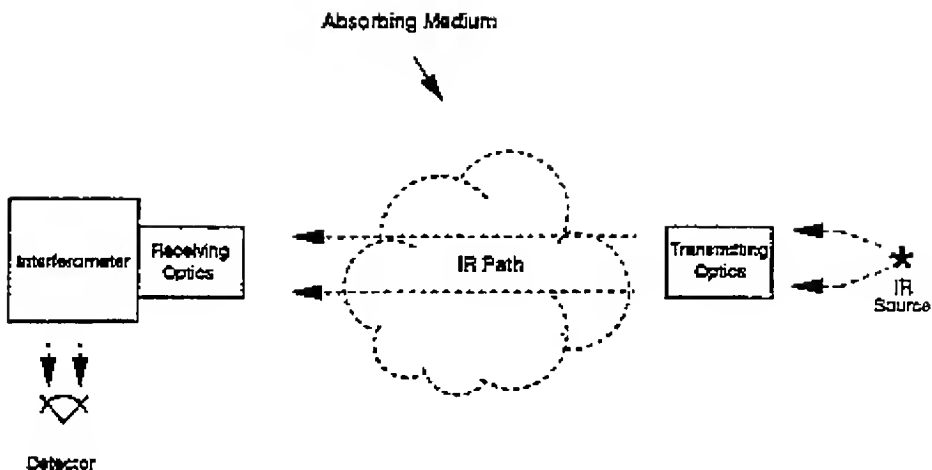


Figure 2.1. Basic schematic of an open-path FTIR system (Source EPA, 92).



Figure 2.2. Midac Corporation open-path FTIR spectrometer (Source: Midac Web page).

After the IR radiation passes through the medium to be sampled, it enters the spectrometer where the beam is split. Some of the radiation is reflected to a stationary mirror then reflected directly into the detector. The waves that pass through the beamsplitter will reflect off a moving, laser-controlled mirror. By moving back and forth at a high frequency, this mirror reflects the full range of wavelengths to the detector. A basic schematic of this system can be seen in Figure 2.3.



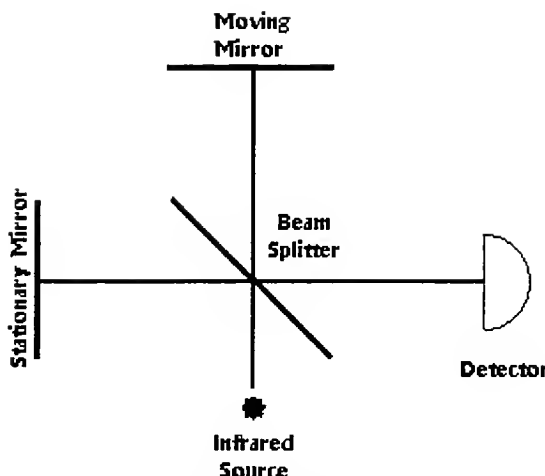


Figure 2.3. Components of a Plane Mirror Michelson spectrometer (Source: EPA, 92).

The two mirrors serve to align the two separate IR waves such that they meet at the detector with some combined amplitude. The energy absorbed by the medium is detected by the change in amplitude of the IR wave at the detector. This concept is illustrated in Figure 2.4. The detector is a liquid nitrogen cooled mercury, cadmium, and telluride (MCT) detector that generates an interferogram in the form of voltage at the path difference based on the location of the two mirrors.

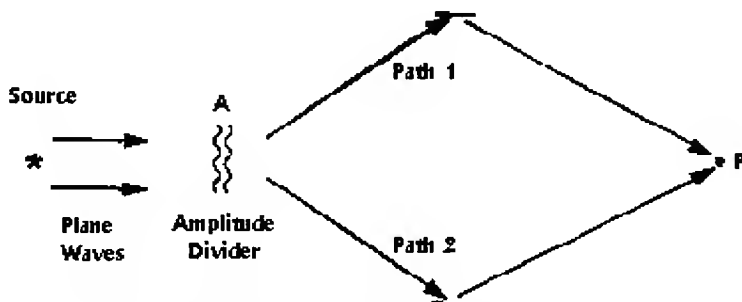


Figure 2.4. Path difference fundamental diagram (Source: EPA, 92).

A computer and software are used to further analyze the interferogram and ultimately generates a concentration reading for the compound of interest. The Midac system comes with a spectral analysis software package called AutoQuant<sup>TM</sup>; a user-friendly version of Grams32<sup>TM</sup>. The interferogram generated by the detector is reduced with a fast fourier transform to generate a single-beam spectrum. A single-beam spectrum is a plot of inverse interferogram intensity versus the wavenumber (inverse



wavelength). This spectrum is compared to a previously recorded background spectrum to generate a transmission spectrum. An absorbance spectrum is then calculated and is defined as the logarithm of the transmission spectrum. This absorbance spectrum is a data set of absorbance versus wavenumber. A schematic of the process to this point is illustrated in Figure 2.5. A predetermined absorption band is set for each compound of interest and is further analyzed to determine a concentration. Beer's law is used and is as follows:  $A = (\alpha)C\lambda$  where, A is the absorbance,  $\alpha$  the absorption coefficient, C the concentration, and  $\lambda$  the path length. The absorbance data is referenced to a data library of known concentration, path length, and absorbance spectrum. The overall equation is as follows:

$$\frac{A_{ref}}{A_{unk}} = \frac{C_{ref} \lambda_{ref}}{C_{unk} \lambda_{unk}}$$

Where the subscripts ‘ref’ and “unk” refer to the reference values and unknown values respectively. Solving this equation for  $C_{unk}$  generates the equation as follows:

$$C_{unk} = \frac{C_{ref} \lambda_{ref} A_{ref}}{\lambda_{unk} A_{ref}}$$

This is the last step in a single-component analysis. For this study, both HCs and CO are studied. For this multicomponent analysis, a classical least squares (CLS) algorithm uses a ratio of path lengths to define the multiplier used to determine the unknown concentration. A classical least squares fitting algorithm simply performs a linear regression over a wave number region, using the unknown and reference spectra.



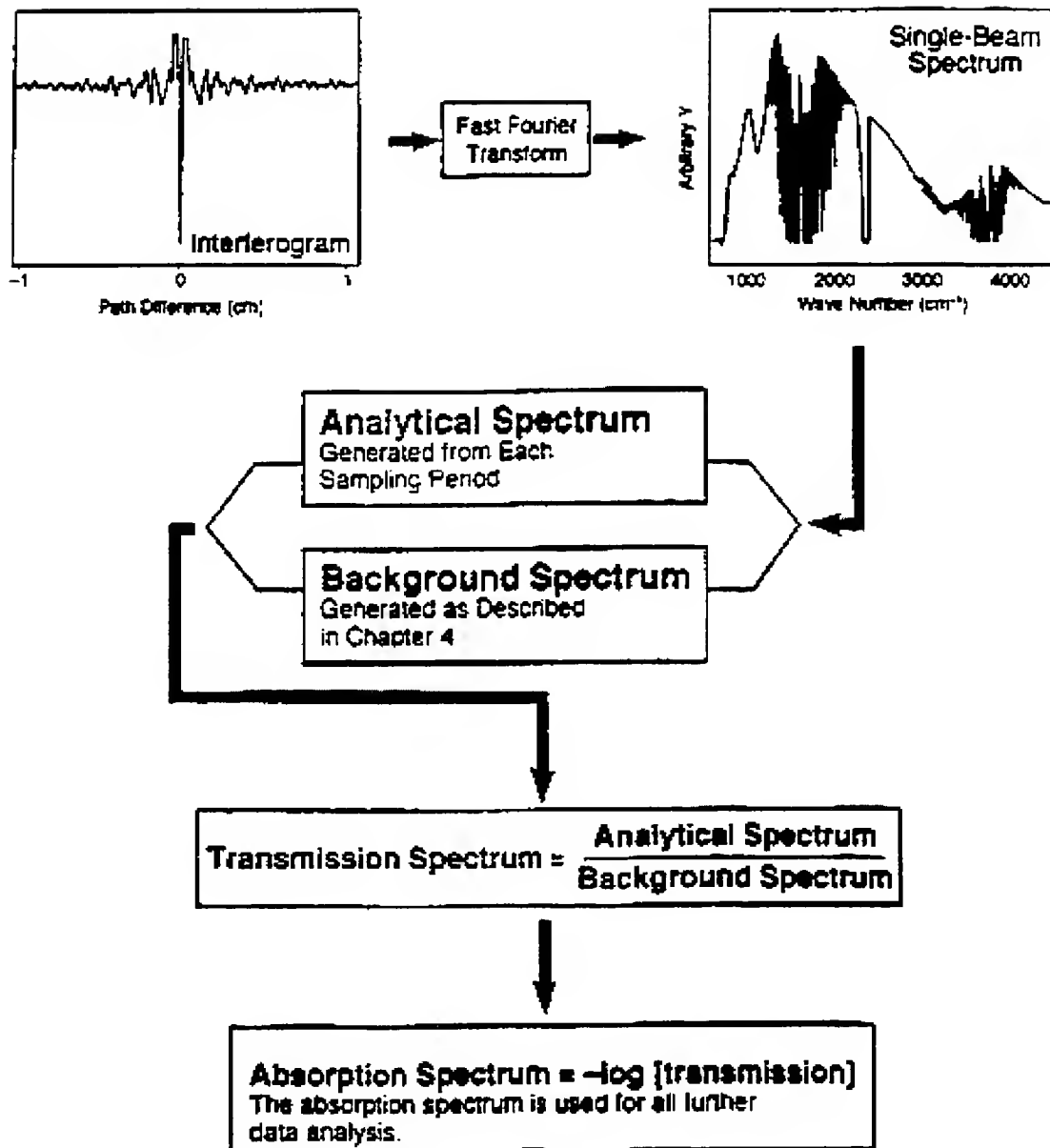


Figure 2.5. The software function diagram (source: EPA 92).



### 3. FIELD EXPERIMENTS

#### 3.1. Preliminary Study

The initial task was to install the 16-bit interface direct access memory (DMA) card into the 486DX2-66 computer that would be used for the research. The computer was configured accordingly and the next step was to confirm that the spectrometer was communicating with the computer. To accomplish this, the system was set up in the laboratory. The appropriate reference files were located, installed, and referenced within the software. Once a background scan was taken, a bottle of hexane was opened in the IR path to confirm detector response (Figure 3.1).

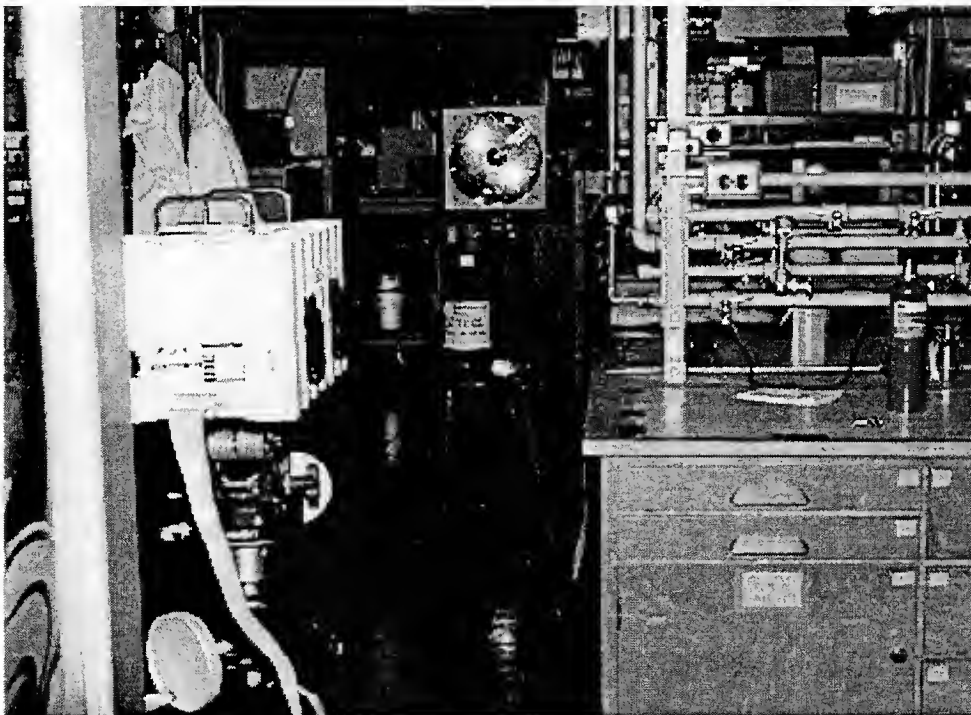


Figure 3.1. Preliminary laboratory setup with hexane bottle in place.

After the laboratory test was complete, a series of trial runs were conducted in a parking lot, across a local road, and in a construction zone on I-65 south of Lafayette. The first trial runs were conducted with stationary emissions sources (Figure 3.2).





Figure 3.2. A stationary trial run using a 1991 Suzuki Sidekick.

At this stage in the project, time was taken to become proficient with the alignment and calibration of the instrument and also to identify the height at which tailpipe emissions were best detected. Once calibrated and aligned, a background scan was taken and then the vehicles were started. After the vehicles had run at idle for a period of time, the engine was revved and the results observed. Figure 3.3 shows the HCs exhaust emission concentration time series of the stationary trial run performed on four vehicles on March 20, 1997 at the parking lot behind the Purdue University Civil Engineering building. There are two alignment procedures that must be followed when using the system. First, the alignment of the IR source with the target angle of the spectrometer. This is accomplished using a scope on the IR source and adjusting the height and angle so that the source reflects in the receiving optics of the spectrometer unit. It is also important to adjust the height of the unit so that the path that is being detected is adjacent to the tailpipes on the passing cars. The second alignment procedure has to do with aligning the mirrors within the interferometer to record the most efficient and accurate detection. This is done with two sets of screws on the side of the spectrometer unit. This is a critical alignment procedure where the parameters indicated on the computer are monitored as



the mirrors are being adjusted. Any vibration or bouncing caused by the passing cars has an obvious effect on this alignment.

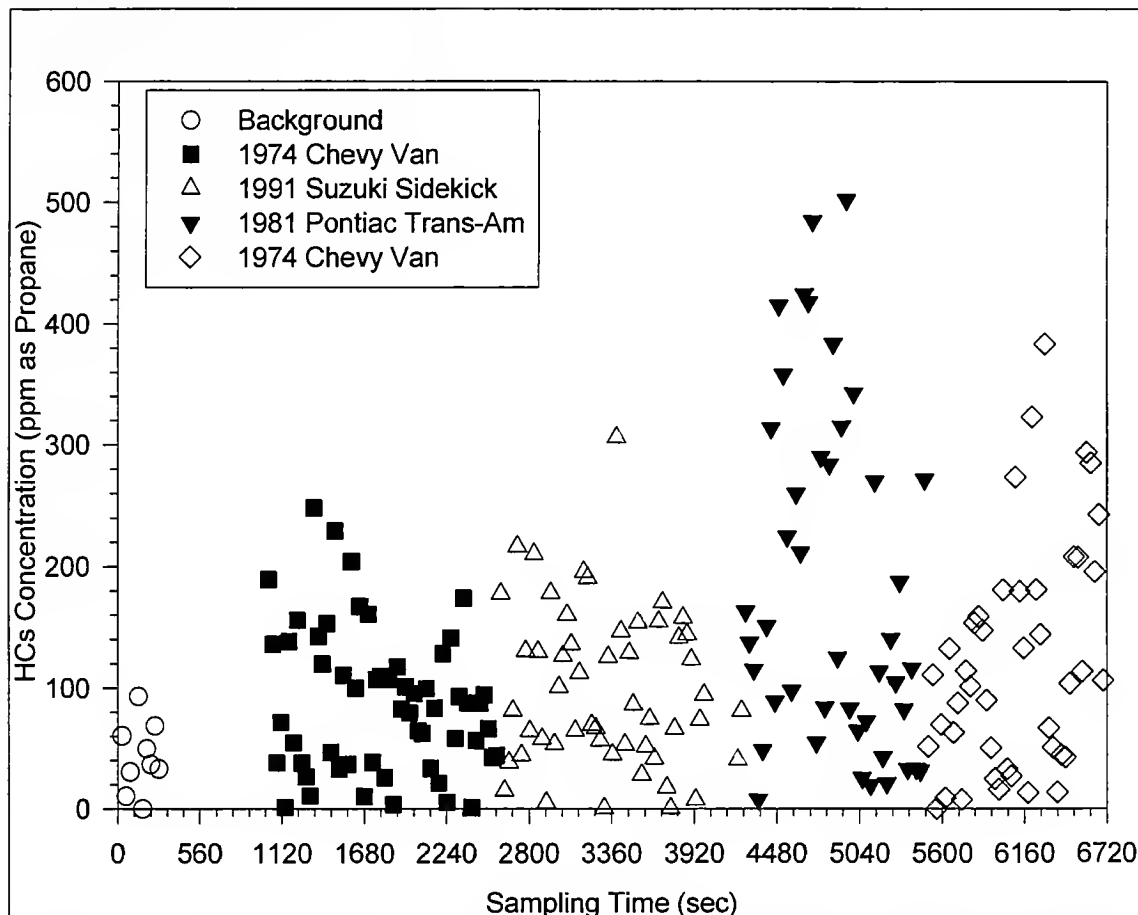


Figure 3.3. HCs Exhaust emission concentrations recorded during a stationary trial run.

A series of dynamic trial runs followed the stationary runs described above. The first was a simple set up where an occasional car would pass. Adjustments in procedure were made to achieve the best detection. The second was done on a local four-lane roadway with a considerable amount of traffic (Figure 3.4). A third one was performed in a construction zone on I-65 south of Lafayette. A considerable amount of data was collected during these trial runs and a camera was incorporated to help identify the vehicle that correlated with the emissions reading. Figure 3.5 shows the CO exhaust emission concentration time series measured during the dynamic trial run performed at the I-65 site on April 18, 1997. As it can be seen, the CO concentrations were very variable due to the differences in vehicle types, age, and operating modes.





Figure 3.4: Four-lane dynamic trial run with a video camera set up.

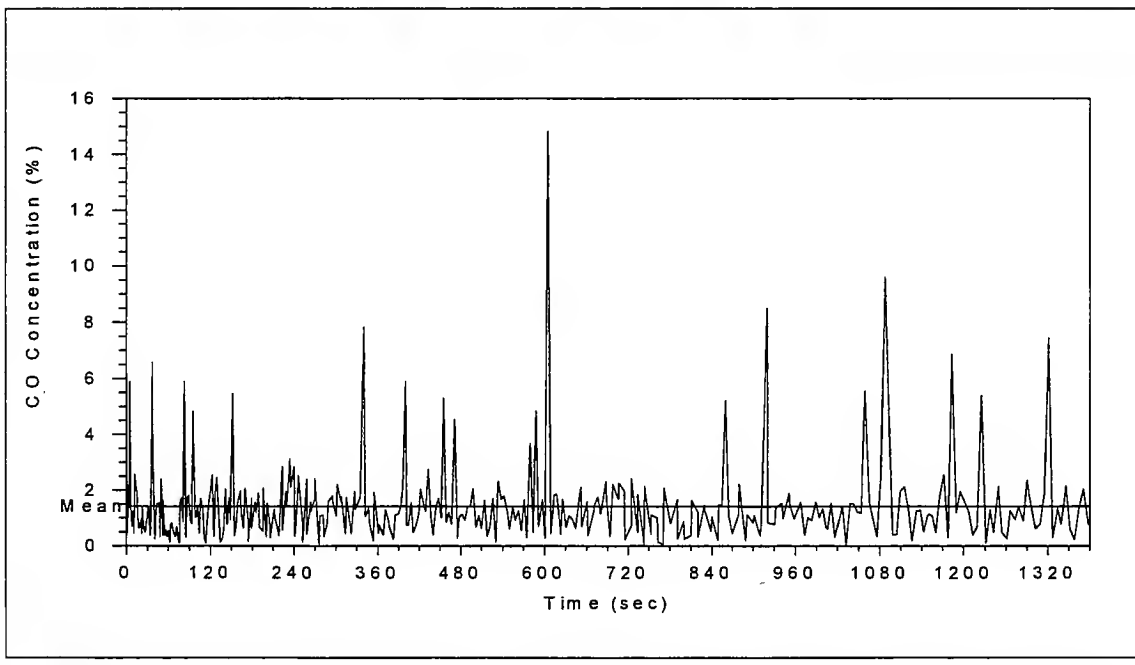


Figure 3.5. CO Exhaust emission concentrations recorded during a dynamic trial run.

An aerodynamic study of the turbulent flow around and behind a moving vehicle was conducted to help identify the height from the road that yielded the best exhaust



emission concentration measurements in the mixed volume behind a moving vehicle. Three basic vehicle types were identified. They included the sedan, the fastback, and the boxier van type. Smoke was used to observe the mixing region behind the van type vehicle (Figure 3.6) while aerodynamic theory was used to define the other two vehicle types. It was found that a vigorous turbulent cavity flow was attached to the back of the vehicles as they move. This mixed volume was identified as the target for exhaust emission concentration measurements.



Figure 3.6. Aerodynamic study of the mixing volume behind a moving van.

### **3.2. Borman Expressway Field Experiments**

For the actual data collection stage of this project, site selection was of utmost importance in order to accomplish the desired results. In order to identify single vehicles, it was necessary to limit the sampling site to a single lane. Since the Borman Expressway is a major three to four lane corridor with very high volume traffic, it was unreasonable to reduce the available lanes to a single lane. This would produce not only an incredible backup of traffic but dangerous operating conditions for the researchers as well. The second criteria for site selection was to have a region of likely acceleration and deceleration similar to what would be characteristic of the stop and go traffic of a construction zone. The location that best suited our needs was the end of the on-ramp from I-65 northbound to the Borman Expressway (Figure 3.7).





Figure 3.7. Sampling site looking east at I-65 on-ramp to the Borman Expressway.

Two lanes take a reduced speed,  $90^0$  turn where they merge into a single lane before further merging with the 55+mph traffic of the Borman Expressway. At this location is an overpass bridge just prior to the merging of the on-ramp traffic with the main flow of traffic on the Borman Expressway. This bridge served additional purposes of hiding the equipment from the drivers and as a protective measure for the equipment and personnel. The equipment was set up just downstream of the bridge abutments on either side of the ramp (Figure 3.8). Because the equipment could not be seen by drivers until it was almost adjacent to the vehicles, the psychological influence of the equipment did not play a role in altering the driving behavior of commuters.

Toward the end of the study, a location on I-65, two miles north of the Frankfort interchange in the northbound lane, was selected to conclude the data collection portion of the study. This site was downstream of a single lane construction zone providing the acceleration that was required (Figure 3.9).



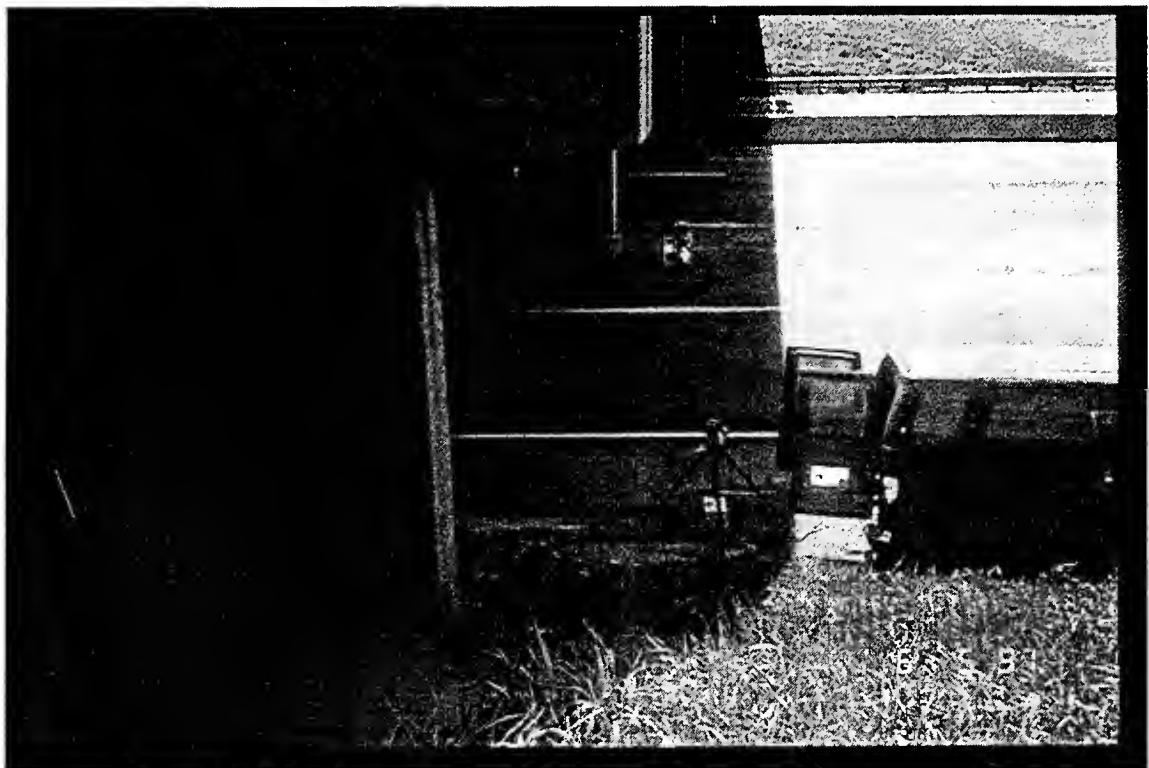


Figure 3.8. Equipment setup at the Borman Expressway sampling site.

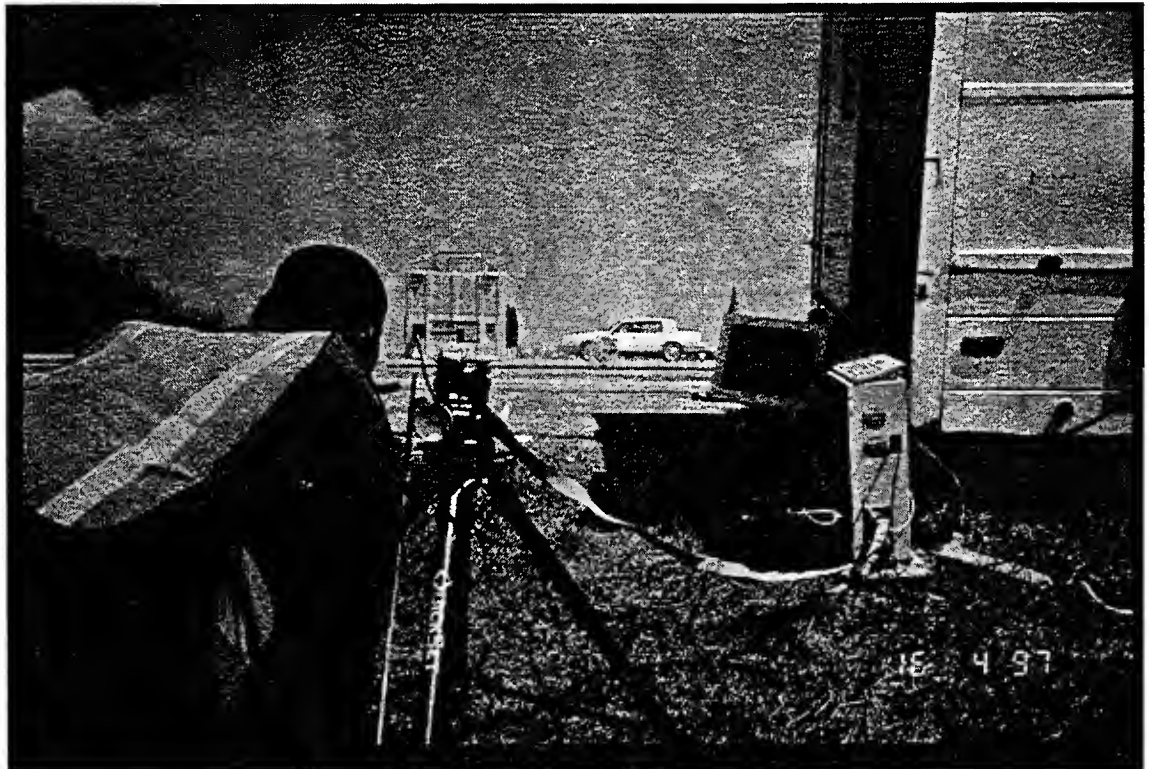


Figure 3.9. Monitoring at I-65 sampling site.



Additional parameters were recorded simultaneously with the emissions data. These parameters included vehicle speed and acceleration, video imageries for vehicle identification, and meteorology (wind speed, wind direction, ambient temperature, dew point temperature, and relative humidity). A camera was set up under the bridge to record the images of vehicles as they passed by the spectrometer. Notice the tripod leg that can be seen in the dark left side of Figure 3.8. This camera had a digital time stamp on the film that was calibrated with the clock on the computer. Later, this video data was used to generate a database of vehicle type versus time at the spectrometer. Speed was measured with a hand held laser speed gun located about 300 feet upstream of the spectrometer. The speed data was collected twice for each vehicle so that acceleration could be determined. A small Hewlet Packard (HP) data logger that through a cable automatically recorded the speed data in a form that could be directly downloaded and analyzed handled the laser gun data collection. Like the video data, the time for the speed gun was correlated with the computer time for data reduction purposes. The third data point recorded by the laser gun was the range to target which would be used to determine the time at which each vehicle passed the spectrometer. This was important because congestion, speed, and laser reading duration made it extremely difficult to catch each vehicle when they passed the spectrometer. Meteorological data were obtained from the Gary and Purdue University airport weather databases.



## 4. DATA REDUCTION AND ANALYSIS

### 4.1. Data Reduction

During the exhaust emission concentration and traffic monitoring, 16,870 vehicles were videotaped. The tapes were manually and visually analyzed in order to determine the vehicle types as well as correlate vehicle occurrence to the time of emission concentration measurements. In doing so, the correlation times included a four-second time lag representing the maximum time for vehicle exhaust plume dissipation (Caddle & Stephens, 1994). Three vehicle types were determined. All the automobiles were represented by type I vehicles. Type II represented all the medium-duty vehicles including light and medium-duty trucks and vans. Heavy-duty trucks were represented by type III. Type III vehicles were not included in the data analysis because their exhaust emission concentrations were not measured due to the fact that the emission sources were in a different plane. However, their number and flow rate were monitored. Figure 4.1.1 summarizes the fleet distribution per vehicle class and Figure 4.1.2 shows their flow rates. 8,478 (50%) were type I vehicles, 4,829 (29%) were type II vehicles, and 3,563 (21%) were type III vehicles. Overall 17.75 vehicles passed the spectrometer in a minute. The flow rates were 8.92, 5.08 and 3.75 vehicles/min for type I vehicles, type II vehicles, and type III vehicles respectively.

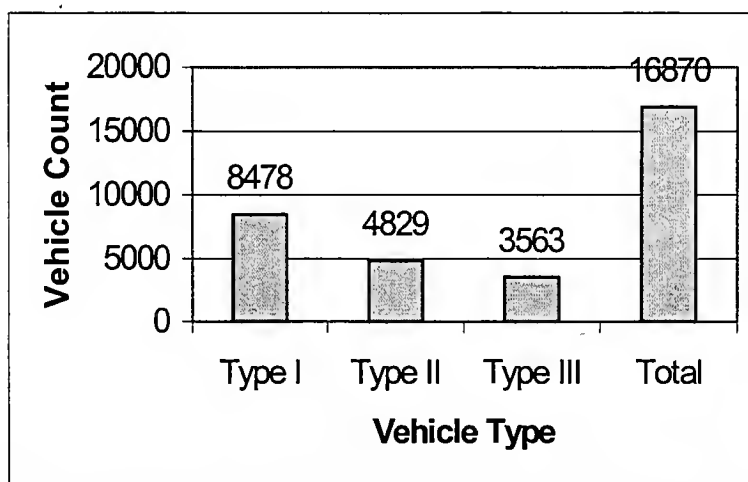


Figure 4.1.1. Total number of vehicles monitored during PVEMP.



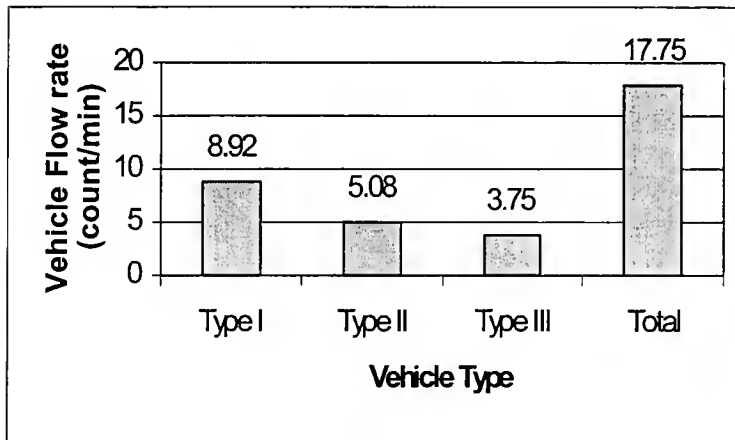


Figure 4.1.2. Average vehicle flow rate recorded during PVEMP.

The measured vehicle speeds were integrated in order to calculate the speeds and accelerations at the spectrometer. These speeds and accelerations were also correlated with vehicle type, time of vehicle at the spectrometer and time of exhaust emission concentration measurement. Hourly meteorological data were then added to the other parameters to develop the PVEMP database.

The integrated final PVEMP database consisted of 4,413 vehicles. 2,848 (65%) were type I vehicles and 1,565 (35%) were type II vehicles (Figure 4.1.3). The decrease in the number of vehicle monitored was due to many factors. These factors included the time correlation of all the measured parameters, the computational time required for emission concentration calculation by the FTIR system, the missing vehicle clocking for speed measurement, the suspect emission concentration values that were discarded, and the subtraction of type III vehicles from the analysis. Appendix A shows a portion and the format of the PVEMP database.

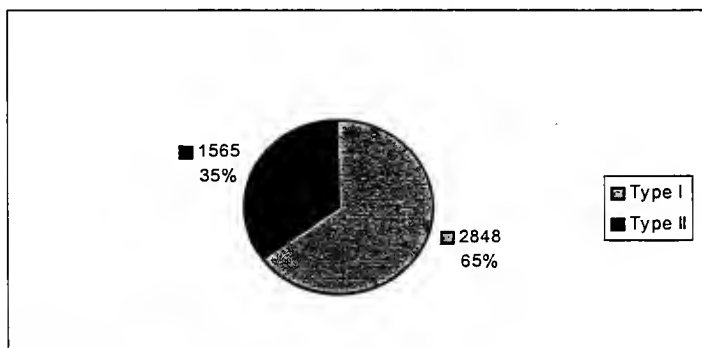


Figure 4.1.3. Total number of vehicles included in the data analysis.



## 4.2. Descriptive Statistics

### 4.2.1. CO and HCs Exhaust Emission Concentrations

The mean, median, minimum, and maximum CO and HCs exhaust emission concentrations for all the vehicles and for the two different vehicle types are presented in figures 4.2.1 and 4.2.2.

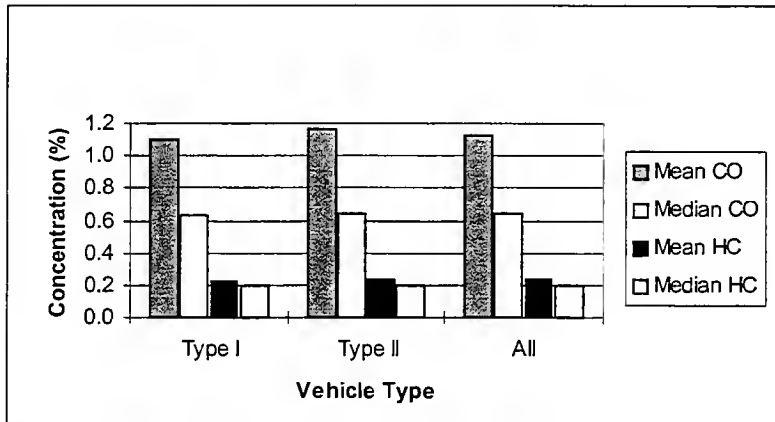


Figure 4.2.1. Mean and median CO and HCs exhaust emission concentrations for type I and type II vehicles, and the combined fleet.

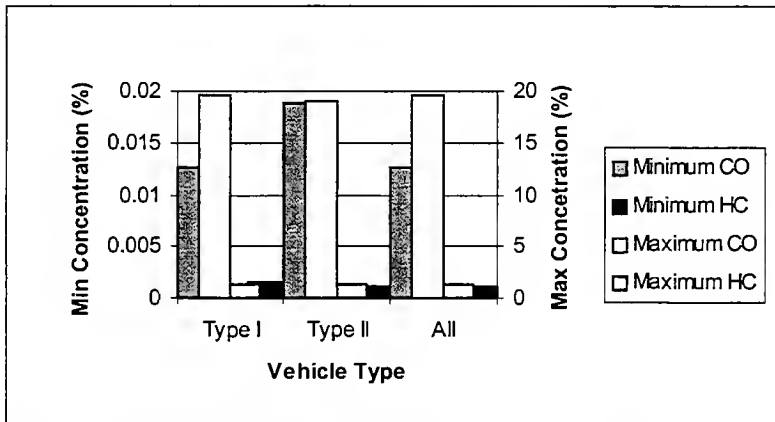


Figure 4.2.2. Minimum and maximum CO and HCs exhaust emission concentrations for type I and type II vehicles, and the combined fleet.

The mean CO exhaust emission concentrations from type I vehicles, type II vehicles, and the combined fleet are 1.10 %, 1.16 %, and 1.12 % respectively. The medians are 0.63 %, 0.64 % and 0.64 % respectively. This suggests that the distributions of CO exhaust emission concentration are severely skewed as seen in Figure 4.2.3. The



skewnesses are equal to 4.05 %, 4.39 %, and 4.21 % for type I vehicles, type II vehicles, and the combined fleet respectively. In fact, CO concentration displays a logarithmic distribution as depicted in Figures 4.2.4.

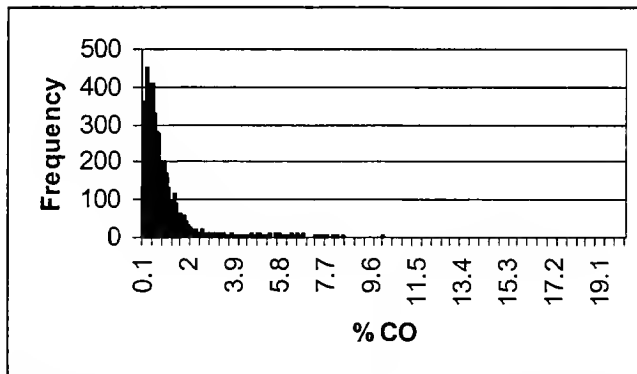


Figure 4.2.3. Histogram of the CO exhaust emission concentration distribution for the combined fleet.

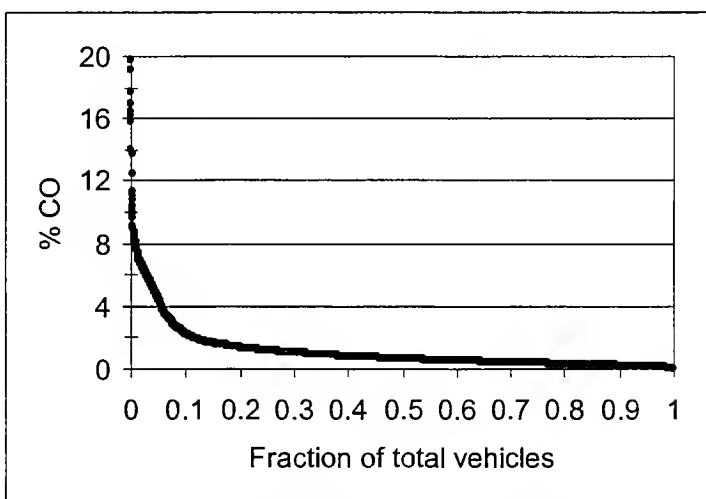


Figure 4.2.4. Logarithmic distribution of CO exhaust emission concentration for the combined vehicle fleet monitored.

The data also show a high variability in CO exhaust emission concentrations. In fact, the minimum, maximum, and standard deviation of CO exhaust emission concentration for the combined fleet are 0.01 %, 19.69 %, and 1.61 % respectively. It is worth mentioning that Type I vehicles registered the highest CO exhaust emission concentration maximum and the lowest mean and type II registered the lowest CO exhaust emission concentration minimum and the highest mean.



The mean HCs exhaust emission concentrations expressed as propane equivalents from type I, type II, and the combined fleet are 0.23 %, 0.24 %, and 0.23 % respectively. The medians are 0.19 %, 0.20 % and 0.20 % respectively. This suggests that the distributions of HCs exhaust emission concentrations are somewhat skewed as displayed in Figure 4.2.5. The skewnesses are equal to 1.28 %, 1.30 %, and 1.30 % for type I vehicles, type II vehicles, and the combined fleet respectively. HCs exhaust emission concentration also displays a logarithmic distribution as depicted in Figures 4.2.6. The variability of the HCs exhaust emission concentration distribution is lower. The minimum, maximum, and standard deviation of HCs exhaust concentration for the combined fleet are 0.00 %, 1.40 %, and 0.17 % respectively. Again, type I vehicles registered the highest HCs exhaust emission concentration maximum while type II registered the highest mean HCs exhaust emission concentration. Appendix B presents the histograms and logarithmic distributions for each vehicle type.

The mean concentrations recorded in this study are in line with the results of the few remote-sensing measurements already done. For example, in a study conducted in Chicago, Illinois in October 1991, Stedman and co-workers reported mean CO and HCs exhaust emission concentrations of 1.10% and 0.14% respectively (Stedman et al, 1991). In the study conducted in El Monte, California in June 1991 by General Motor Research and Development Center and the California Air Resources Board, Stephens reported mean exhaust emission concentrations of 0.86% CO and 0.04% HCs (Stephens, 1994). These data relate to the combined fleet monitored in these studies.

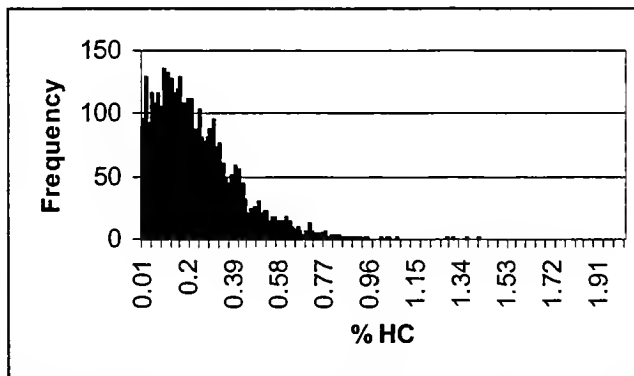


Figure 4.2.5. Histogram of the HCs exhaust emission concentration distribution for the combined fleet.



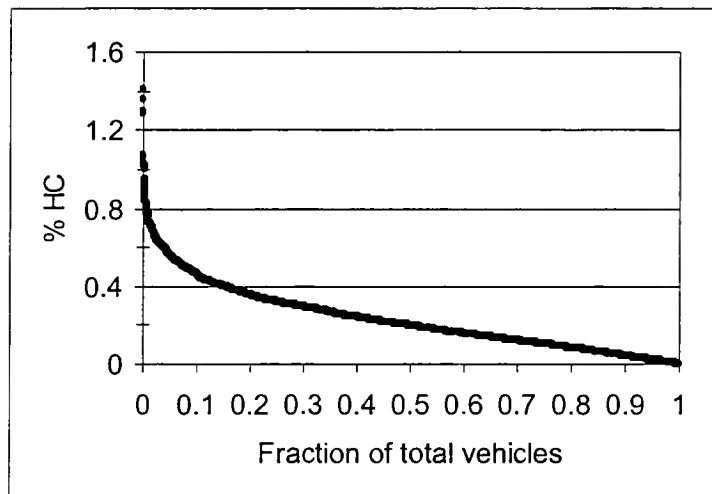


Figure 4.2.6. Logarithmic distribution of HCs exhaust emission concentration for the combined vehicle fleet monitored.

Figures 4.2.7 and 4.2.8 show the mean CO and HCs exhaust emission concentrations for each monitoring session. As expected, the mean concentrations vary from one monitoring session to the other due to changes in the experimental setups, the driving modes, and the atmospheric conditions. The highest mean CO exhaust emission concentrations were obtained during the monitoring session of May 20, 1997, on the Borman Expressway. The lowest were obtained during that of August 21, 1997, on I-65. The highest mean HCs exhaust emission concentrations were obtained during the monitoring session of May 20, 1997 and the lowest during that of August 22, 1997, on I-65. The physical characteristics of these sites are described in Section 3. The atmospheric conditions on these days are described below in the present Section.

Figure 4.2.9 presents the percentiles of the concentrations of CO and HCs for the combined fleet. The plots for the two vehicle types are presented in Appendix B. The interpretation of these figures is critical for the model development and the design of concentration threshold limits for each vehicle type because they can report on the data clusters in the distributions. For example, when all the vehicles are considered, it can be seen that 90% of the HCs exhaust emission concentrations are less than 0.46 % and 10% are less than 0.04 %. Furthermore, 90% of the CO exhaust emission concentrations are less than 2.22 % and 10% are less than 0.18 %. This type of finding will help in deciding which data to include in the development of the exhaust emission concentration model.



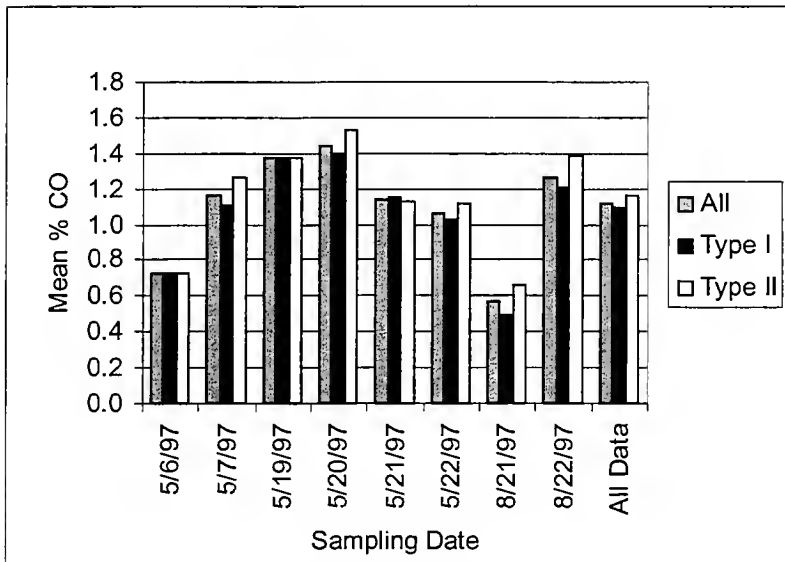


Figure 4.2.7. Mean CO concentrations for type I vehicles, type II vehicles, and the combined fleet recorded during each monitoring session.

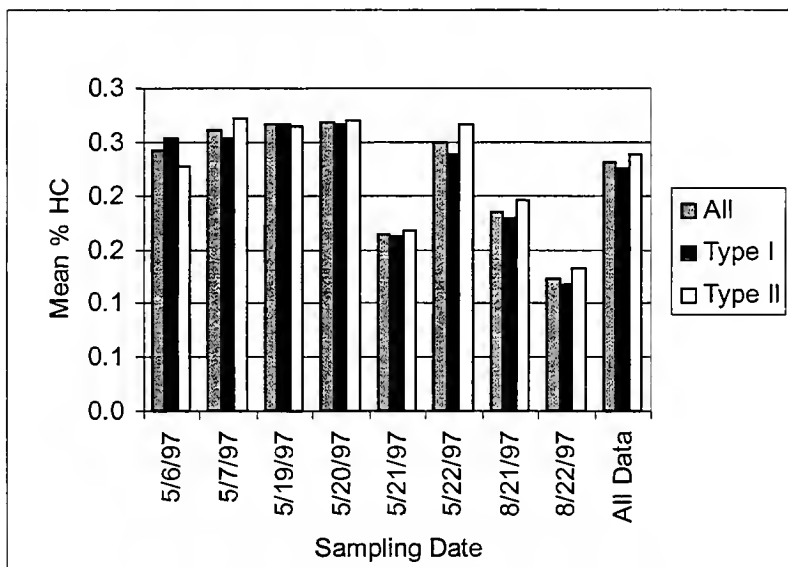


Figure 4.2.8. Mean HCs concentrations for type I vehicles, type II vehicles, and the combined fleet recorded during each monitoring session.



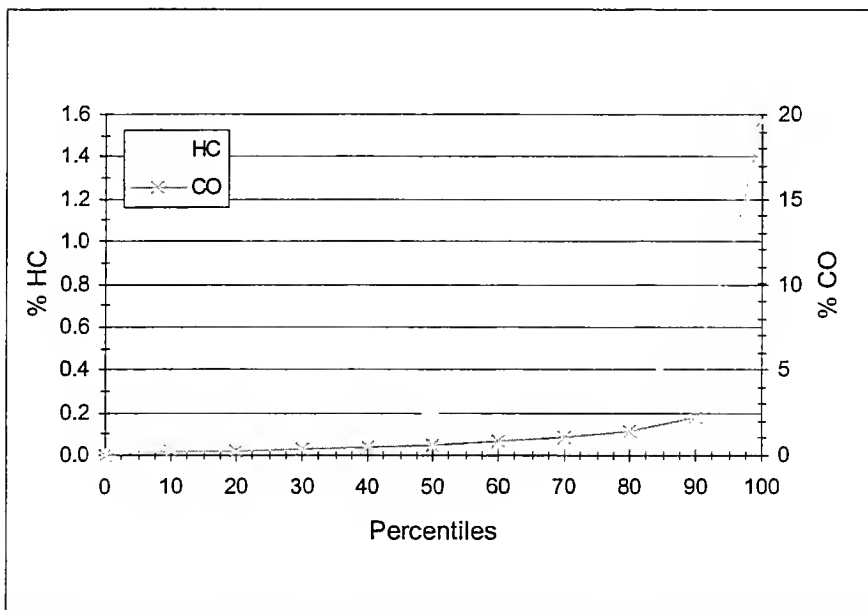


Figure 4.2.9. CO and HCs exhaust emission concentration percentiles for the combined fleet.

#### 4.2.2. Vehicle Speed and Acceleration/Deceleration

The data pertaining to the driving modes is summarized below. Vehicle speeds varied from 34.5 to 83.5 mph with a standard deviation of 5.6 mph. The mean vehicle speed for type I vehicles was 56.74 mph and that of type II vehicles was 56.21 mph. It was 56.56 mph considering the combined fleet. Figure 4.2.10 summarizes the data.

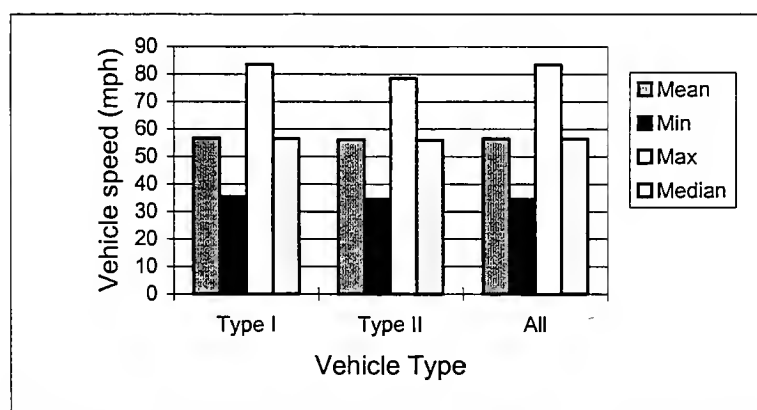


Figure 4.2.10. Mean, median, maximum, and minimum speeds for type I and type II vehicles, and the combined fleet.



The vehicle speed distributions exhibit a near normal characteristic since the means are almost equal to the medians. The day-to-day variations in mean vehicle speeds were between 55.2 mph and 58.5 mph depending on vehicle type (Figure 4.2.11).

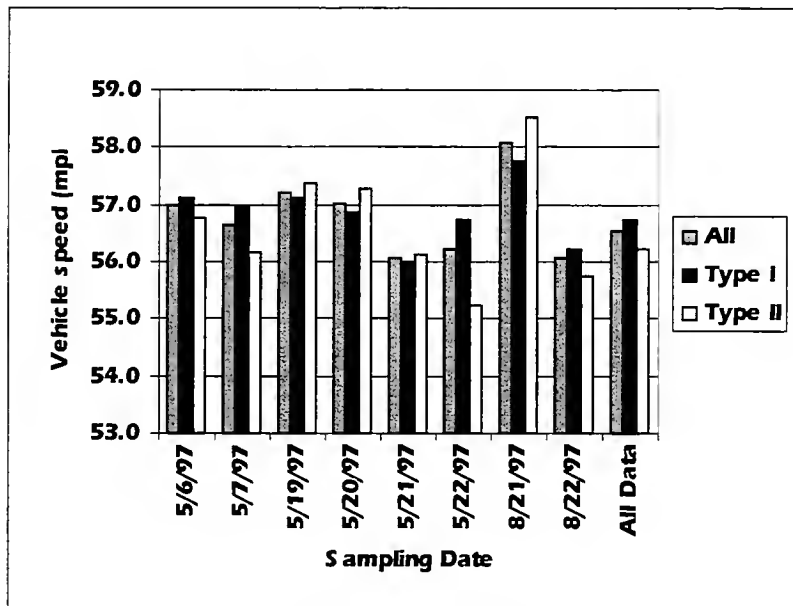


Figure 4.2.11. Mean speeds for type I and type II vehicles, and the combined fleet recorded during each monitoring session.

During the monitoring session of May 20, 1997, when the highest mean CO and HCs exhaust emission concentrations were recorded, the mean vehicle speeds for type I vehicles, type II vehicles, and the combined fleet were 56.9 mph, 57.3 mph, and 57.0 mph respectively. On August 21, 1997, when the lowest mean CO exhaust emission concentrations were recorded, the mean vehicle speeds for type I vehicles, type II vehicles, and the combined fleet were 57.7 mph, 58.5 mph, and 58.1 mph respectively. On August 22, 1997, when the lowest mean HCs exhaust emission concentrations were recorded, the mean vehicle speeds for type I vehicles, type II vehicles, and the combined fleet were 56.2 mph, 55.7 mph, and 56.1 mph respectively. These findings are also depicted on the scatter plots of the mean concentrations versus the mean vehicle speeds for the combined fleet (Figure 4.2.12).



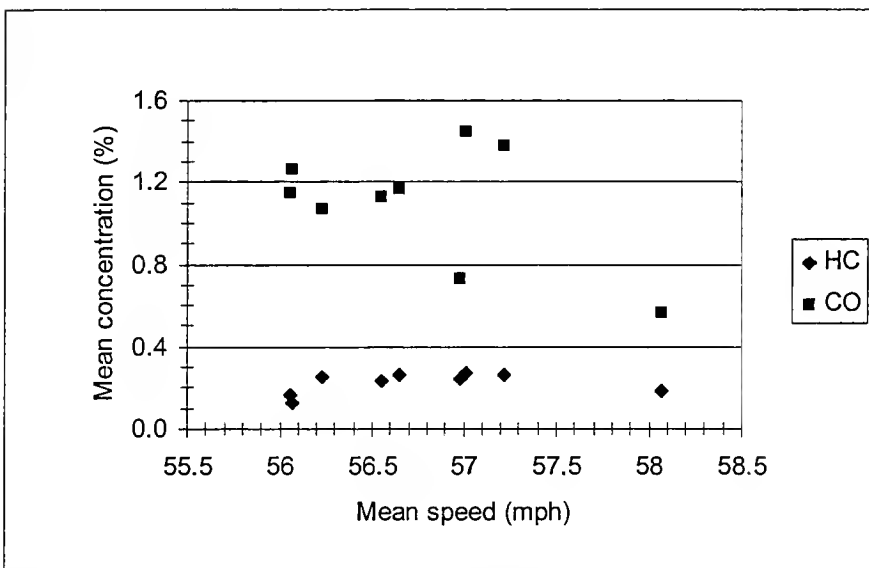


Figure 4.2.12. Variation of mean CO and HCs exhaust emission concentration with mean vehicle speed for the combined vehicle fleet.

The acceleration values varied from -4.5 to 4.0 mph/sec with a mean of 0.17 mph/sec, a median of 0.0 mph/sec, and a standard deviation of 0.71 mph/sec considering all the vehicles (Figure 4.2.13).

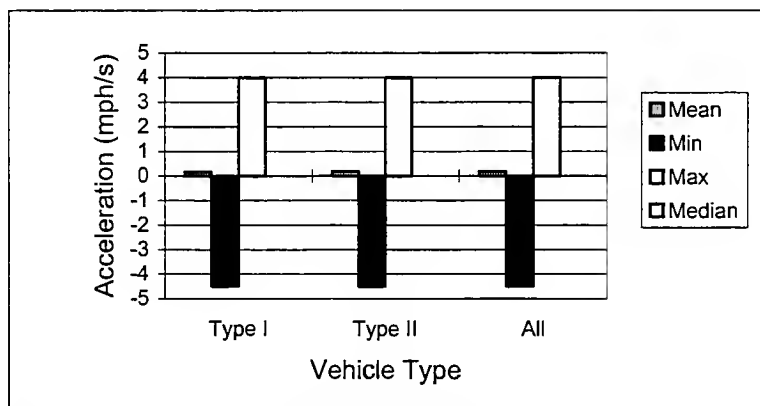


Figure 4.2.13. Mean, median, maximum, and minimum acceleration for type I and type II vehicles and the combined fleet.

The day-to-day variation in mean acceleration values was between 0.04 and 0.13 mph/s depending on car type except on August 21 and 22, 1997 when the mean acceleration values varied from 0.36 to 0.59 mph/s (Figure 4.2.14). This clearly shows the effect of the characteristics of the experimental sites. The I-65 site was unobstructed



and downhill while that of the Borman Expressway was a flat roadway under an overpass. Except for August 22, the mean accelerations for type II vehicles were higher than those of type I vehicles. Note that August 21 and 22, 1997 were the dates when the lowest mean CO and HCs exhaust emission concentrations were respectively recorded. The variations of the mean concentrations with the mean vehicle accelerations are also shown in Figure 4.2.15 for the combined fleet.

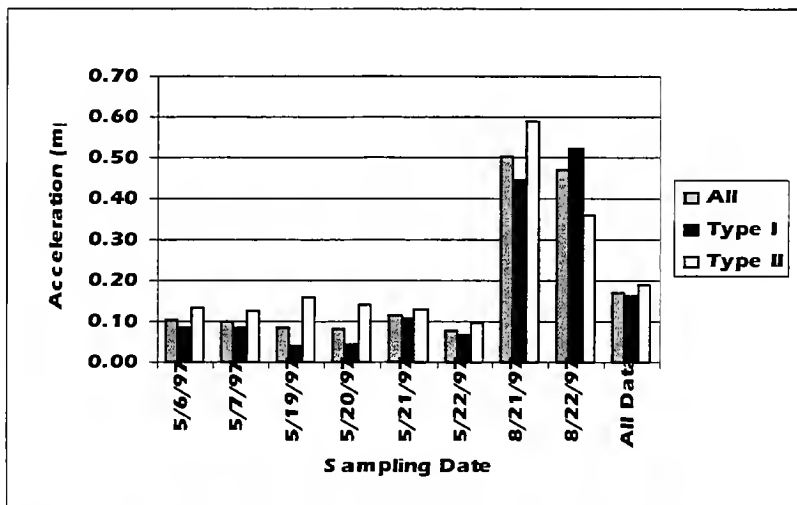


Figure 4.2.14. Mean accelerations for type I and type II vehicles, and the combined fleet recorded during each monitoring session.

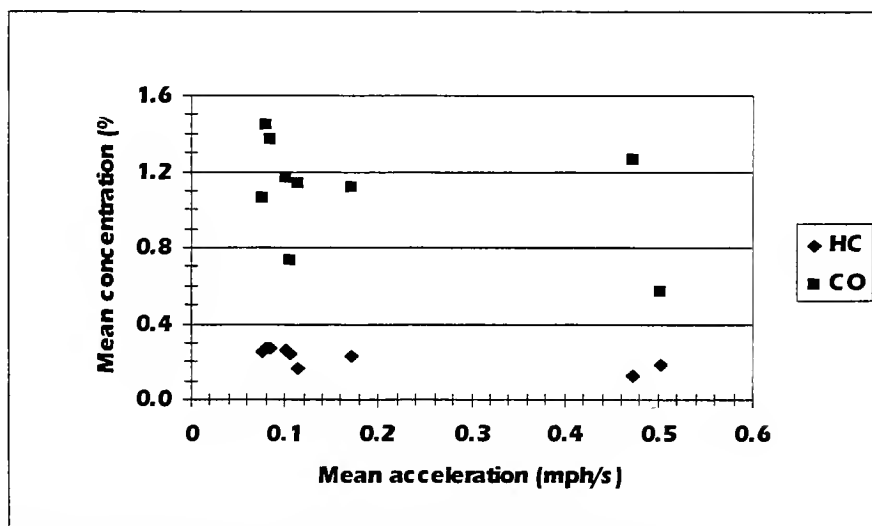


Figure 4.2.15. Variation of the mean CO and HCs concentrations with the mean vehicle acceleration for the combined vehicle fleet.



#### 4.2.3. Meteorology

The mean meteorological data collected during the field experiments is presented in Figure 4.2.16. Ambient temperature varied from 54.6 °F to 72.0 °F with an average of 61.4 °F. Wind speed varied from 8.0 mph to 12.5 mph with an average of 10.4 mph. Relative humidity varied from 34.4% to 79.9% with an average of 46.6%. The winds were from the south-southeast except on May 7, 1997 when they were from the northwest. On May 20, 1997, when the highest mean CO and HCs exhaust emission concentrations were recorded, the mean temperature, wind speed, and relative humidity were 57.1 °F, 11.5 mph, and 70.2% respectively. On August 21, 1997, when the lowest mean CO exhaust emission concentrations were recorded they were 62.6 °F, 10.0 mph, and 79.9% respectively. On August 22, 1997, when the lowest mean HCs exhaust emission concentrations were recorded, they were 72.0 °F, 12.4 mph, and 50.0% respectively.

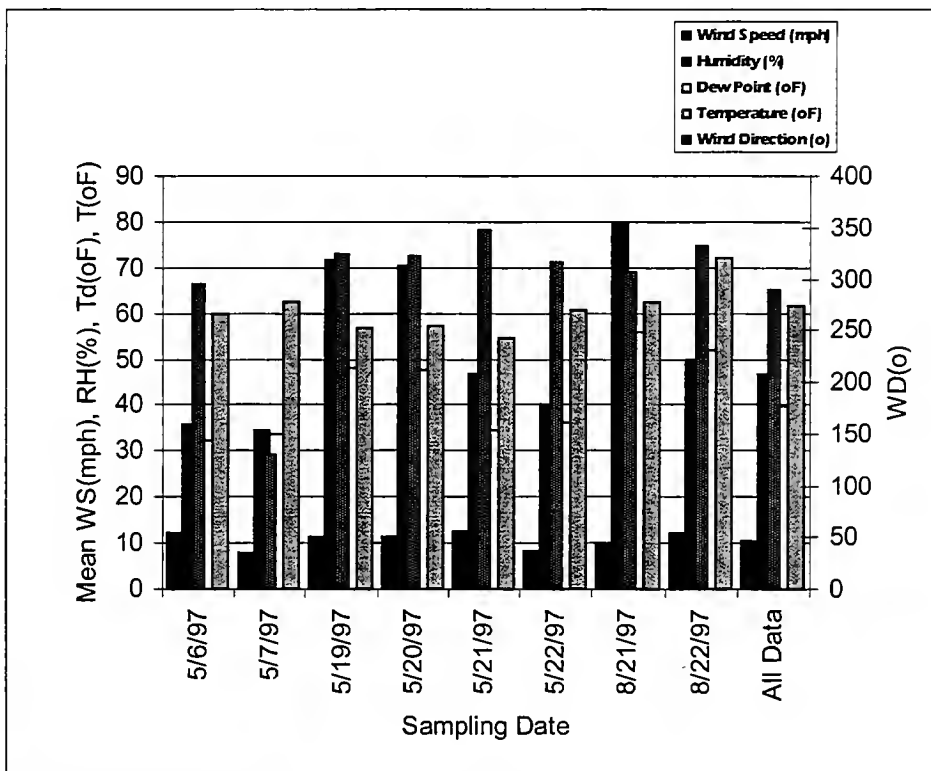


Figure 4.2.16. Mean meteorological data recorded during each monitoring session.



#### **4.3. Observed Emission-Speed-Acceleration Correlations**

The interpretation of the functional relationships between real-time CO and HCs exhaust emission concentrations, vehicle speeds, driving modes (acceleration, deceleration, and cruise), and mean values of atmospheric parameters is very important. It is the key to the development of a sound and efficient modal exhaust emission concentration model that can be used to help improve traffic flow when air quality becomes an important traffic parameter. The first approach is the visual study of the scatter plots of the key parameters. The scatter plots of the mean CO and HCs emission concentrations versus the mean values of vehicle speeds, and accelerations, and atmospheric observations were shown in Section 4.2. The scatter plots of the instantaneous values of CO and HCs exhaust emission concentrations versus vehicle speeds and accelerations, the main parameters of modal emission modeling, are presented in Figures 4.3.1 to 4.3.4 for the combined fleet. Those pertaining to the different vehicle types are presented in Appendix B. These visual correlations do not show any classical mathematical trends except the fact that the emission concentration data are clustered between the speeds of 45.0 and 70.0 mph and the accelerations of -2.0 to + 2.0 mph/sec. These observations may be due to many factors. Because of the nature of the experimental setups and the characteristics of the sites, most of the speed and driving mode data fall in the above speed and acceleration ranges. Moreover, the formation of CO and unburned HCs, as explained in Section 1, makes it apparent that the bulk of the exhaust emissions will occur in these ranges. The Pearson correlation factors between the instantaneous values of CO exhaust emission concentrations and vehicle speeds and accelerations are -0.046 and 0.005 respectively. Those between the instantaneous values of HCs emission concentrations and vehicle speeds and accelerations are 0.001 and -0.033 respectively. This suggests that there is not a linear relationship between emission concentrations, speeds, and accelerations and neither speed nor acceleration alone may explain the emission concentration variations. Therefore both speed and acceleration should be accounted for simultaneously when studying vehicle exhaust emission concentrations. Figures 4.3.5 and 4.3.6 show the three-dimensional plots of the triple correlations for the combined fleet. These surfaces were derived from interpolated meshes using the inverse distance method. The three-dimensional plots of the two



different vehicle types are presented in Appendix B. As it can be seen, the surfaces are neither uniform nor smooth indicating once again the variability and cluster of the exhaust emission concentrations. The determination of these three-dimensional functional relationships will represent the theoretical basis of the model.

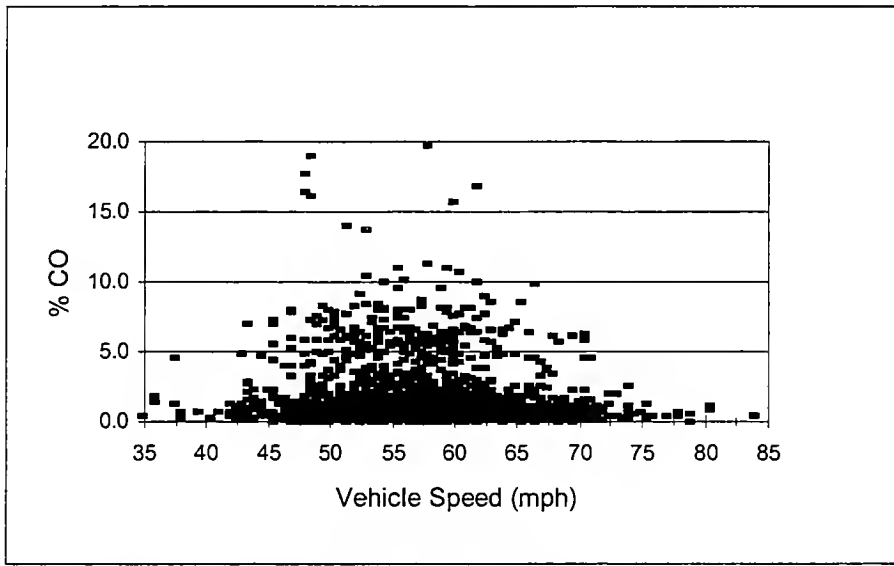


Figure 4.3.1. Variation of instantaneous CO exhaust emission concentrations with vehicle speed for the combined vehicle fleet.

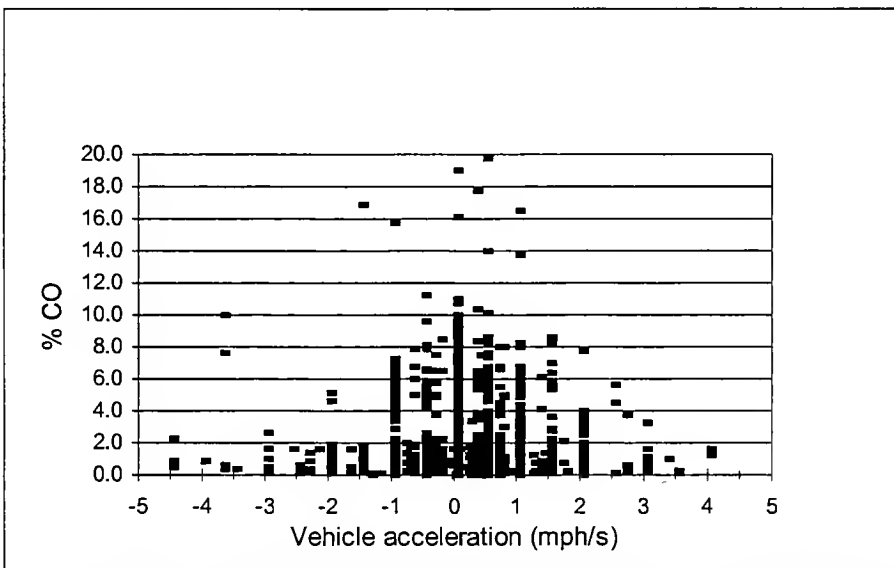


Figure 4.3.2. Variation of instantaneous CO exhaust emission concentrations with vehicle acceleration for the combined vehicle fleet.



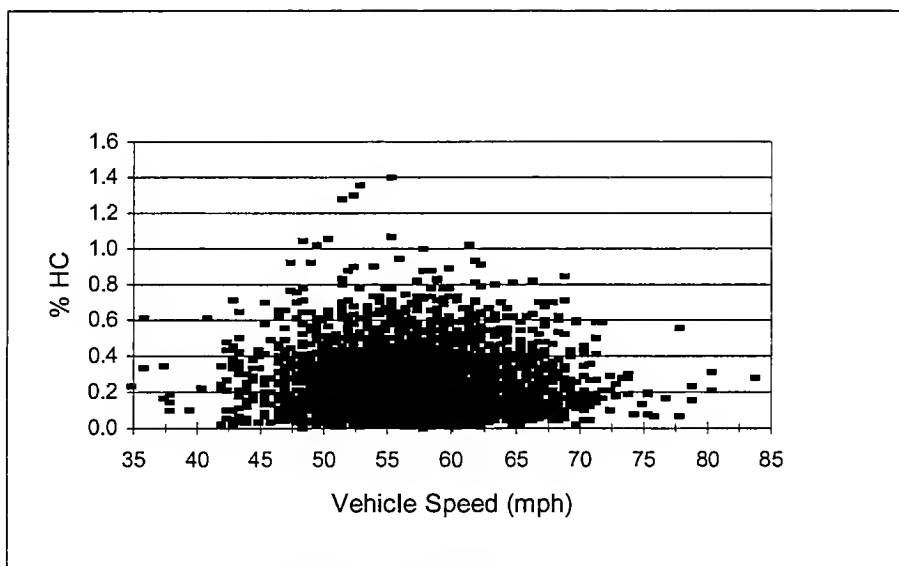


Figure 4.3.3. Variation of instantaneous HCs exhaust emission concentrations with vehicle speed for the combined vehicle fleet.

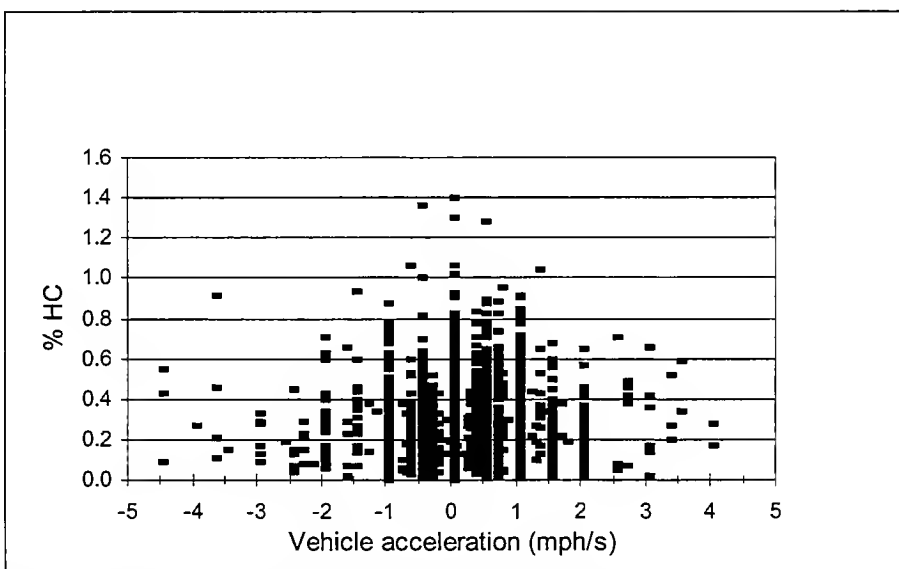


Figure 4.3.4. Variation of instantaneous HCs exhaust emission concentrations with vehicle acceleration for the combined vehicle fleet.



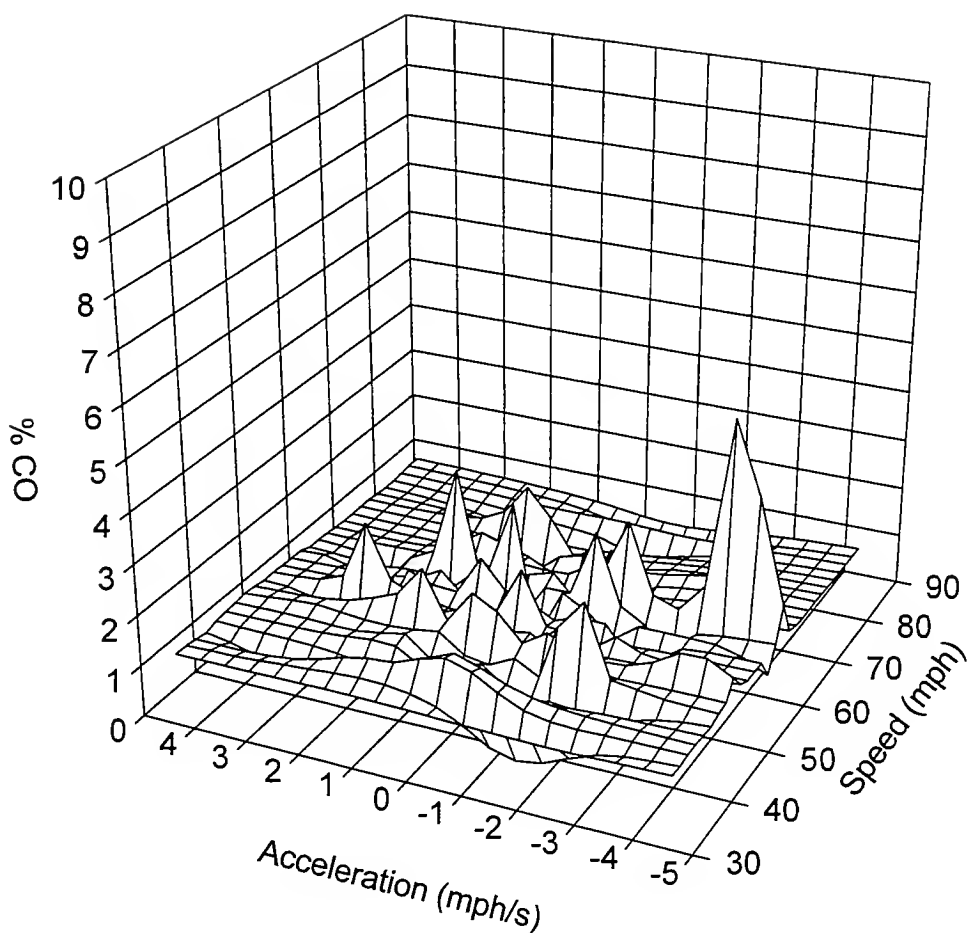


Figure 4.3.5. Three-dimensional plot for the triple correlation of CO exhaust emission concentration, speed, and acceleration for the combined fleet.



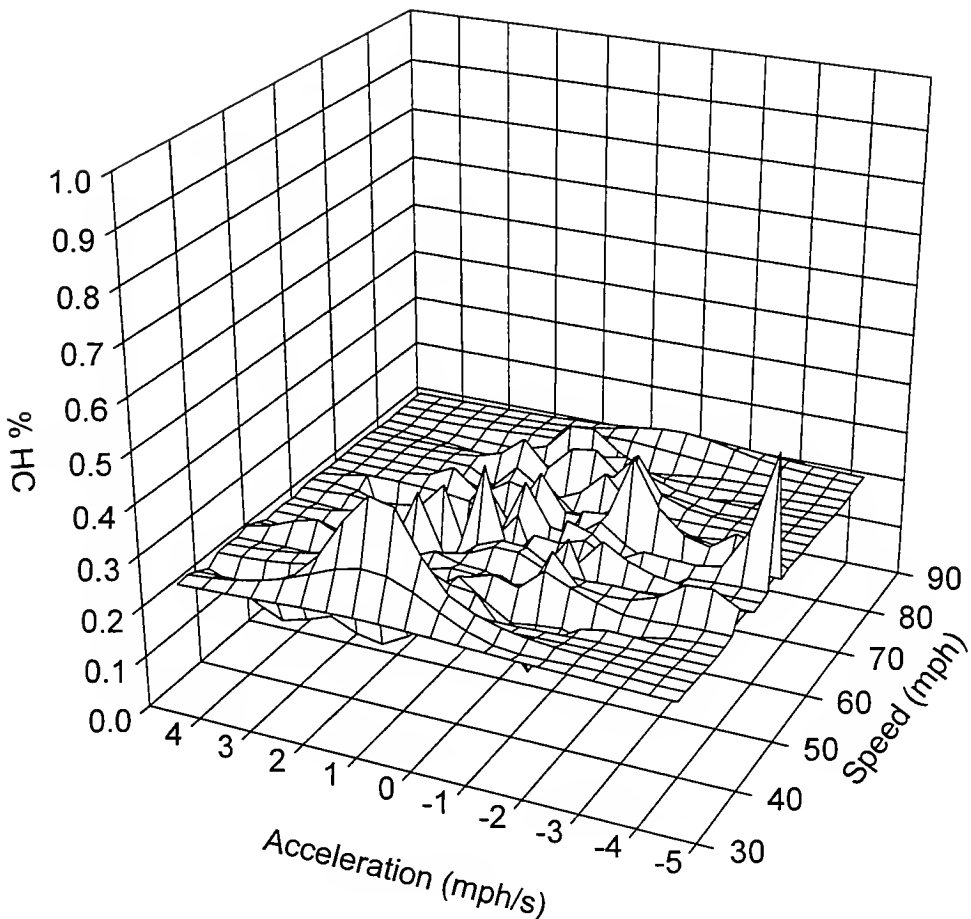


Figure 4.3.6. Three-dimensional plot for the triple correlation of HCs exhaust emission concentration, speed, and acceleration for the combined fleet.

#### 4.4. High Emitters

The CO and HCs high emitting vehicle fractions along with their contribution to the total exhaust emission concentrations are depicted in Figures 4.4.1 and 4.4.2 respectively for the combined fleet. The cut-points for high emitters were selected to be 4.0 % CO and 0.2 % HCs (Jack et al, 1995, Stephens, 1994). The fractions of the total vehicles emitting at or above a given emission concentration level are also presented in Figures 4.1.3 and 4.1.4. Overall, 5.7% of the vehicle fleet emitted more than 4% CO and generated 33.7% of the total CO exhaust emission concentration. 49.2% of the vehicle



fleet emitted more than 0.2% HCs and generated 77.5% of the total HCs exhaust emission concentration. However, Only 3.0% of the total vehicle fleet were high emitters of both CO and HCs together.

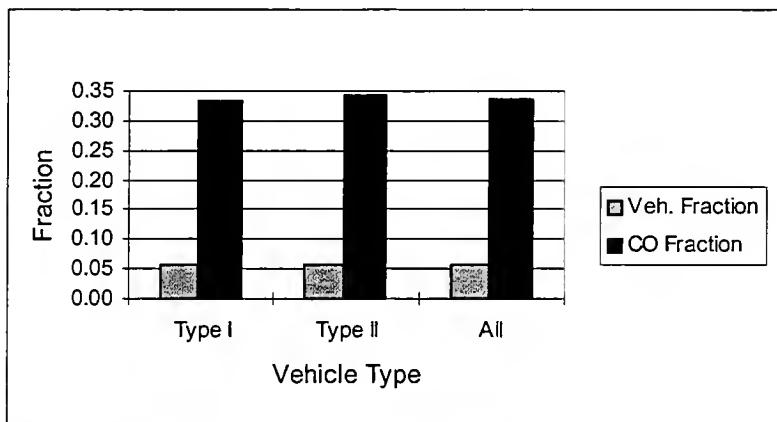


Figure 4.4.1. Fractions of CO high emitters and total CO exhaust emission concentrations for the combined vehicle fleet.

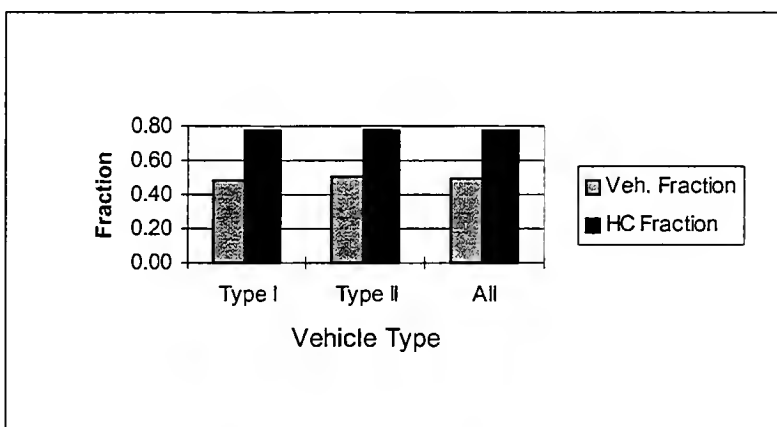


Figure 4.4.2. Fractions of HCs high emitters and total HCs exhaust emission concentrations for the combined vehicle fleet.



## 5. REAL-TIME MODAL MODEL DEVELOPMENT

### 5.1. Modeling Overview

Models are formal set of calculations designed to closely represent reality. Their main roles are to predict or describe unmeasured conditions, predict and examine changes and causalities, and avoid the high costs of data collection and monitoring. The major components of a model are the theories, the input parameters and data, and the underlying assumptions. Since models are set of calculations, they bear inherent errors rising from the assumptions, the limitations of the theories, and the input data.

When modeling traffic emissions, three popular computational methods are used. They are the method based on real driving behavior, the method based on road stretch analysis, and the method based on mileage related emission balances. The scale of applications, the levels of details, and the input data requirements of these computational method are different. The emission calculations based on actual driving behavior (modal modeling) are applied on a local (micro) scale. The emission factors are emission maps for vehicles based on modal data from transient test or real time monitoring. The traffic data are derived from counts or traffic models. The road specific data are represented by actual driving behaviors. The emission calculations based on road stretch analysis are applied on a regional scale. The emission factors are generally from FTP dynamometer tests. The traffic data are derived from counts or traffic models. Mean speed, road gradient, and altitude for each road represent the road specific data. The emission calculations based on mileage-related emission balance are applied on a regional, national, and global scale. The emission factors are generally from FTP dynamometer tests. The traffic data are derived from statistical data for VMTs according to subclasses of vehicles and roads and there is no road specific data.

Modal emission modeling is relatively new and encompasses three different methods. A convenient method to characterize vehicle-operating modes is the development of speed-acceleration matrix that measures emissions associated with each mode. Another modal emissions method develops an emission map based on engine power and speed. These two methods have used second-by-second emission tests performed at numerous engine-operating points, taking an average of steady-state



measurements. St-denis and Winer (1993) have created both a speed-acceleration and a speed-load modal emissions model using data from a single Ford vehicle. Sierra Research has developed a modal emissions model that computes the second-by-second engine speed and load required for a specified driving cycle, then, using an emissions map, second-by-second emissions were approximated (Barth et al, 1998). The other modal emission method is the analytical power-demand modeling. It is based on parameterized analytical representation of emission production. In this extensive treatment, the entire emission process is broken down into components that correspond to physical phenomena associated with vehicle operation and emissions production. Each component is then modeled as an analytical representation consisting of various parameters that are characteristic of the process. These parameters vary according to vehicle type, engine, and emission technology. Researchers at the University of California, Riverside, are currently developing such a model (Barth et al, 1998). However, so far, on-road real-time data have not yet been used in modal emissions modeling. Moreover, modal emission modeling has not yet been used for the estimation of real-time emission production based on input parameters from real-time advanced traffic monitoring systems.

## 5.2. Model Development

### 5.2.1. Description of the current model

The model developed in this study; the Purdue Vehicle Exhaust Emission Model, the Borman Expressway Application (PVEM-BEA) is a real-time, micro-scale, modal exhaust emission concentration model. It is designed to predict average vehicular exhaust emission concentrations of CO and HCs in real-time traffic flow. It is a data driven model based on real driving behavior and derived from the integrated CO and HCs exhaust emission concentrations in terms of the modal value-pairs speeds and accelerations. The regression analyses of the speed-acceleration matrices result from the modal analysis of the PVEMP database described in Section 4. PVEM-BEA is intended to be an integral part of the Borman Expressway Advanced Traffic Management System representing an additional tool for traffic management, especially in construction zones, when air pollution becomes an important decision-making parameter.



Real-time values of vehicle speed and acceleration, traffic composition and volume, and road geometry are the main input parameters. They are the main parameters affecting real-time vehicle exhaust emissions. Even though vehicle age, conditions, and fuel economy affect vehicle exhaust emissions also, they are excluded in PVEM-BEA because they can not be assessed instantaneously. Synoptic meteorology is also excluded because of the small spatial and temporal scale of the model.

For a given location, the real-time input of speed, acceleration, and type of each passing vehicle acquired instantaneously (very short time interval) are used to calculate the mode-average CO and HCs exhaust emission concentrations according to the vehicle type. The program then outputs data about the traffic volume, the fleet composition, the vehicle flow rates, the vehicle speeds and accelerations, the average CO and HCs exhaust emission concentrations, and the emission concentration threshold level exceedences (decision making) for the short time interval.

### **5.2.2. Analytical Background of PVEM-BEA**

It was shown in Section 4 that there were no mathematical relationships between the instantaneous CO and HCs exhaust emission concentration and speeds and accelerations. Consequently, the database has to be reduced further in order to assess the correlations. In doing so, speeds and accelerations were binned and average exhaust CO and HCs emission concentrations were calculated at acceleration midpoints independent of speed, at speed midpoints independent of acceleration, and at the intersection of the speed-acceleration pairs. The acceleration bins were constructed as follows: the midpoints were selected to be -4.0, -3.5, -3.0, ..., -0.5, 0.0, 0.5, ..., 3.0, 3.5, 4.0 mph/sec. The ranges were selected to be [(midpoint - 0.25); (midpoint + 0.25)[ for acceleration and ](midpoint-0.25); (midpoint + 0.25)] for deceleration. Speed values were varied at increment of 1.0 mph from 30.0 mph to 80.0 mph. This methodology was based on the resolution of the measured speed values. Figures 5.2.1 to 5.2.4 show the plots of the bin-average CO and HCs exhaust emission concentrations versus speed and acceleration independent of each other for the combined fleet. The same plots were developed for the two vehicle types and are presented in Appendix C. Both bin-average CO and HCs exhaust emission concentrations exhibit high variabilities at both ends of the speed and



acceleration ranges; that are high acceleration and deceleration, and high and low speeds. Within the common driving mode ranges of the Borman Expressway, i.e., speeds within 45.0 to 70.0 mph and accelerations within -2.0 and 2.0 mph/sec, the bin-average CO and HC exhaust emission concentrations are nearly linear.

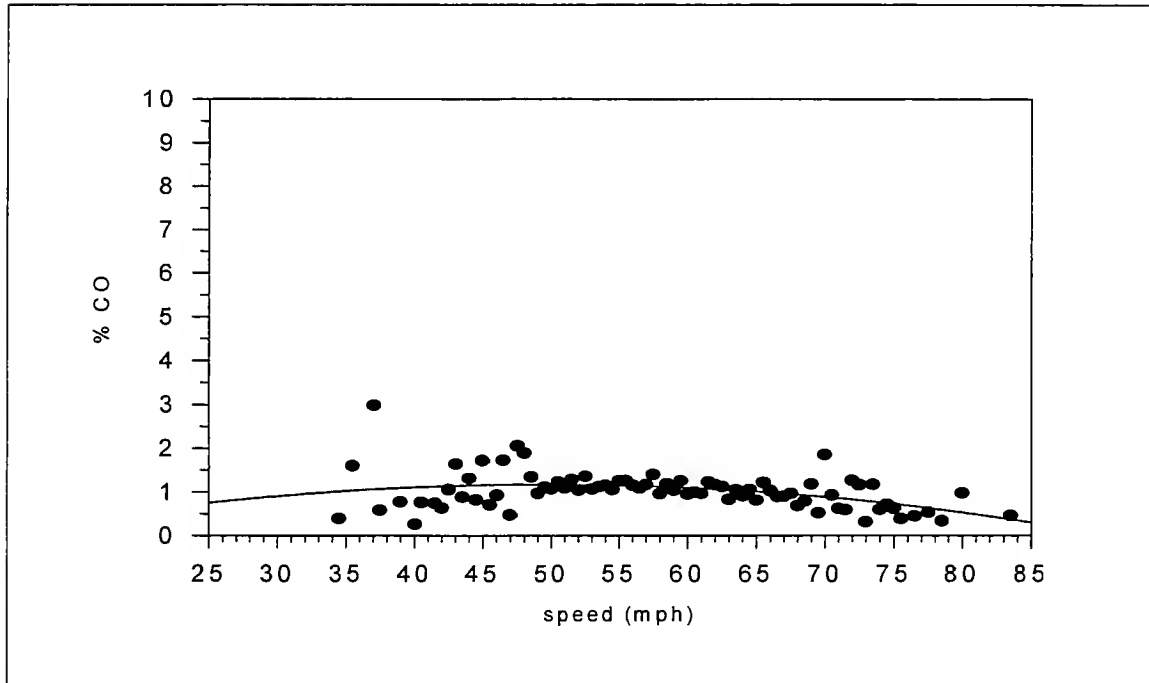


Figure 5.2.1. Bin-average CO exhaust emission concentration versus speed midpoints.

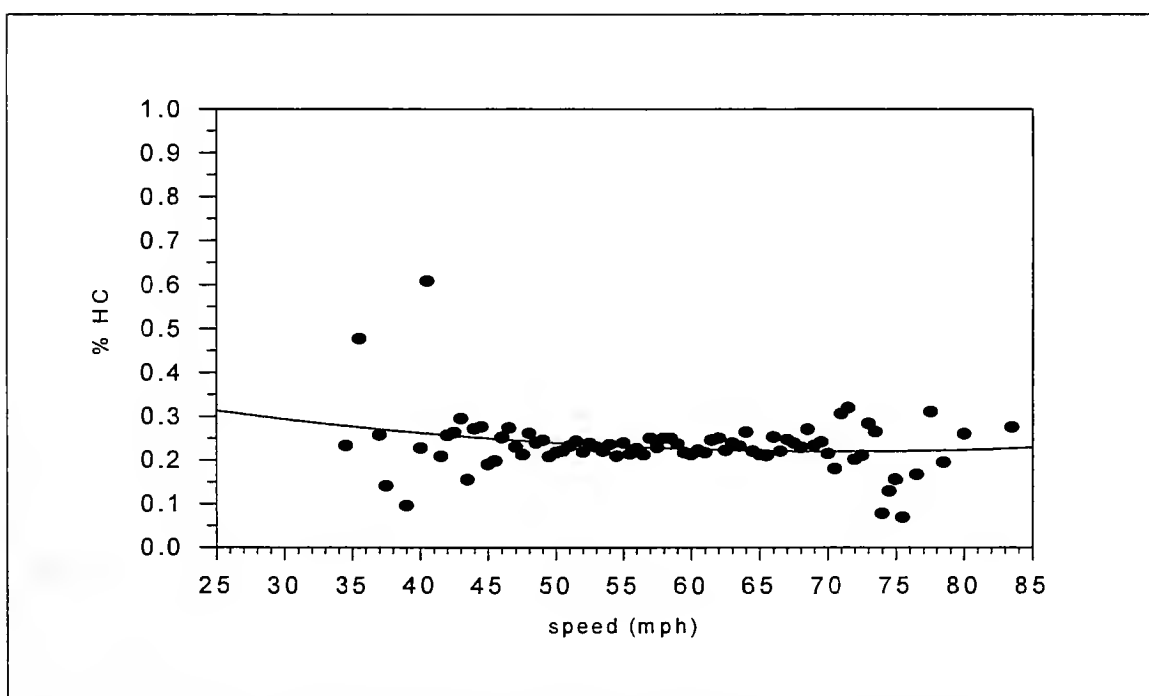


Figure 5.2.2. Bin-average HCs exhaust emission concentration versus speed midpoints.



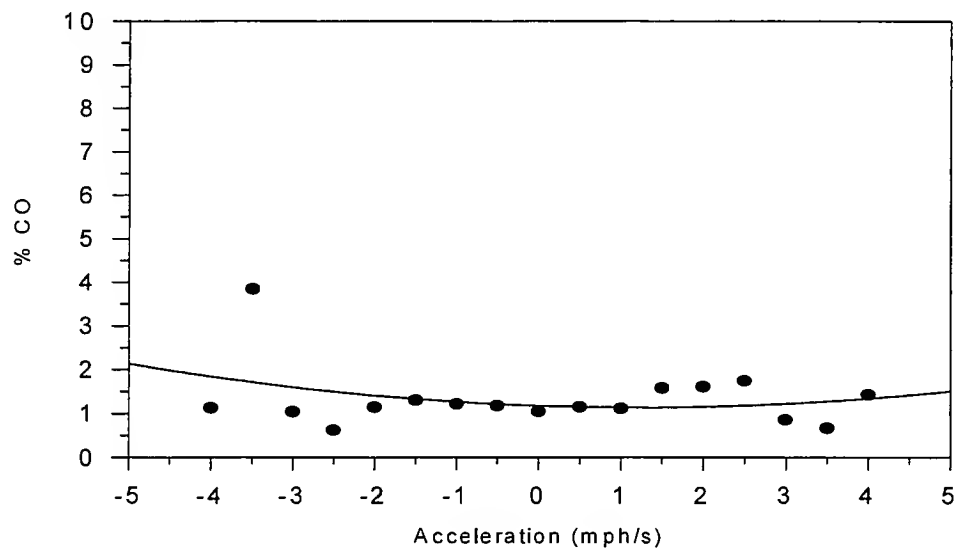


Figure 5.2.3. Bin-average CO exhaust emission concentration versus acceleration midpoints.

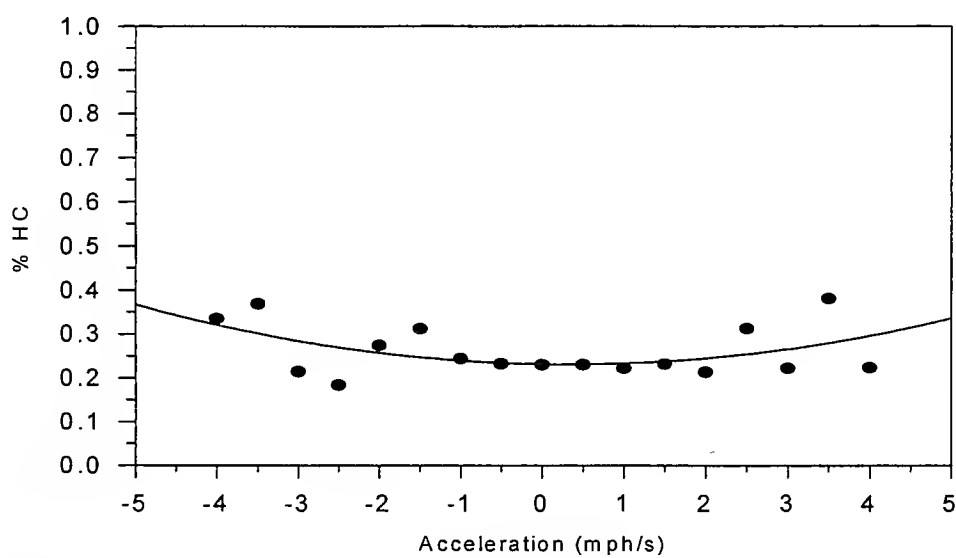


Figure 5.2.4. Bin-average HCs exhaust emission concentration versus acceleration midpoints.



Second order polynomials were fit to the data as shown in the Figures. Because of the high variabilities at both ends of the speed and acceleration spectra, the coefficients of correlation were very low ranging from 20 to 40%. This suggests that neither speed nor acceleration alone may explain all the variations of the bin-average CO and HCs exhaust emission concentrations. However, in real-time monitoring, only these two variables may be assessed. Consequently, the two variables should be used together when analyzing the bin-average CO and HCs exhaust emission concentrations.

Using the acceleration and speed bins developed, the average CO and HCs exhaust emission concentrations were calculated at each speed-acceleration value pairs (or modes). This defined a speed-acceleration matrix for mode-average CO and HCs exhaust emission concentrations (Figure 5.2.5). Figures 5.2.6 and 5.2.7 show the three-dimensional plots of the mode-average CO and HCs exhaust emission concentrations against speed and acceleration midpoints. The surfaces were also derived from interpolated meshes using the inverse distance method. The three-dimensional plots of the two different vehicle types are presented in Appendix C. As it can be seen, the surfaces are neither uniform nor smooth indicating that the mode-average CO and HCs exhaust emission concentrations are also variable and clustered.

|             |    | ACCELERATION (MPH/S) |      |      |     |      |     |      |     |      |      |      |
|-------------|----|----------------------|------|------|-----|------|-----|------|-----|------|------|------|
|             |    | -4.0                 | -3.5 | -3.0 | ... | -0.5 | 0.0 | +0.5 | ... | +3.0 | +3.5 | +4.0 |
| SPEED (MPH) | 30 |                      |      |      |     |      |     |      |     |      |      |      |
|             | 31 |                      |      |      |     |      |     |      |     |      |      |      |
|             | 32 |                      |      |      |     |      |     |      |     |      |      |      |
|             | -- |                      |      |      |     |      |     |      |     |      |      |      |
|             | 55 |                      |      |      |     |      | Eij |      |     |      |      |      |
|             | -- |                      |      |      |     |      |     |      |     |      |      |      |
|             | 80 |                      |      |      |     |      |     |      |     |      |      |      |
|             | -- |                      |      |      |     |      |     |      |     |      |      |      |
|             | 85 |                      |      |      |     |      |     |      |     |      |      |      |

Figure 5.2.5. Speed-acceleration matrix for Eij (Eij = mode-average exhaust emission concentration at speed i and acceleration j).



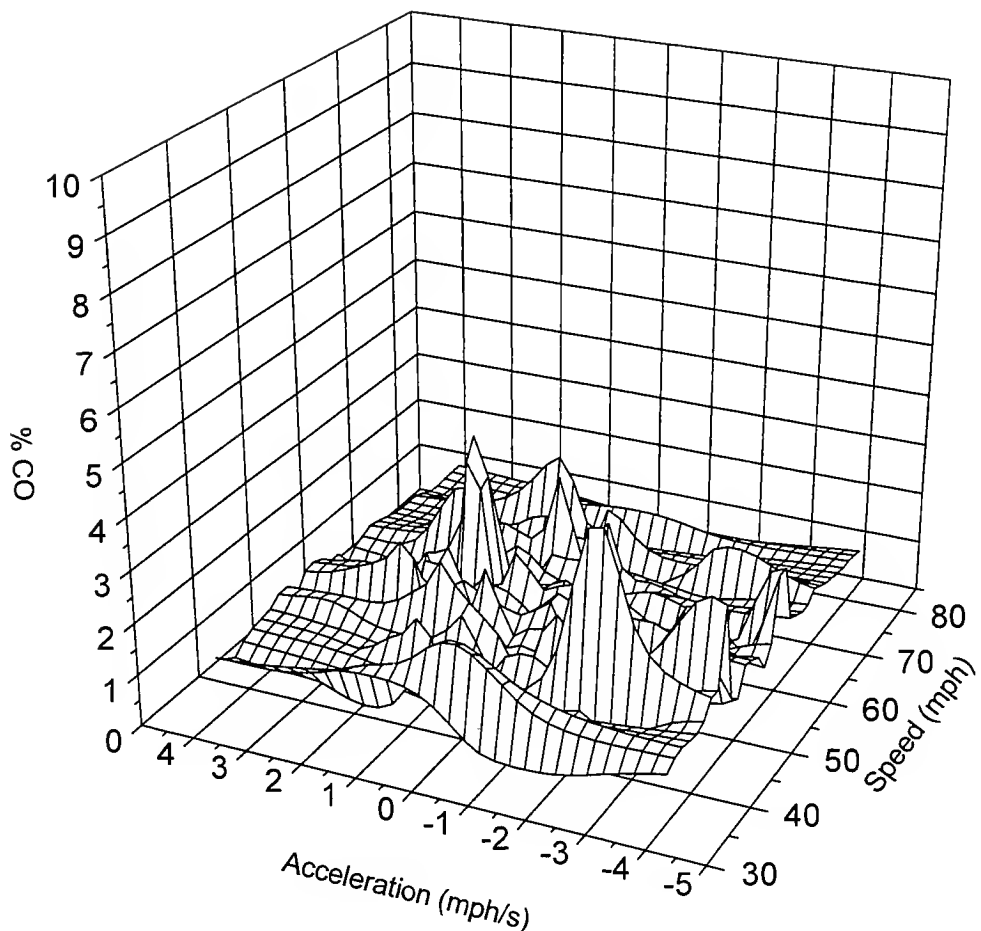


Figure 5.2.6. Three-dimensional plot of the mode-average exhaust CO emission concentration versus speed and acceleration midpoints for the combined fleet.



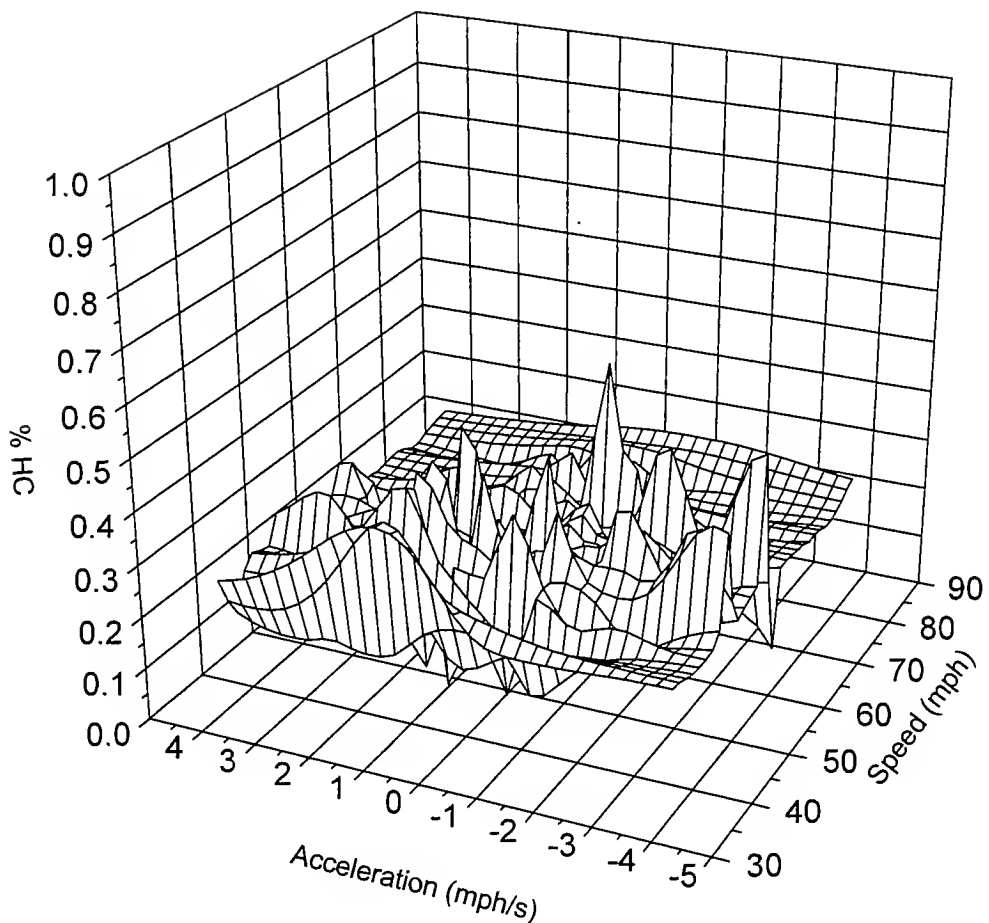


Figure 5.2.7. Three-dimensional plot of the mode-average exhaust HCs emission concentration versus speed and acceleration midpoints for the combined fleet.

Using a non-linear multivariate regressive approach, the mode-average CO and HCs exhaust emission concentrations variations with speed and acceleration midpoints could be smoothed out for estimation purposes. Based on the variations of Figures 5.2.1 to 5.2.4, a second order multiple regression on both speed and acceleration was used. The interactions between speed and acceleration were also included. The Marquardt-Levenberg algorithm was used to find the coefficients (parameters) of the independent variables (speed and acceleration) that give the best fit between the equation and the data. This algorithm seeks the values of the parameters that minimize the sum of the squared



differences between the values of the observed and predicted values of the dependent variable. This process is iterative. It begins with a guess at the parameters, checks to see how well the equation fits, then continues to make better guesses until the differences between the residual sum of squares no longer decreases significantly or converges. The following predictive equation for the mode-average CO and HC exhaust emission concentrations was determined based on this method.

$$\begin{aligned} E = C_0 + C_1 * ((S-55.0)/30.0) + C_2 * ((S-55.0)/30.0)^2 \\ + C_3 * (A/4.0) + C_4 * (A/4.0)^2 + C_5 * ((S-55.0)/30.0) * (A/4.0) \end{aligned} \quad (1)$$

where  $C_0, C_1, C_2, C_3, C_4$ , and  $C_5$  are the regression coefficients.  $E$  represents the mode-average CO and HC exhaust emission concentrations in %,  $S$  the speed in mph, and  $A$  the acceleration in mph/sec. Tables 5.2.1 and 5.2.2 show the values of the regression coefficients and that of the multiple coefficient of determination for the mode-average CO and HC exhaust emission concentrations for the different vehicle classes.

The multiple coefficient of determination is defined as

$$R^2 = \text{sum}[(O-P)^2] / \text{sum}[(O-\text{avg}(O))^2] \quad (2)$$

$O$  and  $P$  are the observed and predicted mode-average CO or HC exhaust emission concentrations. The very high values of the multiple coefficient of determination implies that the model fits very well the data and that at least 96% of the variation in the mode-average CO and HC exhaust emission concentrations are attributable to speed and acceleration.

| Parameters | Vehicle types |         |         |
|------------|---------------|---------|---------|
|            | Type I        | Type II | All     |
| $C_0$      | 1.2490        | 1.3240  | 1.1780  |
| $C_1$      | -0.2855       | 0.0908  | -0.2403 |
| $C_2$      | -0.6823       | -1.0890 | -0.6993 |
| $C_3$      | 0.0013        | 0.1417  | 0.0225  |
| $C_4$      | 0.2185        | -0.2069 | 0.4413  |
| $C_5$      | 1.0440        | -0.0418 | 0.4337  |
| $R^2$      | 0.9792        | 0.9934  | 0.9682  |

Table 5.2.1. Regression parameters for the mode-average CO exhaust emission concentration against speed and acceleration.



| Parameters     | Vehicle types |         |         |
|----------------|---------------|---------|---------|
|                | Type I        | Type II | All     |
| C0             | 0.2324        | 0.2471  | 0.2367  |
| C1             | -0.0231       | -0.0385 | -0.0261 |
| C2             | 0.0080        | -0.0494 | -0.0068 |
| C3             | -0.0274       | -0.0396 | -0.0278 |
| C4             | 0.0373        | 0.0233  | 0.0292  |
| C5             | 0.0539        | -0.0375 | -0.0330 |
| R <sup>2</sup> | 0.9905        | 0.9799  | 0.9841  |

Table 5.2.1. Regression parameters for the mode-average HCs exhaust emission concentration against speed and acceleration.

Figures 5.2.8 and 5.2.9 show the three-dimensional plots of the application of the mathematical relationships for the combined fleet. Those for the two different vehicle types are included in Appendix C. These surfaces were also derived from interpolated meshes using the inverse distance method. As it can be seen, the mode-average CO and HCs exhaust emission concentrations are highest at hard accelerations and decelerations and flatten off at mild accelerations. This finding is in agreement with the theories of the formation of CO and HCs exhaust emissions described in the Introduction section (Turns, 1996). It can also be seen that the CO surfaces are smoother than the HCs surfaces.



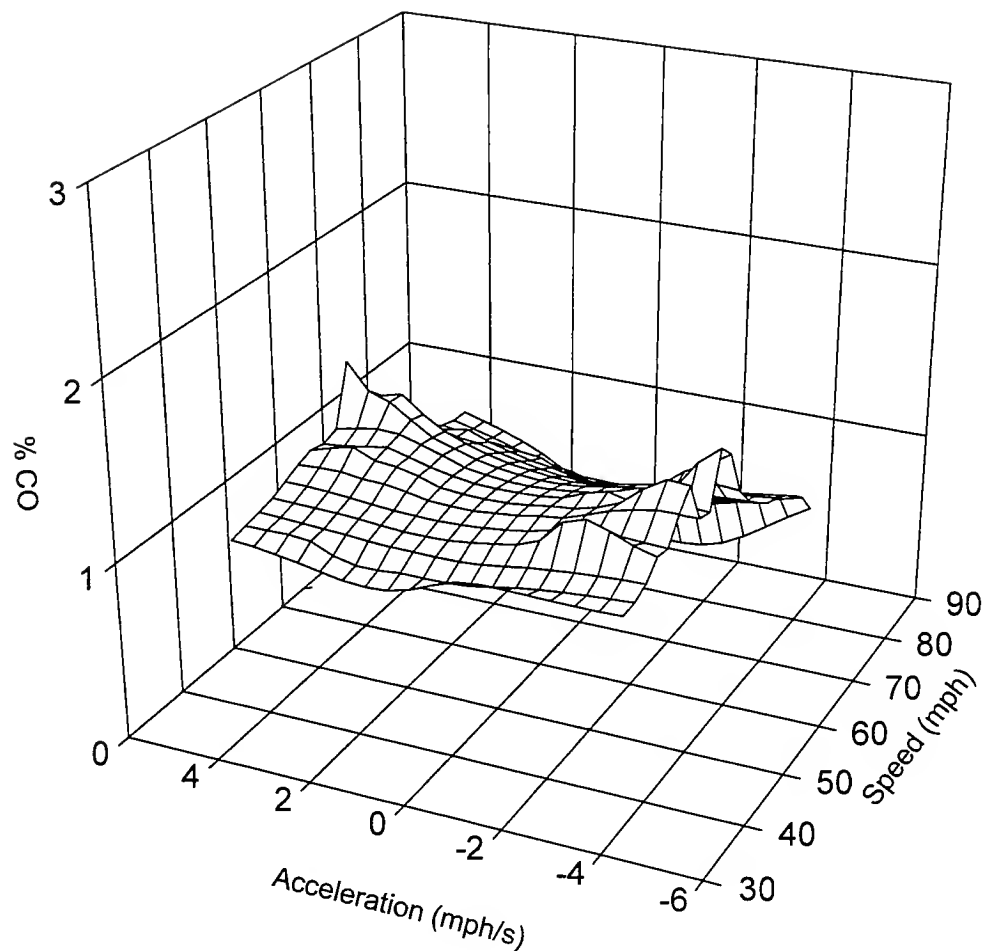


Figure 5.2.8. Three-dimensional plot of the mode-average CO exhaust emission concentration obtained from the mathematical relationship for the combined fleet.



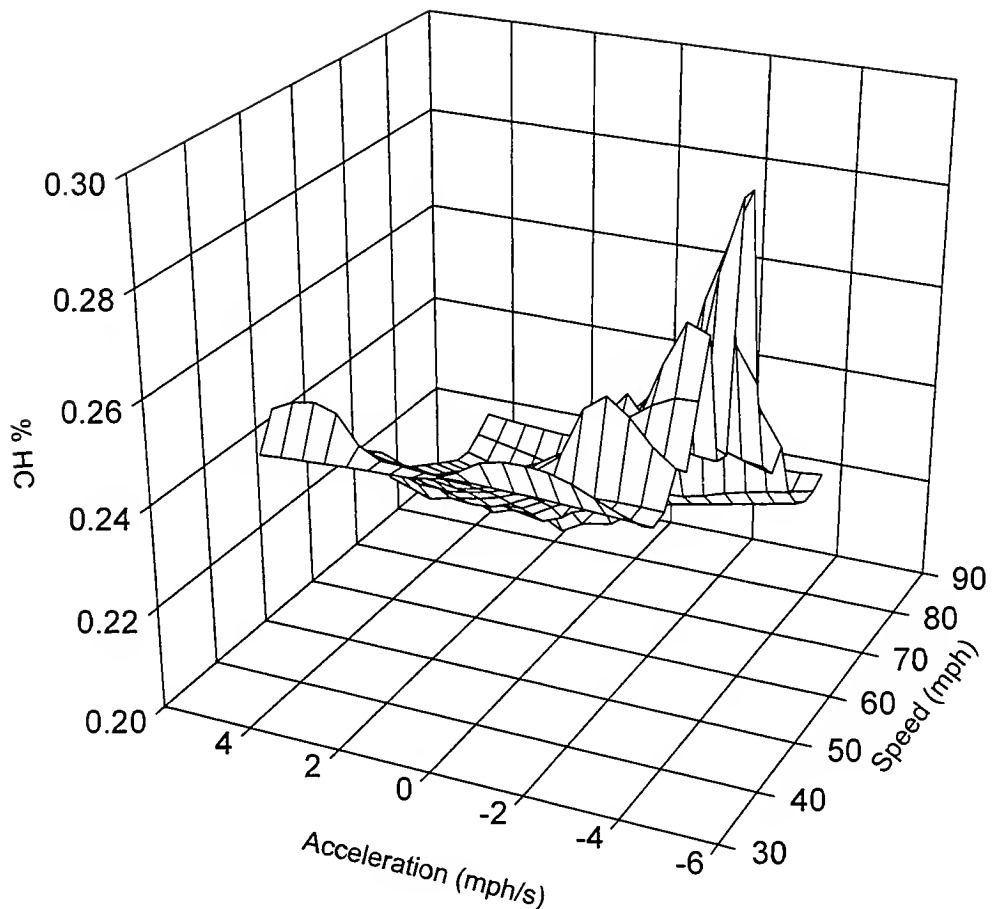


Figure 5.2.9. Three-dimensional plot of the mode-average HCs exhaust emission concentration obtained from the mathematical relationship for the combined fleet.

### 5.2.3. Limitations and Extrapolations of PVEM-BEA

The mathematical relationships built from the multivariate regression approach may not be applied outside the ranges of the supporting experimental data that are speeds between 30.0 mph and 80.0 mph and accelerations between -4.0 mph/sec and 4.0 mph/sec. Since the model is primarily intended to be used at construction zones, extrapolation of the estimation method is necessary in order to include lower speed values. The extrapolation method used in this study depends solely on acceleration since it represents the critical and limiting variable as far as real-time estimation of exhaust



emission concentrations is concerned. Therefore, for speed values outside the experimental data range, the model will switch to an acceleration alone mode. Thus the best fit of the mode-average CO and HCs exhaust emission concentrations against acceleration alone (Figures 5.2.3 and 5.2.4) given in Equation 2 will be used for the estimations

$$E = C_0 + C_1 * (A/4.0) + C_2 * (A/4.0)^2 \quad (3)$$

Tables 5.2.3 and 5.2.4 summarize the parameters of Equation 3.

| Parameters     | Vehicle types |         |         |
|----------------|---------------|---------|---------|
|                | Type I        | Type II | All     |
| C <sub>0</sub> | 1.1890        | 1.173   | 1.0830  |
| C <sub>1</sub> | -0.3745       | -0.2512 | -0.2112 |
| C <sub>2</sub> | 0.5304        | 0.4121  | 0.2590  |

Table 5.2.2. Regression parameters for the mode-average CO exhaust emission concentration against acceleration alone.

| Parameters     | Vehicle types |         |         |
|----------------|---------------|---------|---------|
|                | Type I        | Type II | All     |
| C <sub>0</sub> | 0.2357        | 0.2293  | 0.2315  |
| C <sub>1</sub> | -0.0243       | 0.0020  | -0.0124 |
| C <sub>2</sub> | 0.0703        | 0.1026  | 0.0766  |

Table 5.2.3. Regression parameters for the mode-average HCs exhaust emission concentration against acceleration alone.

#### 5.2.4. Design of Concentration thresholds for decision-making

For individual vehicles, the design of the CO and HCs concentration thresholds was based on the statistical characteristics of the regression analysis of the triple correlation between exhaust emission concentrations, speeds, and accelerations. The instantaneous values of the mode-average CO and HCs exhaust emission concentration thresholds were set to the upper limits of the 99% confidence intervals of the regression means. Thus, for individual type I vehicles, the exhaust emission concentration thresholds were 1.24 % CO and 0.24 % HCs. For individual type II vehicles, they were



1.26 % CO and 0.25 % HCs. For the combined fleet they were 1.25 % CO and 0.24 % HCs.

For classes of vehicles modeled within the maximum averaging time, the design method was different. Here, the measured 99<sup>th</sup> percentile of CO and HCs exhaust emission concentrations were multiplied by the measured vehicle flow rates. This product was called the concentration threshold limit (CTL) and expressed in %/sec. The product of the estimated class-average CO and HCs exhaust emission concentrations by the flow rate and the total number of traffic lanes are compared to the CTLs in the model to arrive at a decision about concentration levels within the maximum averaging time. For type I vehicles, the CTLs were 1.16 %/sec CO and 0.11 %/sec HCs. For type II vehicles, they were 0.68 %/sec CO and 0.06 %/sec HCs. For the combined fleet they were 1.86 %/sec CO and 0.17 %/sec HCs.

### **5.2.5. Computer Algorithm of PVEM-BEA**

The current version of PVEM-BEA is written in FORTRAN for the PC computing environment. It requires a FORTRAN compiler such as the Microsoft FORTRAN Visual Workbench™ for its execution. It can be run as a stand-alone program or as integrated in the Borman Expressway Traffic Management Center (TMC). It also requires input from Advanced Traffic Monitoring systems such as the Autoscope™ or two consecutive pre-installed conventional inductive loops. Figure 5.2.10 shows a top down flow chart of PVEM-BEA execution algorithm. Figure 5.2.11 shows a sample output of PVEM-BEA obtained from a hypothetical simulation input. The main program makes a sequential call of ten different subroutines whose operations are described below.

**INCLUDE:** this not a subroutine but a call to an included file that initializes all the constant parameters including the regression parameters and CO and HCs emission concentration thresholds.

**SUBROUTINES:**

**OPENER:** Opens all the input and output files.

**READER1:** Inputs the simulation location name, the number of traffic lanes, and the distance between loops or consecutive speed measurement points.



WRITER1: Outputs the model description, and the variables read by READER1.

READER2: Inputs real-time traffic parameters including speeds, and vehicle type.

Calculates traffic volumes and flow rates by vehicle class within the maximum time interval.

CALCACCEL: Calculates average speed and acceleration of each passing vehicle within the time interval of speed-readings, and average speed and acceleration by vehicle type within the maximum time interval.

CALCEMISSION: Calculates the mode-average CO and HCs exhaust emission concentration for each passing vehicle as well as for classes of vehicles within the maximum time interval. Compares instantaneous emission concentrations for each vehicle to threshold values. Calculates the product of flow rates and average emission concentration per vehicle type for decision-making purposes.

DECMAKER: Makes decision about average CO and HCs exhaust emission concentrations by comparing the product of flow rates and average concentration per vehicle type to designed threshold levels of the same product.

WRITER2: Outputs all the relevant information concerning calculated traffic parameters, exhaust emission concentration, decision made within the maximum time interval for each vehicle as well as for each class of vehicles.

RESETER: Loops through the program for the next simulation time or calls an end to the program if the simulation is over.

CLOSER: Closes all the input and output files when the simulation ends.



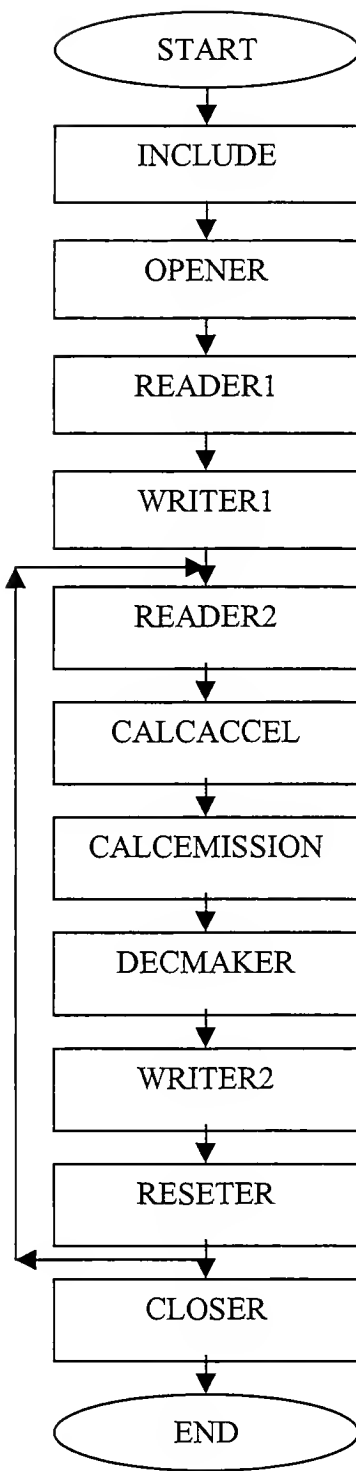


Figure 5.2.10. Top-down flow chart of the PVEM-BEA subroutines.



\*\*\*\*\*
\* Purdue Real-Time Vehicle Exhaust Emission Modal Model V 1.0 (PVEM1.0)
\* Developed by Dr. Ouattara Fatogoma, Civil Engineering, Purdue University. All Rights Reserved.
\*\*\*\*\*

## NOTES

=====
CO and HCs instantaneous exhaust  
emission concentration thresholds(%)

| VT | CO     | HCs   |
|----|--------|-------|
| 1  | 1.3300 | .3300 |
| 2  | 1.3500 | .3300 |
| 3  | .0000  | .0000 |
| 4  | 1.3400 | .3300 |

Designed CO and HCs threshold limit values  
by vehicle type(%/sec)

| VT | CO     | HCs   |
|----|--------|-------|
| 1  | 1.2500 | .2000 |
| 2  | .7700  | .1500 |
| 3  | .0000  | .0000 |
| 4  | 1.9500 | .2600 |

Notes: bt = below threshold, at = above threshold

1=type 1 vehicles (LDV), 2=type 2 vehicles (MDV), 3=type 3 vehicles (HDV), 4=Combined 1&2

PCFNL=product concentration, flow rate, number of lanes

Modeling location: Borman Expressway Mileage 100

Number of lanes: 3

Distance between 2 speed detection points (ft): 100.00

=====
Run#: 000001

## SIMULATION DATA

| Date<br>(mmddyy) | Time<br>(hhmmss) | Vt | Spd<br>(mph) | Acc<br>(mph/s) | CO<br>(%) | COfg | HC<br>(%) | HCfg |
|------------------|------------------|----|--------------|----------------|-----------|------|-----------|------|
| 020998           | 120000           | 3  | 50.00        | .00            | .0000     | bt   | .0000     | bt   |
| 020998           | 120000           | 2  | 57.50        | -1.50          | 1.2431    | bt   | .2628     | bt   |
| 020998           | 120000           | 1  | 57.50        | -4.00          | 1.3507    | at   | .2907     | bt   |

## SUMMARY DATA

|  | Type_1 | Type_2 | Type_3 | CF_1&2 |
|--|--------|--------|--------|--------|
| Number of vehicles:                        | 1      | 1      | 1      | 2      |
| Vehicle Flow rate(#veh/sec/lane):          | .08    | .08    | .08    | .17    |
| Average speed(mph):                        | 57.50  | 57.50  | 50.00  | 57.50  |
| Average acceleration(mph/sec):             | -4.00  | -1.50  | .00    | -2.75  |
| Average CO emission concentration(%):      | 1.3507 | 1.2431 | .0000  | 1.2969 |
| Average HC emission concentration(%):      | .2907  | .2628  | .0000  | .2768  |
| Number of vehicles exceeding CO threshold: | 1      | 1      | 0      | 0      |
| Number of vehicles exceeding HC threshold: | 1      | 1      | 0      | 0      |
| CO PCFNL(%/sec):                           | .3377  | .3108  | .0000  | .6484  |
| HCs PCFNL(%/sec):                          | .0727  | .0657  | .0000  | .1384  |
| CO PCFNL flag:                             | bt     | bt     | bt     | bt     |
| HCs PCFNL flag:                            | bt     | bt     | bt     | bt     |

Figure 5.2.11. Sample output of PVEM-BEA for single simulation



## 6. IMPLEMENTATION SUGGESTIONS

The PVEM-BEA Model is used to estimate the exhaust emission concentrations of CO and HCs in real-time traffic flow. The only inputs required of the model are two consecutive speed-readings for a single vehicle and the vehicle type identification. The output from the model is the input traffic parameters, the emissions concentrations with decision making threshold trigger, and the time-average data for each class of vehicle.

With these requirements in mind, the model can be implemented in a variety of ways. It can be used prior to a project to assess the possible CO and HCs impacts of a construction project lane closure, during a project to confirm the impact and to monitor the situation, or after the fact as an emissions inventory or airshed impact tool. Data from current Advanced Traffic Management System (ATMS) can be transmitted to a central station where they can be processed, or the data can be collected in-situ and processed real-time via a laptop computer.

The ATMS currently under development on the Borman Expressway can seamlessly integrate the PVEM-BEA model into the network. Any data that is collected and stored as a database of specified format can be read into the model to produce an emissions concentration estimate. It may also be possible to read the data into the model real-time once the system is up and running.

In the field, the Hoosier Helper vehicles equipped with a video camera on a vertically telescoping mount can be implemented in conjunction with an Autoscope™ system made by Image Sensing Systems Incorporated. The method of detection used by this system requires no permanent detector installation and no disruption of traffic or the roadway. This allows the system to be highly mobile and be transported to the site of concern for quick and easy determination of traffic parameters. Since construction zones are of main concern, this mobility is of critical importance.

With the Autoscope™ system, a video image is analyzed up to 30 times per second and is capable of determining vehicle speed, count, and type. The Autoscope™ unit shown in Figure 6.1, detects vehicle presence by monitoring the video image at a specified location on the roadway. These locations are essentially sensors on the roadway defined by the interface computer. The video image of the roadway is displayed on the



interface computer screen and boxes are drawn with the mouse to identify regions where the image is to be analyzed and then identified for the type of analysis to be

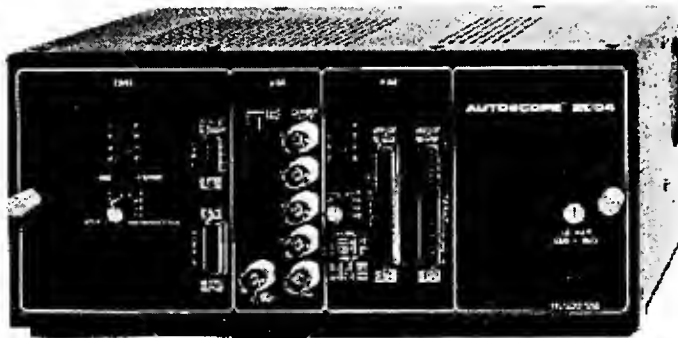


Figure 6.1. The Autoscope™ Video Detection Processor Unit.

conducted (see Figure 6.2). Changes in the image attributes at these specified locations are used to identify and measure the vehicle type, count, and speed. The detector regions will indicate a detected vehicle visually on the computer screen by changing color during setup to assure proper operation (see Figure 6.2).

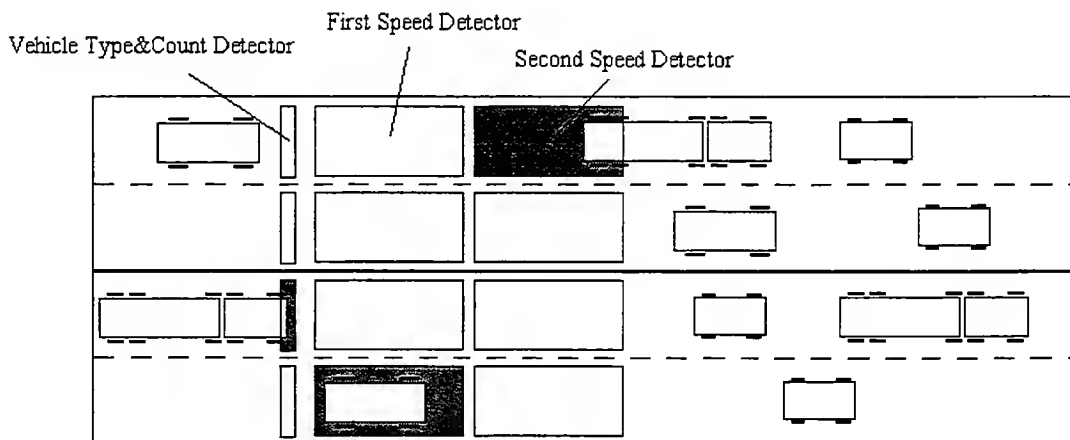


Figure 6.2. Schematic of Video Detection.

Data can be collected for multiple lanes on either an instantaneous or a time-averaged basis. The instantaneous data can be read directly into the model for instantaneous vehicle emissions determination. The interval data is a time average



dataset and can be generated for time intervals of 10, 20, and 30sec, or 1, 5, 10, 15, 30, and 60 minutes. In all cases, the acceleration parameter will be calculated within the PVEM-BEA model from multiple speed-readings of the same vehicle. This in-situ method of data collection can give a real-time evaluation of the effects of both local ATMS efforts and any traffic obstruction such as an incident or a construction zone.

The PVEM-BEA model can be a valuable planning tool as well. Prior to the beginning of a construction project, vehicle data can be gathered and modified to represent the event of a lane closure. Once modified, the dataset can be input into the model to estimate the emissions impact of the lane closure or speed reduction. In this way, multiple scenarios can be analyzed and decisions made to minimize the actual impact of the traffic pattern change.



## 7. CONCLUSION

The Midac FTIR air monitoring system was used to measure real-time on-road vehicular CO and HCs exhaust emission concentrations in spring and summer 1997. Concurrently, two vehicle speed-readings were acquired from the passing vehicles in the vicinity of the spectrometer using a hand-held laser gun. The speed data were integrated to calculate average vehicle speed and acceleration at the spectrometer. Furthermore, an 8-mm camcorder was set up to videotape the passing vehicles. These video imageries were reduced in order to classify the passing vehicles. Meteorology data were also acquired from the nearest surface meteorological stations.

Overall, 16,870 vehicles were monitored. 8,478 were type I vehicles (automobiles), 4,829 were type II (medium-duty vehicles), and 3,563 were type III (heavy-duty vehicles). The flow rates of the vehicles in count/min, were 8.92 for type I vehicles, 5.08 for type II, 3.75 for type III, and 17.75 for the combined fleet. 4,413 vehicles were retained for data analysis after reduction. 2,848 were type I vehicles, and 1,565 were type II. Type III vehicles were not included in the analysis because their CO and HCs exhaust emission concentrations were not measured due to the fact that their sampling points were in a different plane. The analysis of the retained data showed that the instantaneous CO and HCs exhaust emission concentrations were very variable and their distributions severely skewed. For example, the average, median, standard deviation, minimum, and maximum CO exhaust emission concentrations for the combined fleet were 1.12 %, 0.64%, 1.61 %, 0.01 %, and 19.69 % respectively. Those of HCs exhaust emission concentration for the combined fleet were 0.23 %, 0.20 %, 0.17 %, 0.00%, and 1.40 % respectively. The mean vehicle speed and acceleration were 56.56 mph and 0.17 mph/sec respectively for the combined fleet. Setting high emitters concentration cut-points to 4.0 % CO and 0.2 % CO, it was found that 5.7% and 49.2% of the combined vehicle fleet were CO and HCs high emitters respectively.

The PVEMP database was then used to develop a modal CO and HCs exhaust emission concentration model. The underlying theory used a multivariate regressive approach applied to the speed-acceleration matrices of the modal-average CO and HCs exhaust emission concentrations to determine the three-dimensional mathematical



relationships between mode-average CO and HCs exhaust emission concentrations and speed and acceleration midpoints. The regressions were found to fit the data very well. For example, the multiple coefficient of determination was equal to 0.9792 for the combined fleet, 0.9934 for type I vehicles, and 0.9682 for type II vehicles. Based on the mathematical relationships, the real-time CO and HCs exhaust emission concentration model (PVEM-BEA) was developed in FORTRAN for the PC computing environment. It may be executed as an integrated program to the Borman Expressway Traffic Management Center or as a stand-alone mobile program. It requires real-time input parameters (speeds, vehicle class, and road geometry) from advanced traffic monitoring systems such as the Autoscope<sup>TM</sup>. It can also get its inputs from two consecutive pre-installed conventional loops as long as means to assess real-time vehicle types exist.

The implementation of the research is the integration of the real-time modal model to the Borman Expressway ATMS. It represents a tool to estimate real-time vehicular exhaust emission concentration, especially in construction work zones.



## REFERENCES

- Barth, M.J., J.M. Norbeck, and M. Ross, *Development of a Comprehensive Modal Emissions Model*, TRB Conference, Washington, DC, 1998.
- Caddle, S.H. and R.D. Stephens, *Remote Sensing of Vehicle Exhaust Emissions*, ES&T, V 28, 1994.
- EPA, FTIR Guidance Document, 1992.
- Image Sensing Systems Word Wide Web Home Page.
- INDOT Word Wide Web Home Page.
- Jack, M.D., *Remote and On-Board Instrumentation for Automotive Emissions Monitoring*, Transaction SAE, V 104, 1995.
- Midac Corporation Word Wide Web Home Page.
- Seinfeld, J.H., *Atmospheric Chemistry and Physics of Air Pollution*, John Wiley & Son, New York, NY, 1986.
- St-Denis, M. and A.M. Winer, *Prediction of On-Road Emissions and Comparison of Modeled On-Road Emissions to Federal Test Procedure*. A&WMA the Emission Inventory: Perception and Reality, Pasadena, CA, 1993.
- Stedman, D.H., J.E. Peterson, P.L. Guenther, I.F. Mcvey, and S.P. Beaton, *On-Road Carbon Monoxide and Hydrocarbon Remote Sensing in the Chicago Area*, Final Report, ILENR/RE-AQ-40, 1991.
- Stephens R.D., *Remote Sensing Data and a Potential Model of Vehicle Exhaust Emissions*, J. Air & Waste Manage. Assoc. V 44, 1994.
- Turns, S.R., *An Introduction to Combustion. Concepts and Applications*, McGraw-Hill, Inc., New York, NY, 1996.



## **APPENDICES**



## APPENDIX A

### A Portion of the Integrated PVEMP Database



| Date    | Time     | CO (%)    | HC (%)     | VT | VS (mph) | VA (mph/s) | T (oF) | Td (oF) | WS (mph) | WD(o) | RH(%) | Sky |
|---------|----------|-----------|------------|----|----------|------------|--------|---------|----------|-------|-------|-----|
| 5/19/97 | 13:16:21 | 1.2427110 | 0.3569540  | 1  | 54.0     | -1.0       | 57     | 49      | 10       | 320   | 74    | OVC |
| 5/19/97 | 13:16:22 | 2.0345000 | 0.3265460  | 1  | 54.0     | -1.0       | 57     | 49      | 10       | 320   | 74    | OVC |
| 5/19/97 | 13:16:24 | 7.2548070 | 0.1647530  | 1  | 54.0     | -1.0       | 57     | 49      | 10       | 320   | 74    | OVC |
| 5/19/97 | 13:16:26 | 0.1753420 | 0.2539020  | 2  | 54.0     | -1.0       | 57     | 49      | 10       | 320   | 74    | OVC |
| 5/19/97 | 13:16:27 | 0.5815650 | 0.1694290  | 2  | 54.0     | -1.0       | 57     | 49      | 10       | 320   | 74    | OVC |
| 5/19/97 | 13:16:29 | 0.3967560 | 0.3135310  | 2  | 52.0     | 0.0        | 57     | 49      | 10       | 320   | 74    | OVC |
| 5/19/97 | 13:16:31 | 0.8495580 | 0.1339370  | 2  | 52.0     | 0.0        | 57     | 49      | 10       | 320   | 74    | OVC |
| 5/19/97 | 13:16:32 | 0.3557870 | 0.2803900  | 2  | 52.0     | 0.0        | 57     | 49      | 10       | 320   | 74    | OVC |
| 5/19/97 | 13:16:34 | 0.8481560 | 0.0900560  | 2  | 52.0     | 0.0        | 57     | 49      | 10       | 320   | 74    | OVC |
| 5/19/97 | 13:16:40 | 0.7519070 | 0.2359130  | 1  | 68.5     | 1.0        | 57     | 49      | 10       | 320   | 74    | OVC |
| 5/19/97 | 13:16:41 | 1.2931750 | 0.2773640  | 1  | 68.5     | 1.0        | 57     | 49      | 10       | 320   | 74    | OVC |
| 5/19/97 | 13:16:42 | 0.8187710 | 0.1650900  | 1  | 68.5     | 1.0        | 57     | 49      | 10       | 320   | 74    | OVC |
| 5/19/97 | 13:16:45 | 0.8199290 | 0.8478700  | 1  | 68.5     | 1.0        | 57     | 49      | 10       | 320   | 74    | OVC |
| 5/19/97 | 13:16:47 | 1.7030590 | 0.3411360  | 1  | 68.5     | 1.0        | 57     | 49      | 10       | 320   | 74    | OVC |
| 5/19/97 | 13:16:50 | 1.1370830 | 0.3452310  | 1  | 70.0     | 0.0        | 57     | 49      | 10       | 320   | 74    | OVC |
| 5/19/97 | 13:17:42 | 1.7942660 | 0.3581360  | 2  | 59.0     | 0.7        | 57     | 49      | 10       | 320   | 74    | OVC |
| 5/19/97 | 13:17:44 | 1.7330280 | 0.1251040  | 2  | 59.0     | 0.7        | 57     | 49      | 10       | 320   | 74    | OVC |
| 5/19/97 | 13:17:47 | 1.6214710 | 0.1480710  | 2  | 59.0     | 0.7        | 57     | 49      | 10       | 320   | 74    | OVC |
| 5/19/97 | 13:17:49 | 1.0422930 | 0.07151330 | 2  | 59.0     | 0.7        | 57     | 49      | 10       | 320   | 74    | OVC |
| 5/19/97 | 13:18:15 | 1.8830890 | 0.4906280  | 2  | 53.5     | 0.5        | 57     | 49      | 10       | 320   | 74    | OVC |
| 5/19/97 | 13:18:17 | 1.2674650 | 0.1457750  | 2  | 53.5     | 0.5        | 57     | 49      | 10       | 320   | 74    | OVC |
| 5/19/97 | 13:18:20 | 0.2471490 | 0.3226260  | 2  | 53.5     | 0.5        | 57     | 49      | 10       | 320   | 74    | OVC |
| 5/19/97 | 13:18:22 | 0.4372230 | 0.2813480  | 1  | 62.5     | -3.0       | 57     | 49      | 10       | 320   | 74    | OVC |
| 5/19/97 | 13:18:25 | 0.4825810 | 0.0931810  | 2  | 62.5     | -3.0       | 57     | 49      | 10       | 320   | 74    | OVC |
| 5/19/97 | 13:18:27 | 0.1477660 | 0.1263550  | 2  | 62.5     | -3.0       | 57     | 49      | 10       | 320   | 74    | OVC |
| 5/19/97 | 13:18:30 | 1.2499790 | 0.3361590  | 1  | 59.5     | -0.5       | 57     | 49      | 10       | 320   | 74    | OVC |
| 5/19/97 | 13:18:33 | 0.9853400 | 0.1554820  | 1  | 59.5     | -0.5       | 57     | 49      | 10       | 320   | 74    | OVC |
| 5/19/97 | 13:18:37 | 0.3703550 | 0.2991990  | 2  | 59.5     | -0.5       | 57     | 49      | 10       | 320   | 74    | OVC |
| 5/19/97 | 13:18:38 | 1.1111520 | 0.1784550  | 2  | 59.5     | -0.5       | 57     | 49      | 10       | 320   | 74    | OVC |
| 5/19/97 | 13:18:57 | 0.8096620 | 0.2065390  | 1  | 56.0     | 0.0        | 57     | 49      | 10       | 320   | 74    | OVC |
| 5/19/97 | 13:19:00 | 0.3539590 | 0.5757670  | 1  | 56.0     | 0.0        | 57     | 49      | 10       | 320   | 74    | OVC |
| 5/19/97 | 13:19:05 | 7.9410810 | 0.1779940  | 1  | 56.0     | 0.0        | 57     | 49      | 10       | 320   | 74    | OVC |
| 5/19/97 | 13:19:05 | 1.0354450 | 0.2422850  | 1  | 56.0     | 0.0        | 57     | 49      | 10       | 320   | 74    | OVC |
| 5/19/97 | 13:19:11 | 1.0902230 | 0.2324970  | 1  | 50.0     | 0.0        | 57     | 49      | 10       | 320   | 74    | OVC |
| 5/19/97 | 13:19:16 | 1.3545480 | 0.2105060  | 1  | 50.0     | 0.0        | 57     | 49      | 10       | 320   | 74    | OVC |
| 5/19/97 | 13:19:16 | 1.3356420 | 0.1609930  | 1  | 50.0     | 0.0        | 57     | 49      | 10       | 320   | 74    | OVC |
| 5/19/97 | 13:19:20 | 1.5676080 | 0.2397820  | 1  | 50.0     | 0.0        | 57     | 49      | 10       | 320   | 74    | OVC |
| 5/19/97 | 13:19:49 | 1.0888730 | 0.2114300  | 1  | 80.0     | 0.0        | 57     | 49      | 10       | 320   | 74    | OVC |
| 5/19/97 | 13:19:52 | 0.8509020 | 0.3076100  | 1  | 80.0     | 0.0        | 57     | 49      | 10       | 320   | 74    | OVC |
| 5/19/97 | 13:19:57 | 0.6348100 | 0.1260900  | 1  | 63.5     | -0.5       | 57     | 49      | 10       | 320   | 74    | OVC |
| 5/19/97 | 13:19:58 | 0.2442420 | 0.2431580  | 1  | 63.5     | -0.5       | 57     | 49      | 10       | 320   | 74    | OVC |
| 5/19/97 | 13:20:07 | 0.7756060 | 0.1819080  | 1  | 60.5     | 0.5        | 57     | 49      | 10       | 320   | 74    | OVC |
| 5/19/97 | 13:20:10 | 0.7616880 | 0.2965870  | 2  | 60.5     | 0.5        | 57     | 49      | 10       | 320   | 74    | OVC |
| 5/19/97 | 13:20:13 | 1.3108910 | 0.1931510  | 2  | 61.0     | 0.0        | 57     | 49      | 10       | 320   | 74    | OVC |
| 5/19/97 | 13:20:17 | 0.1730580 | 0.2536170  | 2  | 61.0     | 0.0        | 57     | 49      | 10       | 320   | 74    | OVC |
| 5/19/97 | 13:20:31 | 0.4773770 | 0.1448860  | 1  | 57.0     | 1.0        | 57     | 49      | 10       | 320   | 74    | OVC |
| 5/19/97 | 13:20:32 | 1.0582980 | 0.2251370  | 1  | 57.0     | 1.0        | 57     | 49      | 10       | 320   | 74    | OVC |
| 5/19/97 | 13:20:38 | 1.3212230 | 0.1023880  | 2  | 57.0     | 1.0        | 57     | 49      | 10       | 320   | 74    | OVC |
| 5/19/97 | 13:20:39 | 1.6152110 | 0.2113900  | 2  | 57.0     | 1.0        | 57     | 49      | 10       | 320   | 74    | OVC |

Figure A.1. A portion of the integrated PVEMP database.



## APPENDIX B

Graphical Representations for Data Pertaining to the Two Vehicle Types



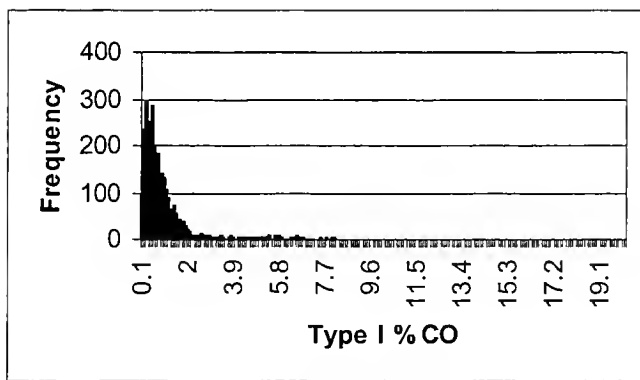


Figure B1.1.1. Histogram of the CO exhaust emission concentration distribution for type I vehicles.

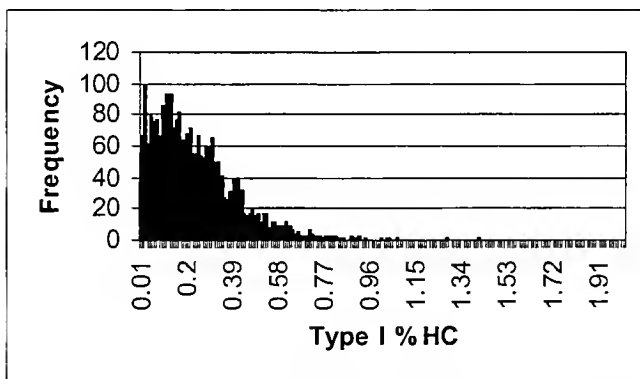


Figure B1.1.2. Histogram of the HCs exhaust emission concentration distribution for type I vehicles.

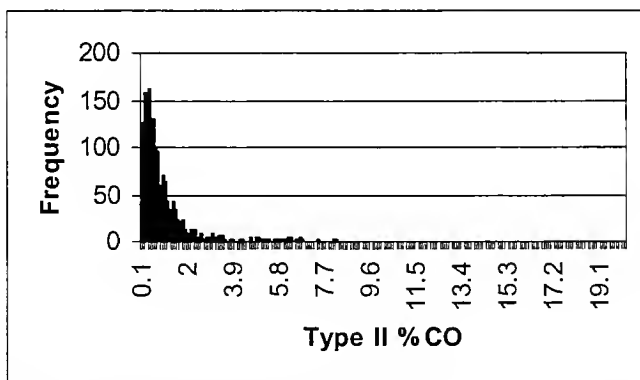


Figure B1.2.1. Histogram of the CO exhaust emission concentration distribution for type II vehicles.



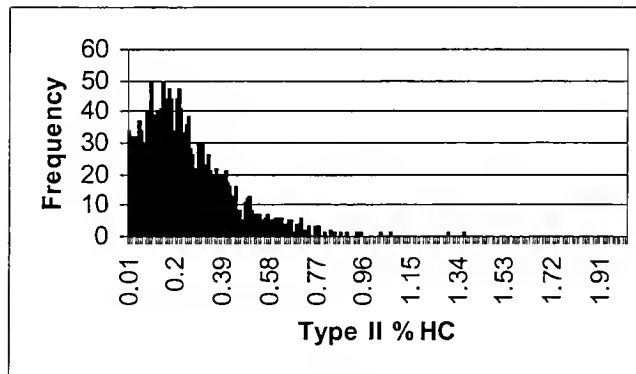


Figure B1.2.2. Histogram of the HCs exhaust emission concentration distribution for type II vehicles.

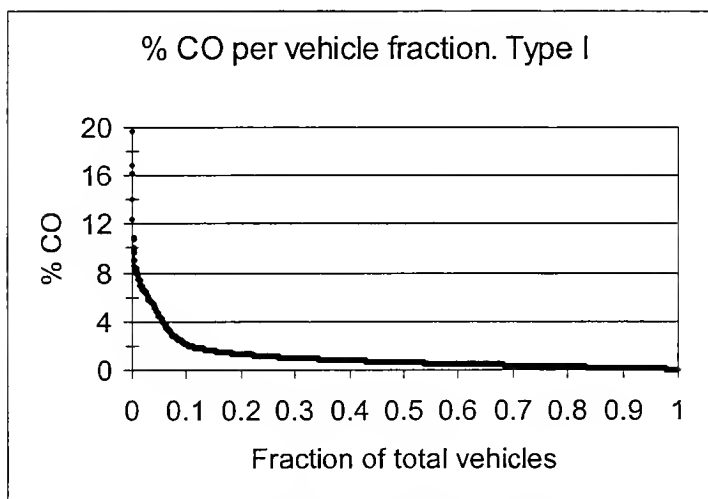


Figure B2.1.1. Logarithmic distribution of CO exhaust emission concentration for type I vehicles.

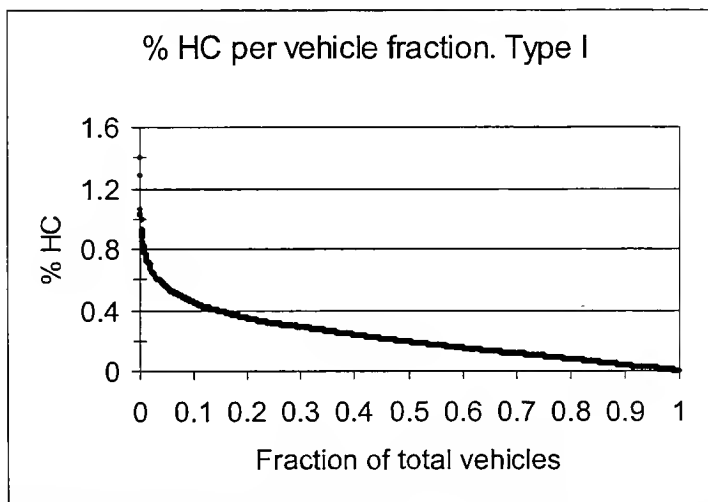


Figure B2.1.2. Logarithmic distribution of HCs exhaust emission concentration for type I vehicles.



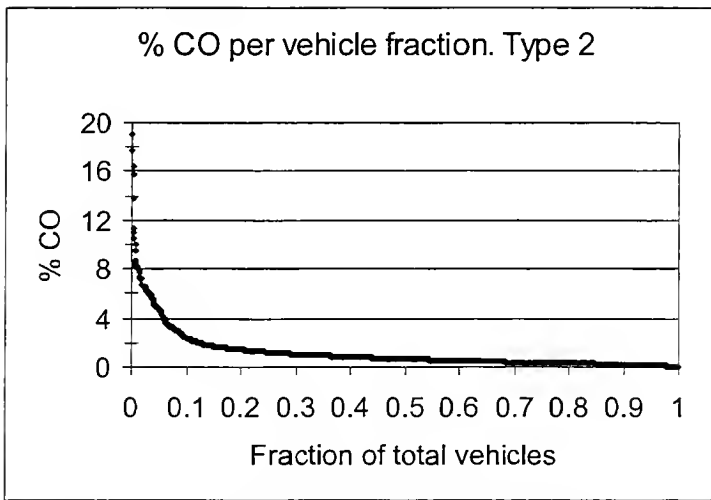


Figure B2.2.1. Logarithmic distribution of CO exhaust emission concentration for type II vehicles.

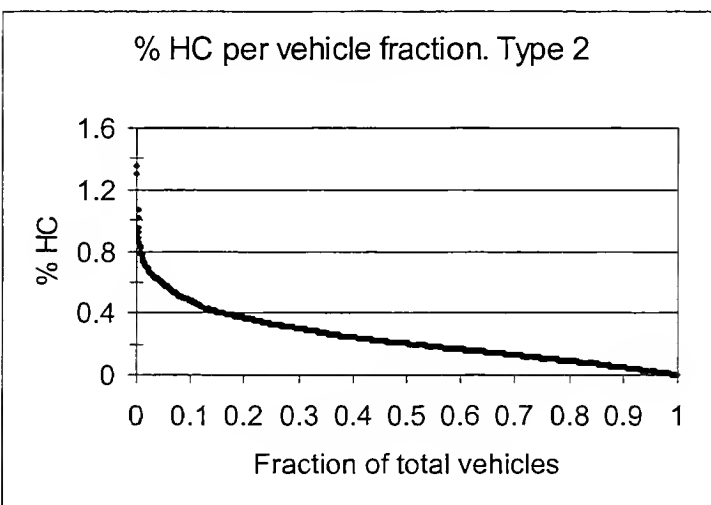


Figure B2.2.2. Logarithmic distribution of HCs exhaust emission concentration for type II vehicles.



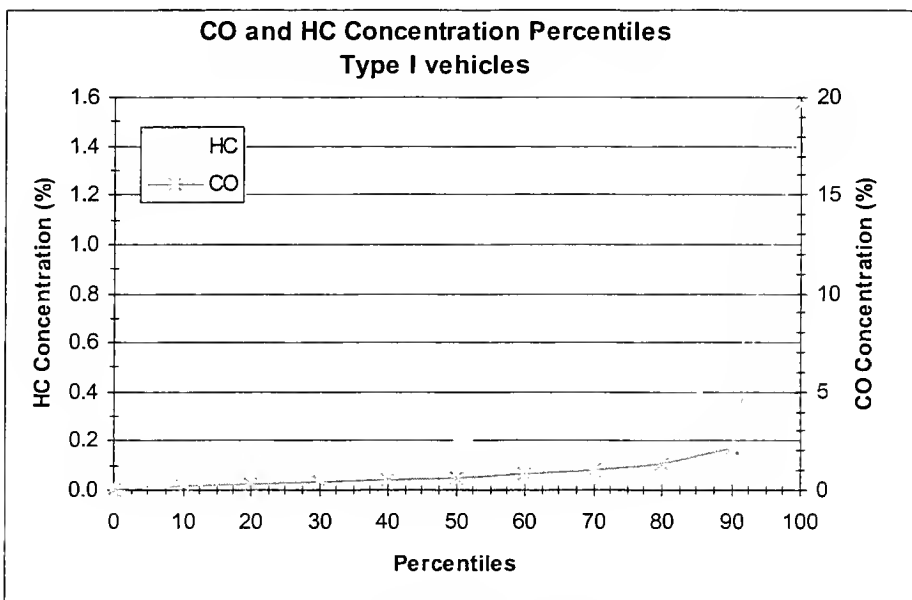


Figure B3.1. CO and HCs exhaust emission concentration percentiles for type I vehicles.

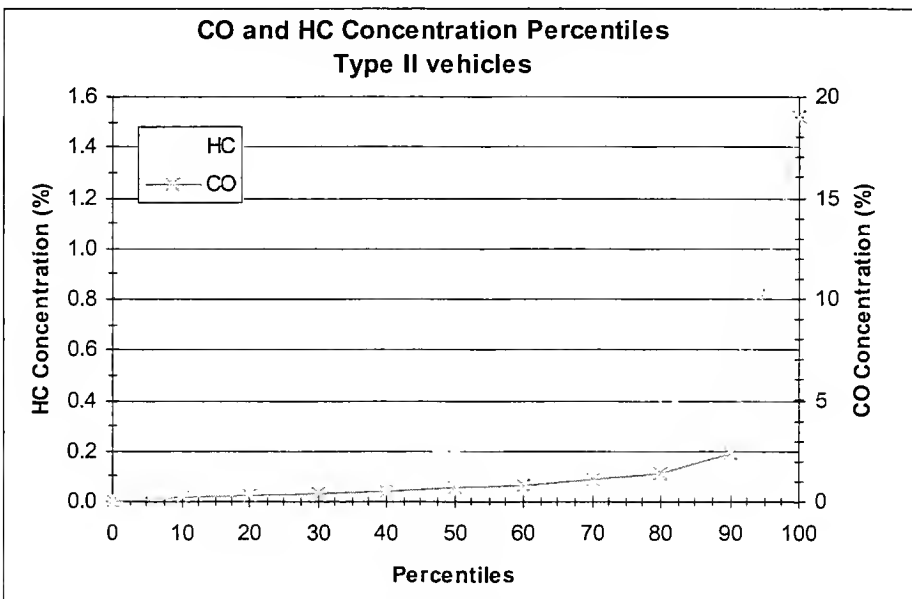


Figure B3.2. CO and HCs exhaust emission concentration percentiles for type II vehicles.



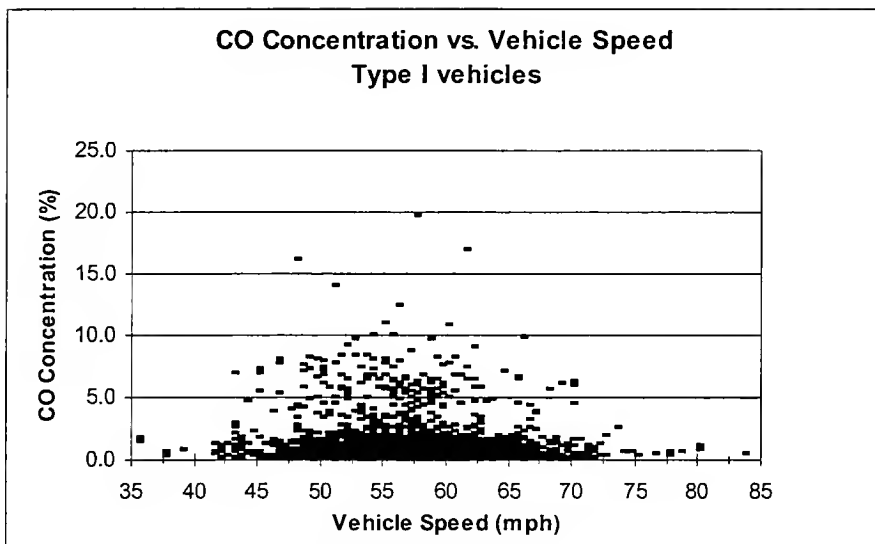


Figure B4.1.1. Variation of instantaneous CO exhaust emission concentrations with vehicle speed for type I vehicles.

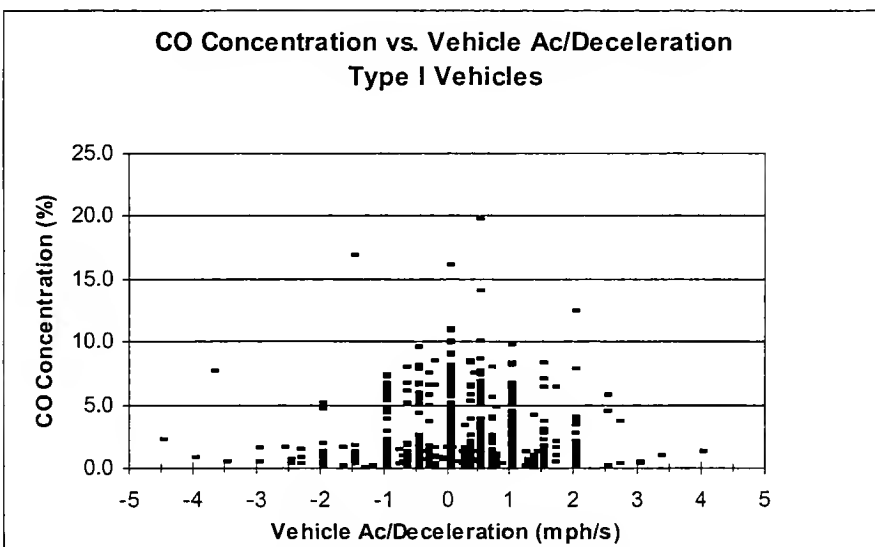


Figure B4.1.2. Variation of instantaneous CO exhaust emission concentrations with vehicle acceleration for type I vehicles.



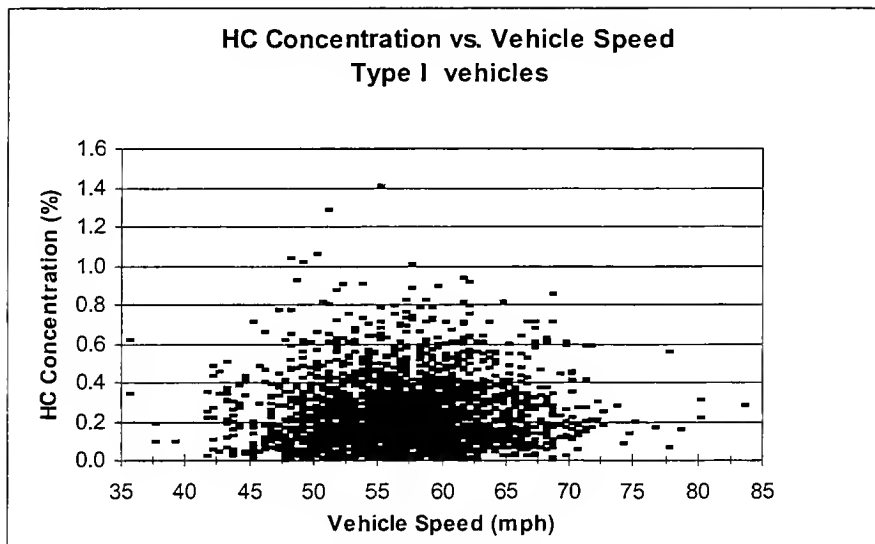


Figure B4.1.3. Variation of instantaneous HCs exhaust emission concentrations with vehicle speed for type I vehicles.

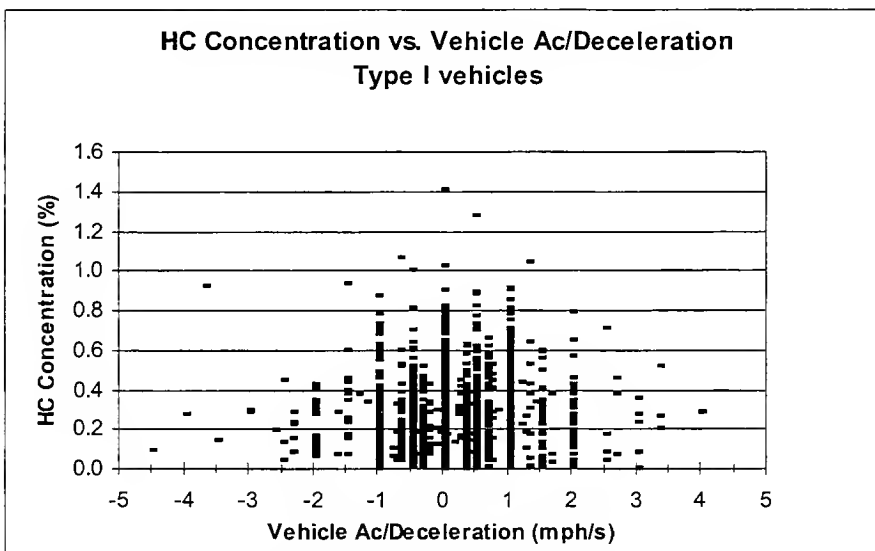


Figure B4.1.4. Variation of instantaneous HCs exhaust emission concentrations with vehicle acceleration for type I vehicles.



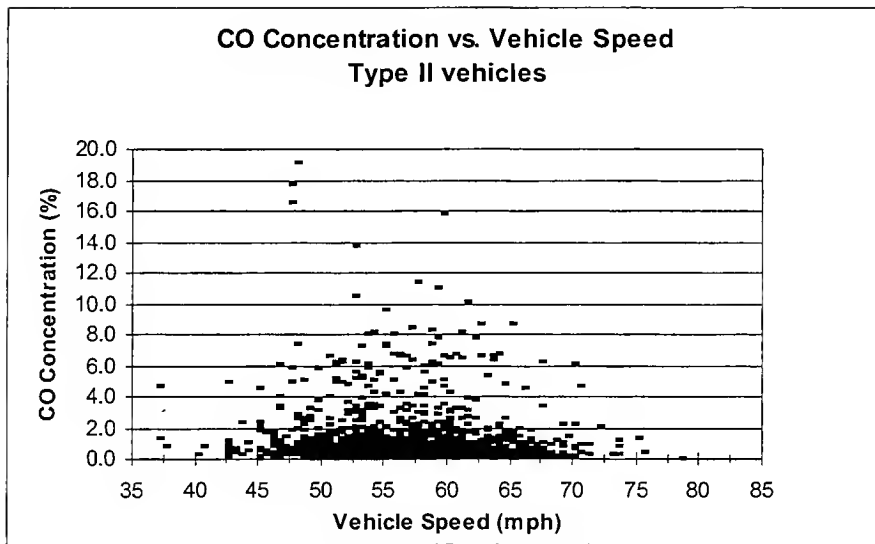


Figure B4.2.1. Variation of instantaneous CO exhaust emission concentrations with vehicle speed for type II vehicles.

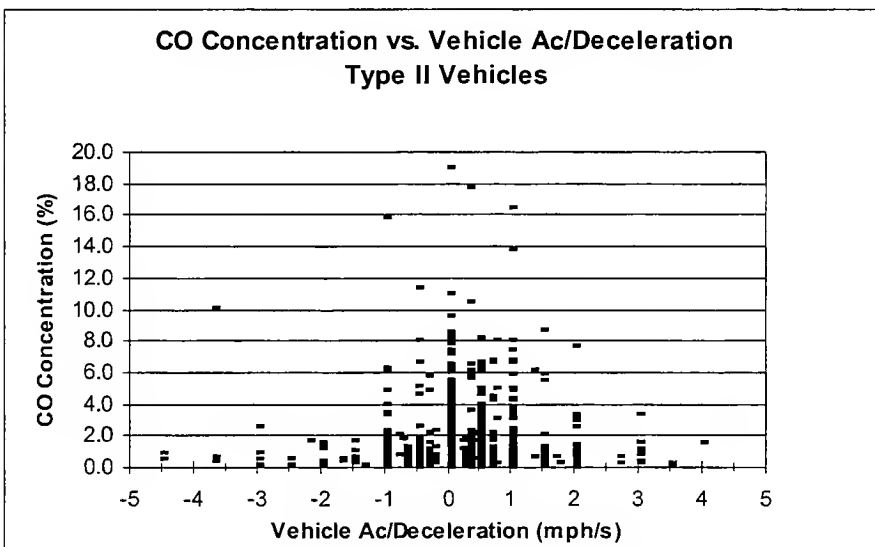


Figure B4.2.2. Variation of instantaneous CO exhaust emission concentrations with vehicle acceleration for type II vehicles.



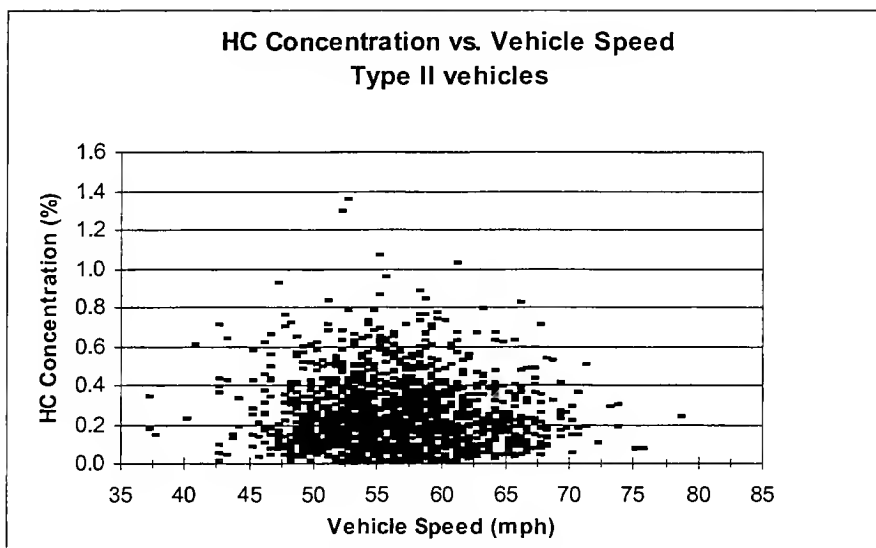


Figure B4.2.3. Variation of instantaneous HCs exhaust emission concentrations with vehicle speed for type II vehicles.

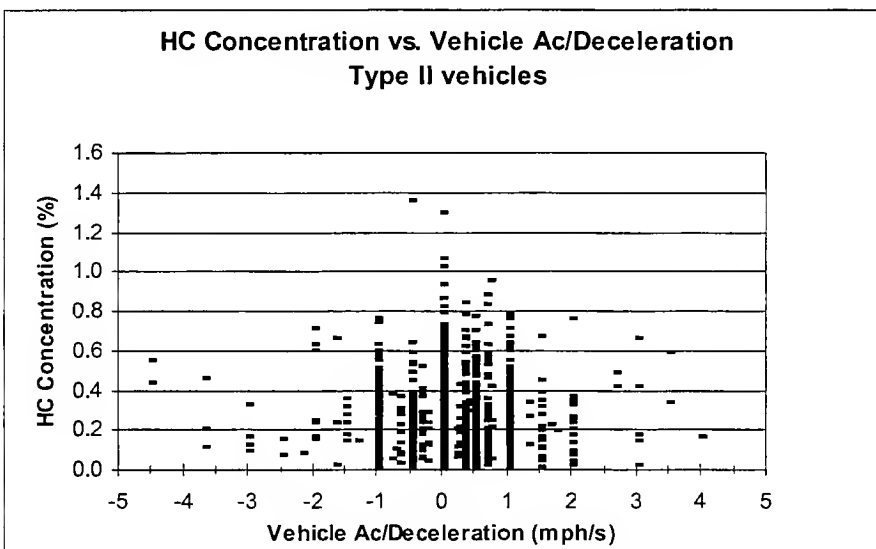


Figure B4.2.4. Variation of instantaneous HCs exhaust emission concentrations with vehicle acceleration for type II vehicles.



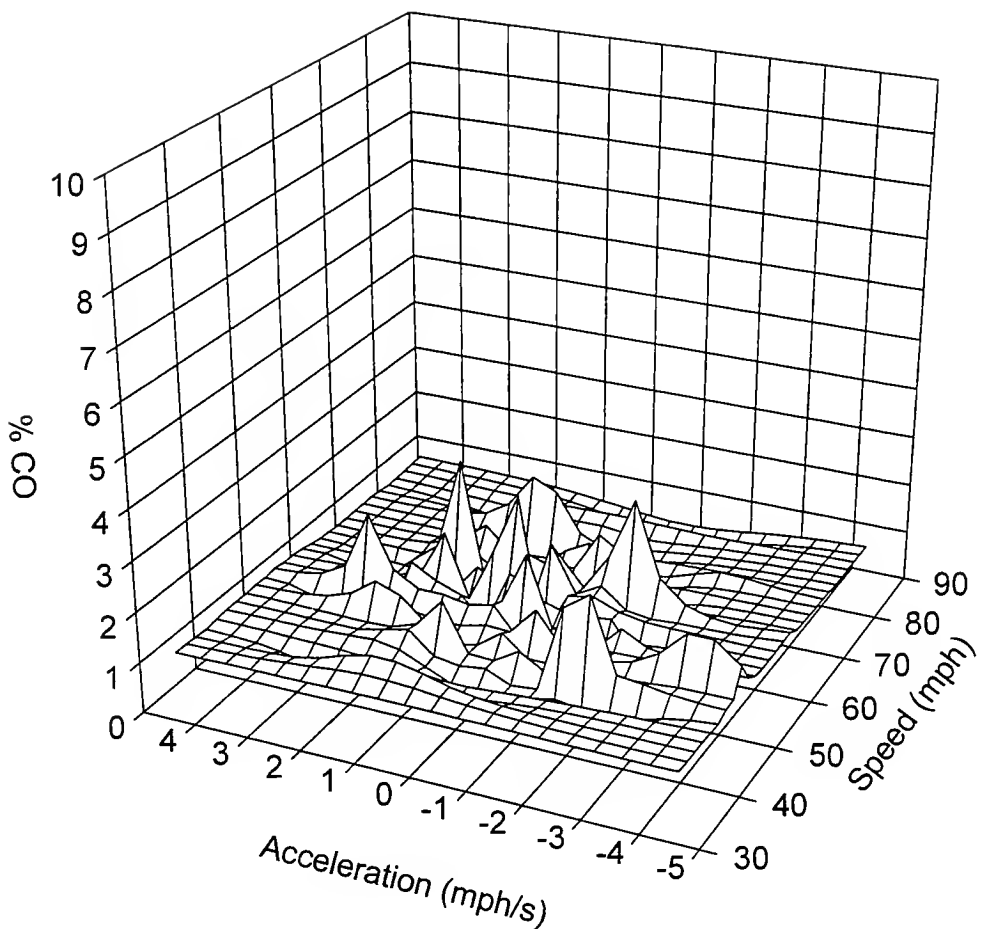


Figure B5.1.1. Three-dimensional plot for the triple correlation of CO emission concentration, speed, and acceleration for type I vehicles.



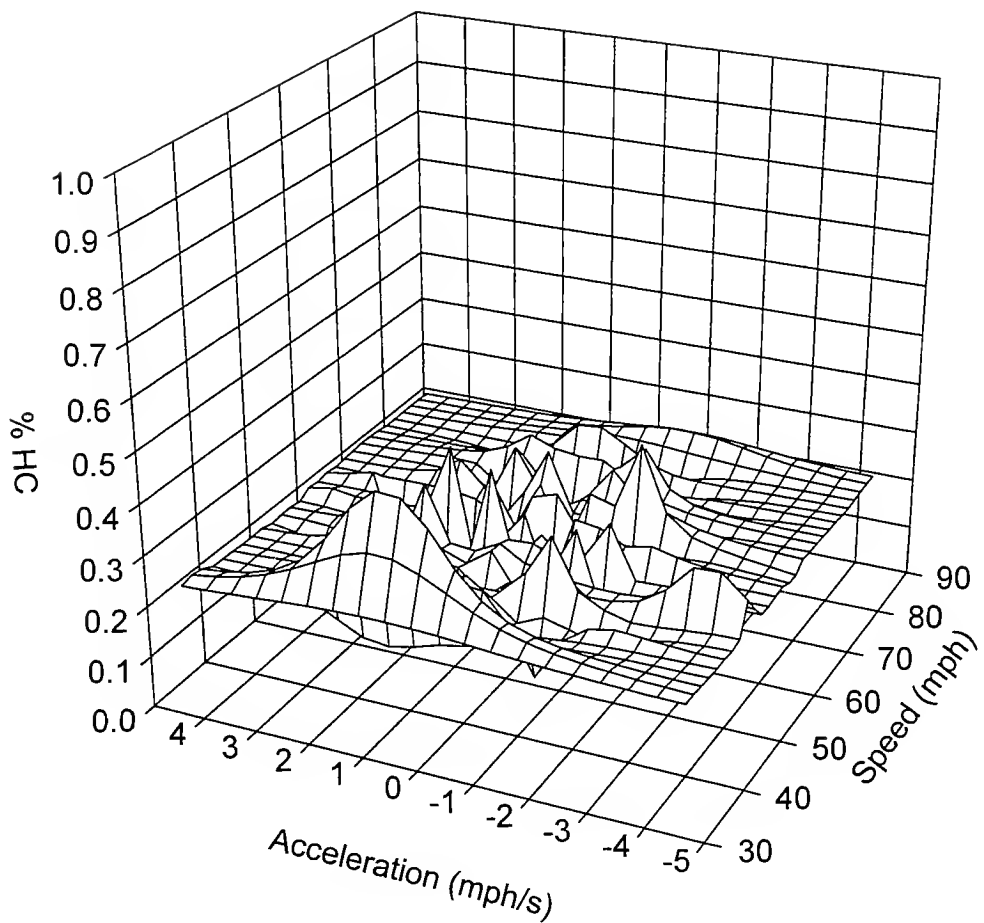


Figure B5.1.2. Three-dimensional plot for the triple correlation of HCs emission concentration, speed, and acceleration for type I vehicles.



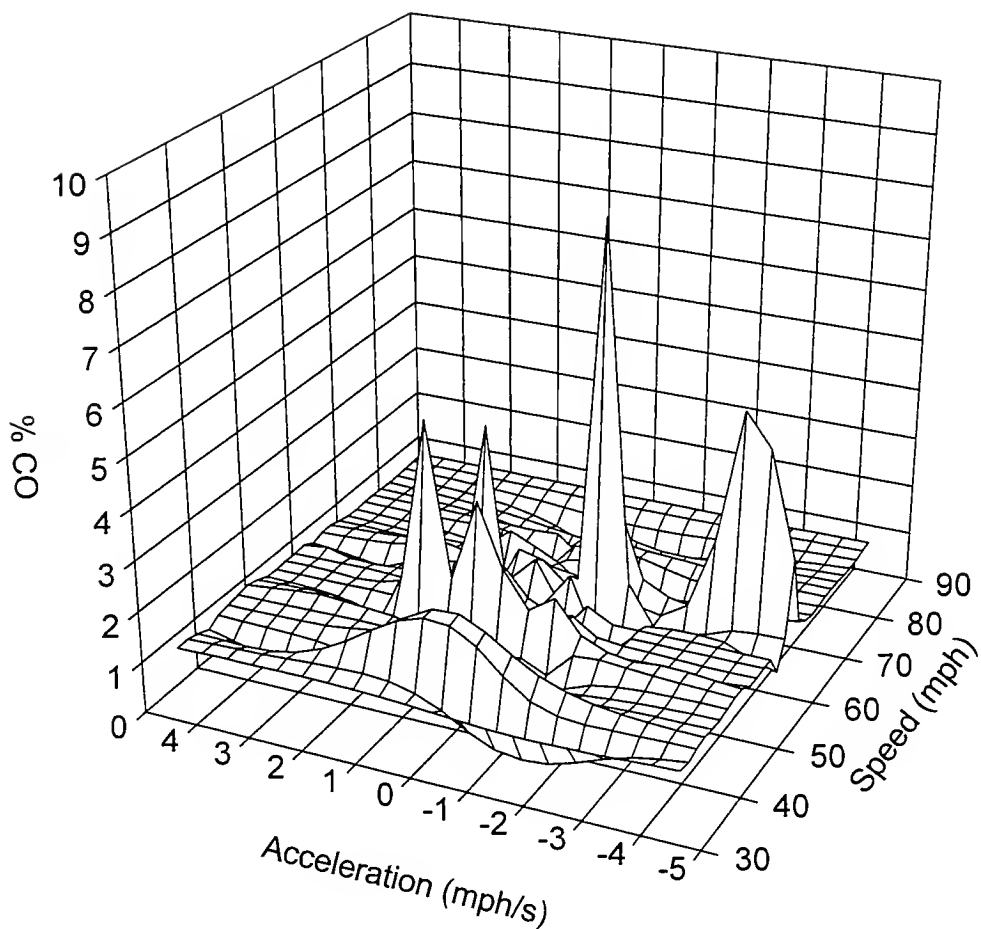


Figure B5.2.1. Three-dimensional plot for the triple correlation of CO emission concentration, speed, and acceleration for type II vehicles.



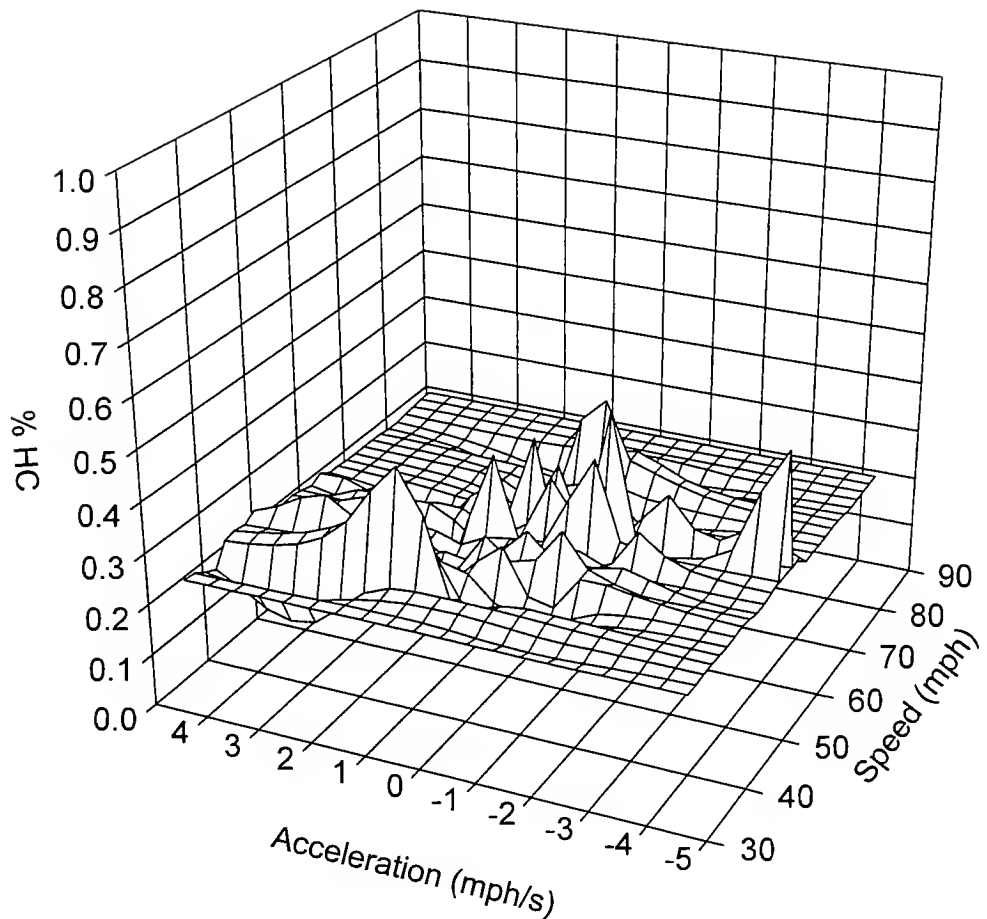


Figure B5.2.2. Three-dimensional plot for the triple correlation of HCs emission concentration, speed, and acceleration for type II vehicles.



## APPENDIX C

**Graphical Representations of the Regression Data for the Two Vehicle Types**



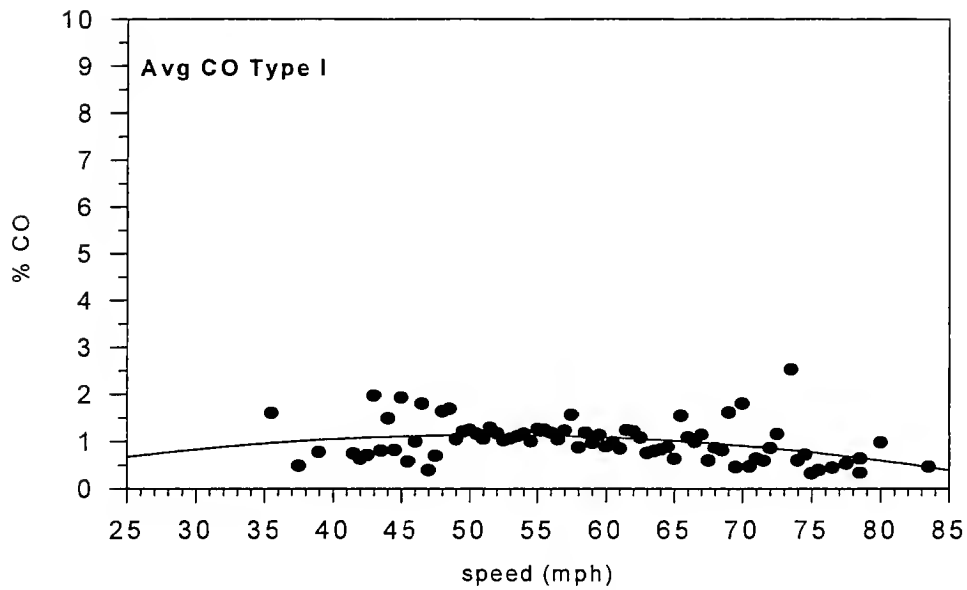


Figure C1.1.1. Bin-average CO exhaust emission concentration versus speed midpoints for type I vehicles.

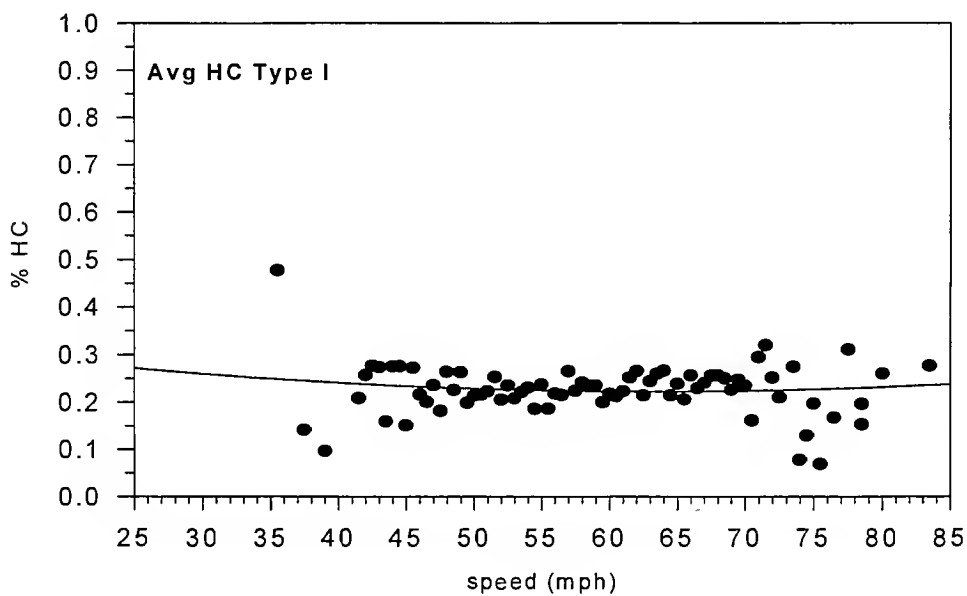


Figure C1.1.2. Bin-average HCs exhaust emission concentration versus speed midpoints for type I vehicles.



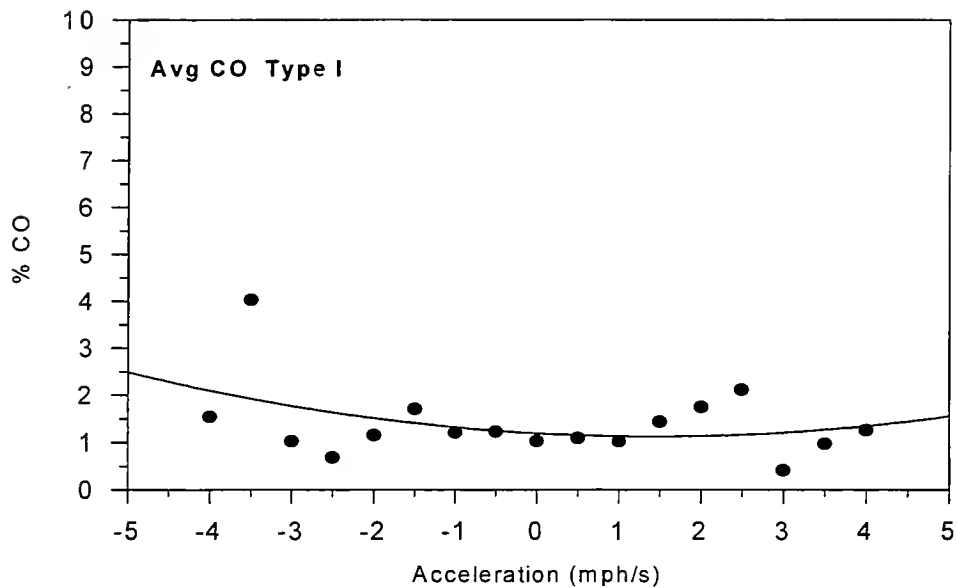


Figure C1.2.1. Bin-average CO exhaust emission concentration versus acceleration midpoints for type I vehicles.

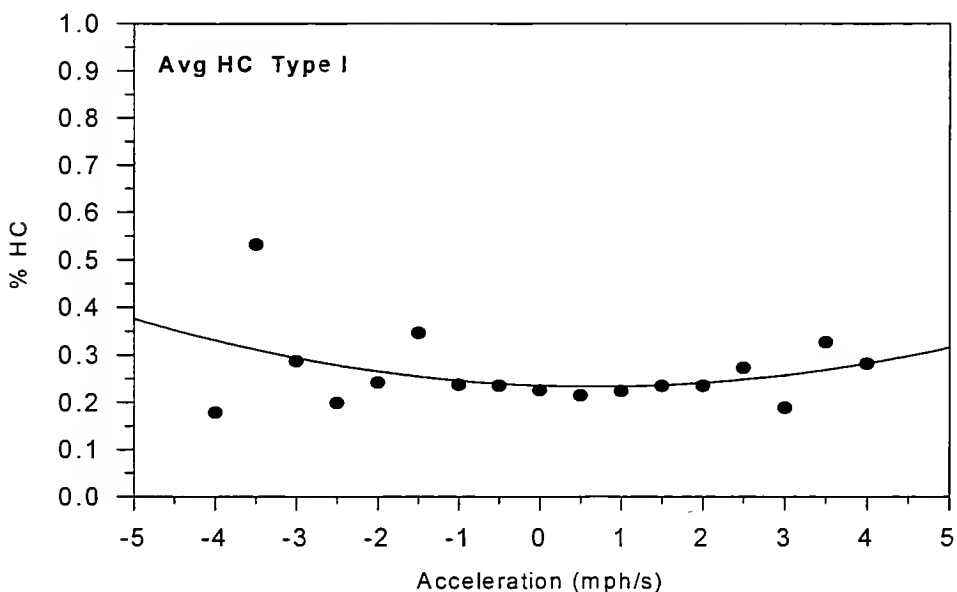


Figure C1.2.2. Bin-average HCs exhaust emission concentration versus acceleration midpoints for type I vehicles.



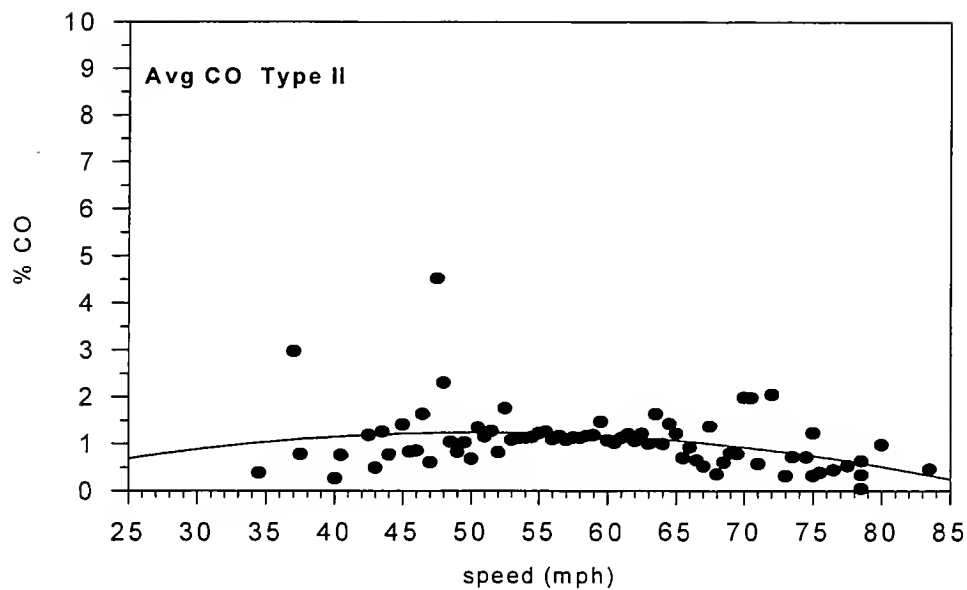


Figure C2.1.1. Bin-average CO exhaust emission concentration versus speed midpoints for type II vehicles.

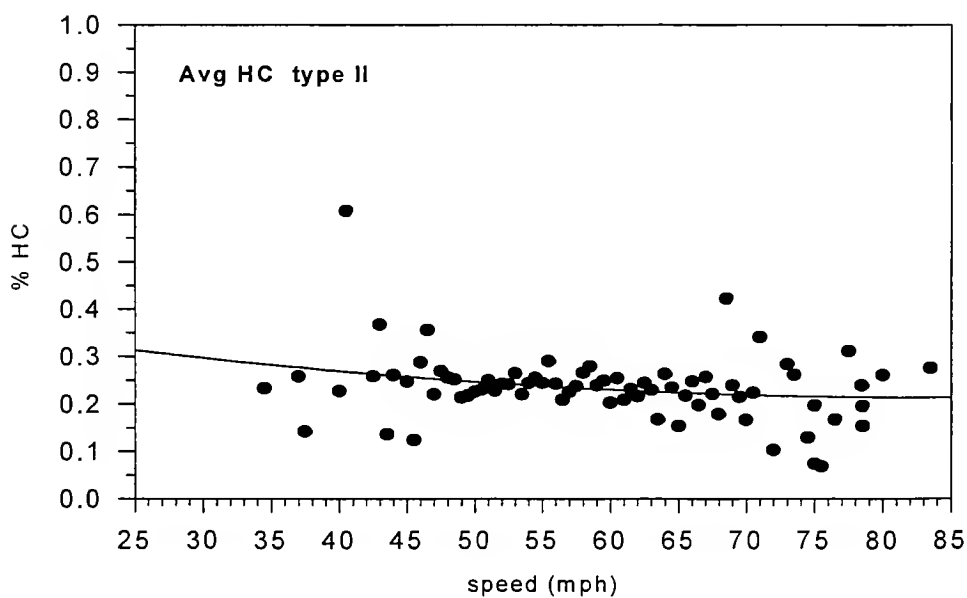


Figure C2.1.2. Bin-average HCs exhaust emission concentration versus speed midpoints for type II vehicles.



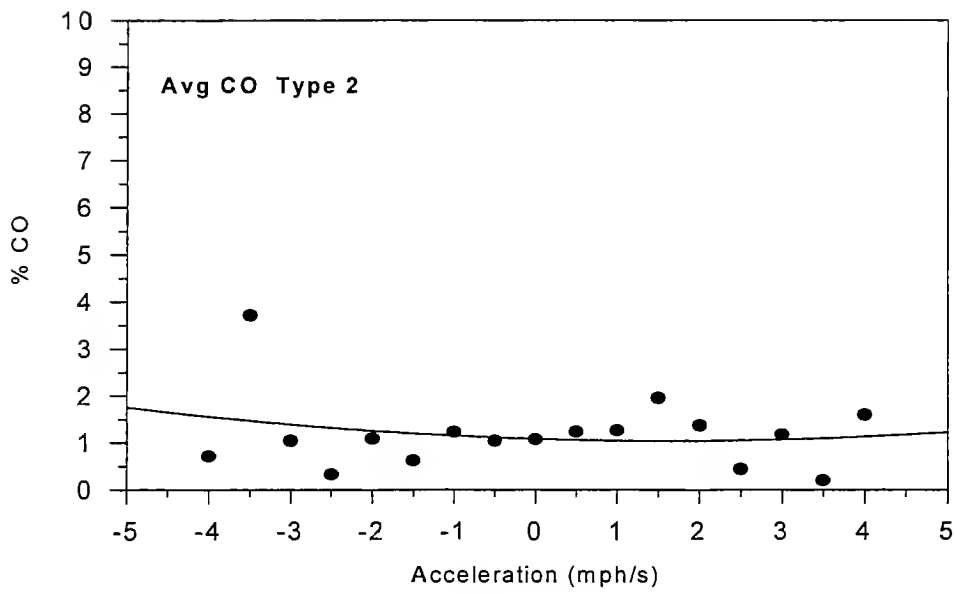


Figure C2.2.1. Bin-average CO exhaust emission concentration versus acceleration midpoints for type II vehicles.

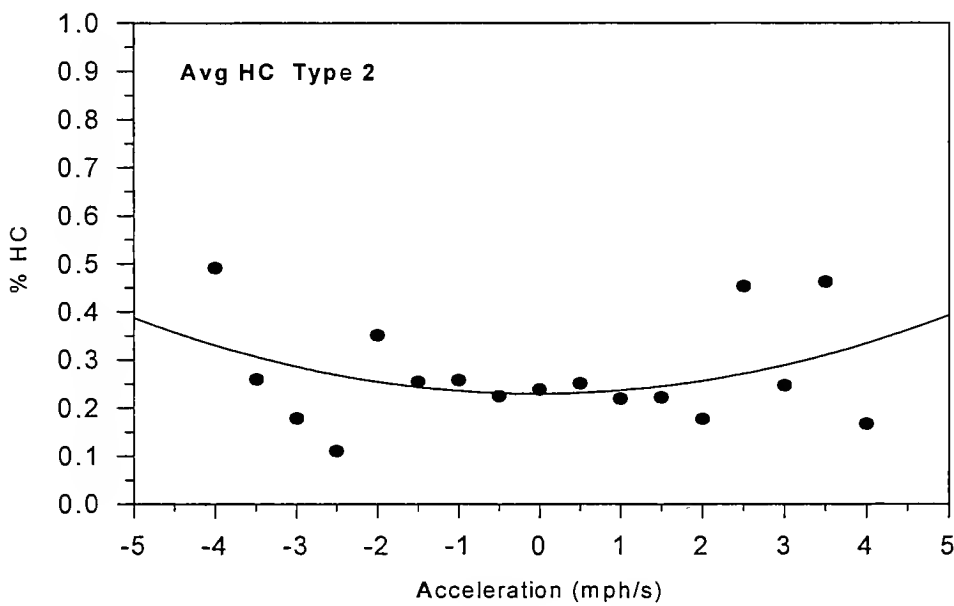


Figure C2.2.2. Bin-average HCs exhaust emission concentration versus acceleration midpoints for type II vehicles.



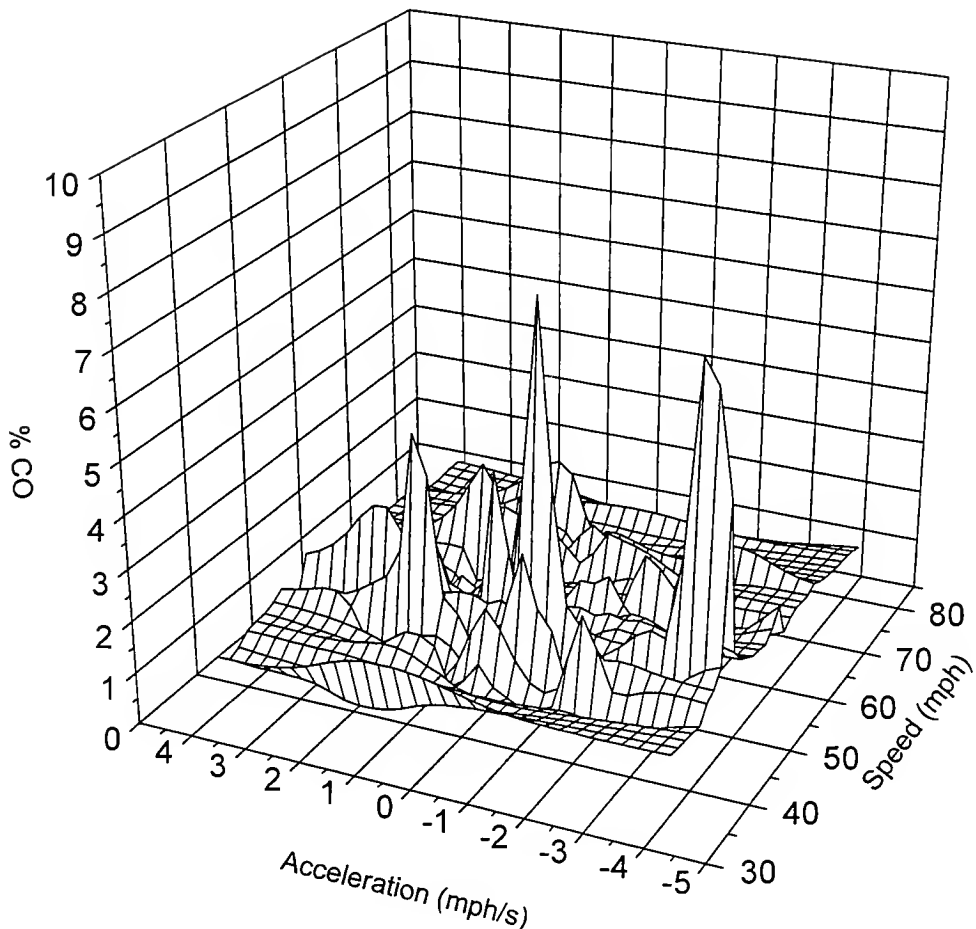
**3D CO Type I mode-avg**

Figure C3.1.1. Three-dimensional plot of the mode-average exhaust CO emission concentration versus speed and acceleration midpoints for type I vehicles.



3D HC Type I mode-avg

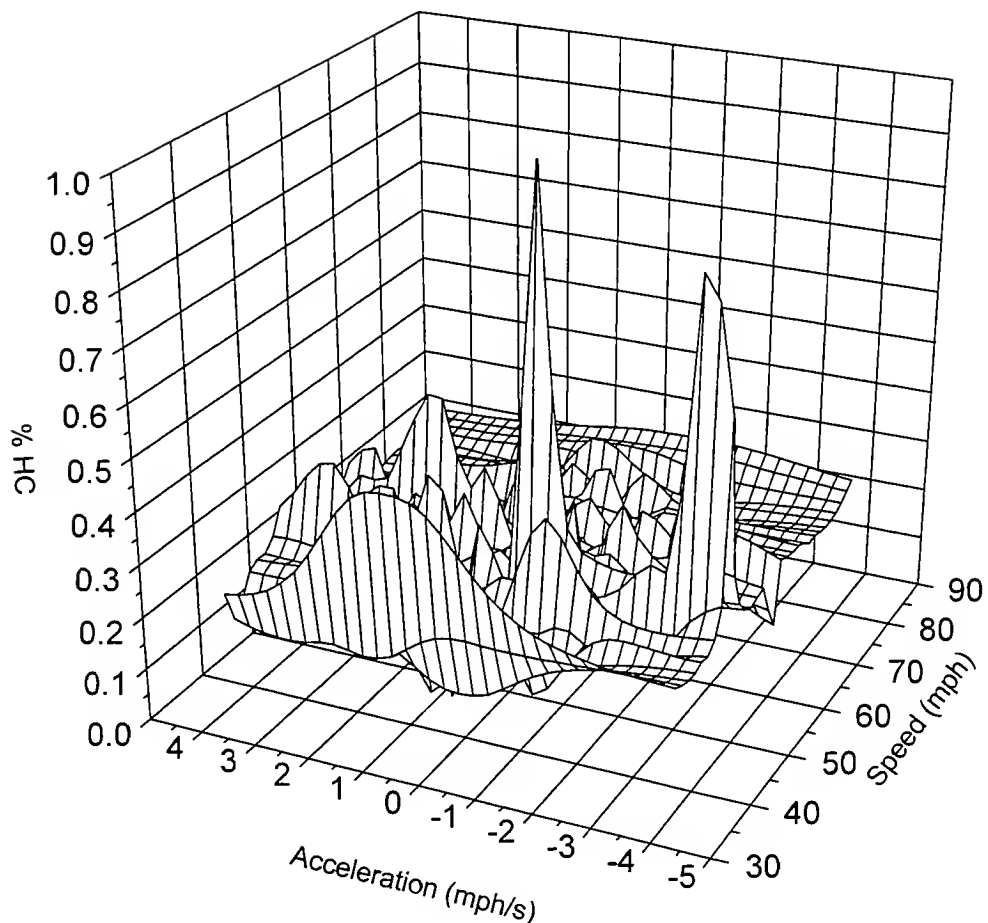


Figure C3.1.2. Three-dimensional plot of the mode-average exhaust HCs emission concentration versus speed and acceleration midpoints for type I vehicles.



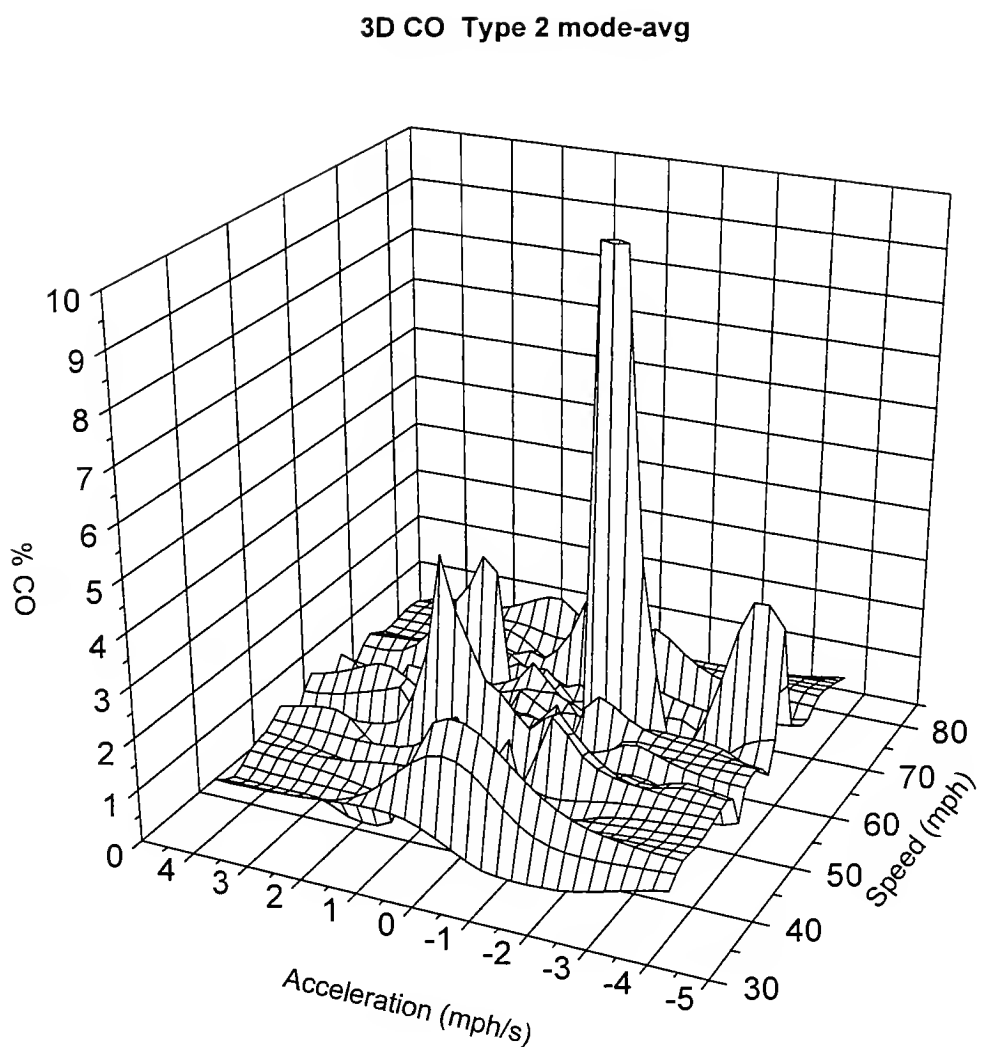


Figure C3.2.1. Three-dimensional plot of the mode-average exhaust CO emission concentration versus speed and acceleration midpoints for type II vehicles.



3D HC Type II mode-avg

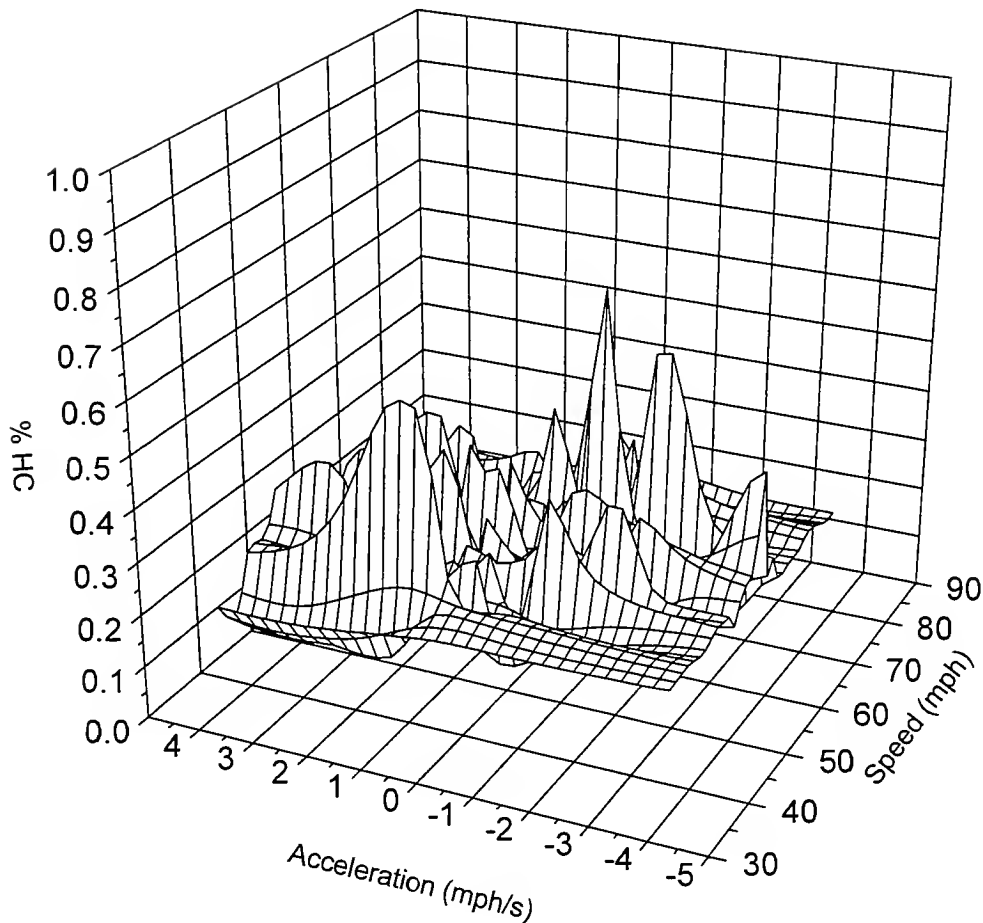


Figure C3.2.2. Three-dimensional plot of the mode-average exhaust HCs emission concentration versus speed and acceleration midpoints for type II vehicles.



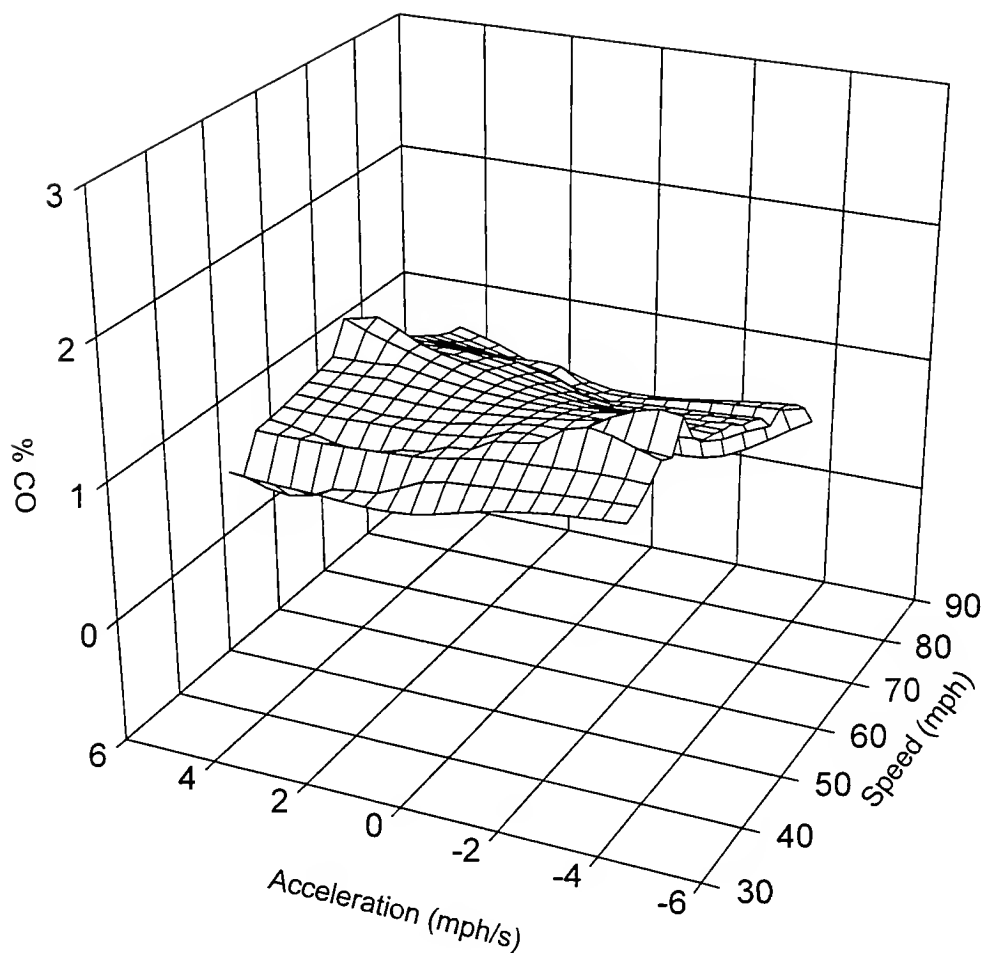


Figure C4.1.1. Three-dimensional plot of the mode-average CO exhaust emission concentration obtained from the mathematical relationship for type I vehicles.



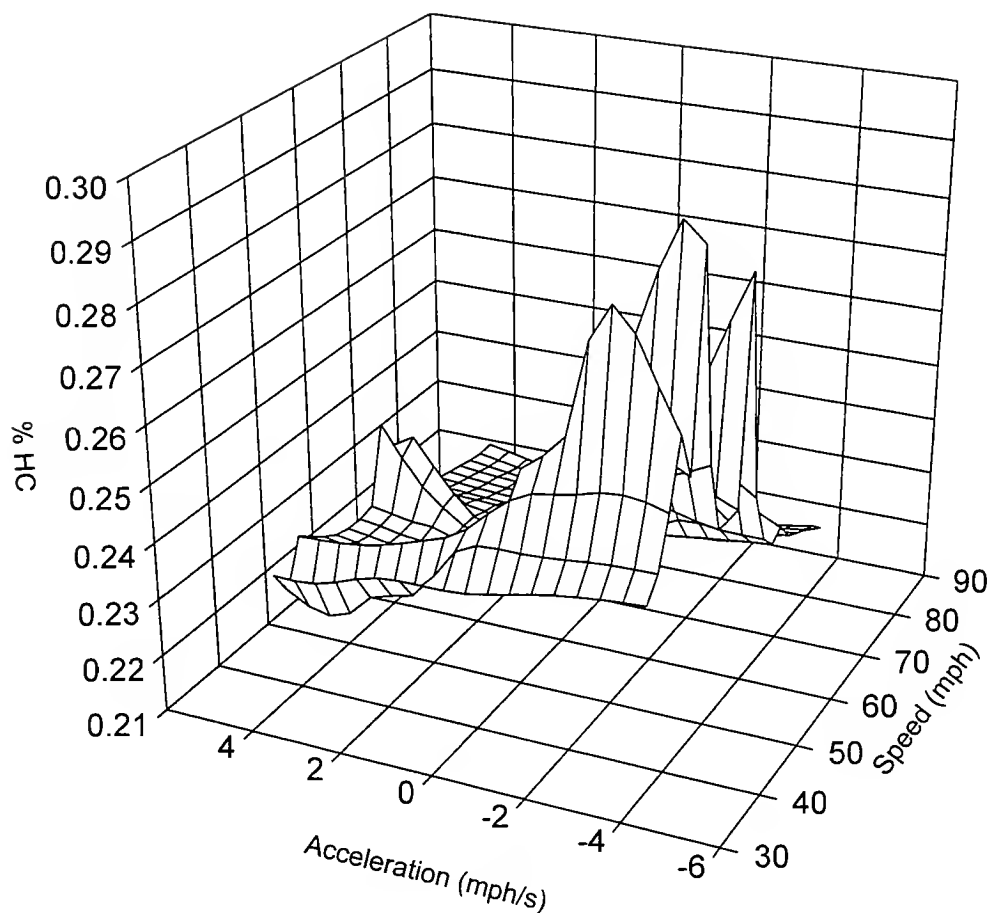


Figure C4.1.2. Three-dimensional plot of the mode-average HCs exhaust emission concentration obtained from the mathematical relationship for type I vehicles.



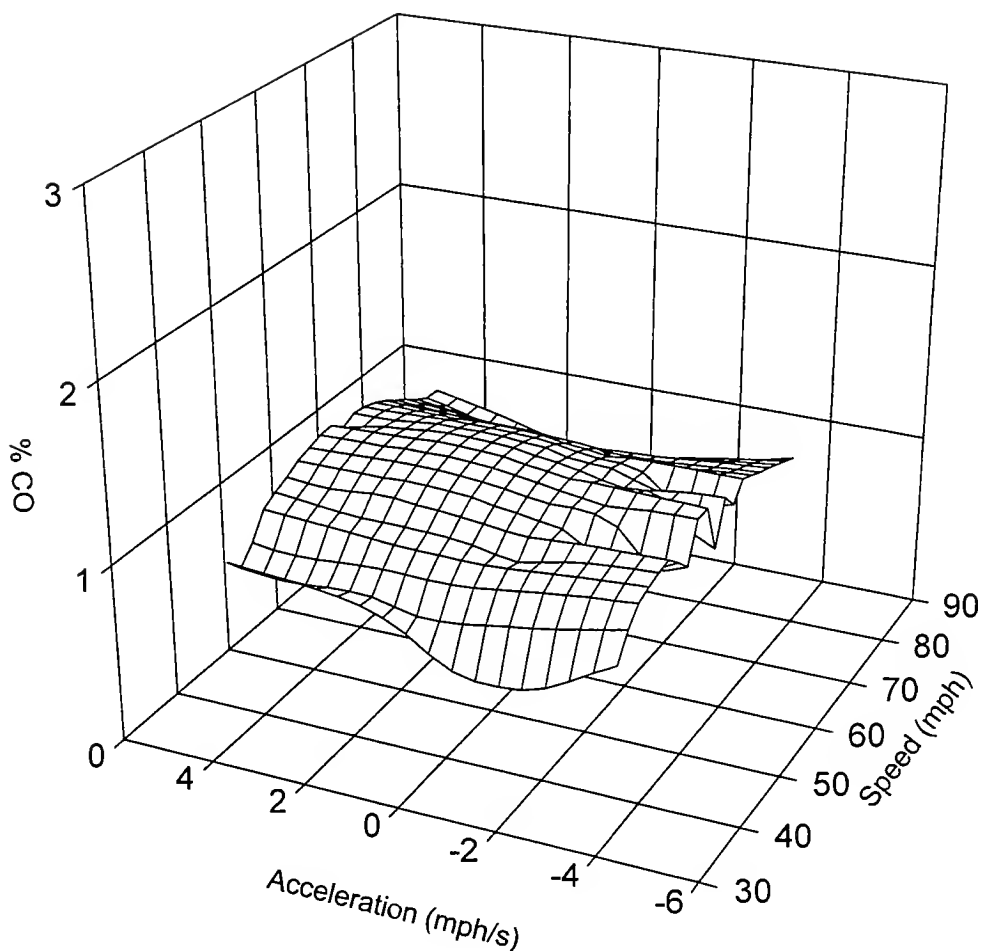


Figure C4.2.1. Three-dimensional plot of the mode-average CO exhaust emission concentration obtained from the mathematical relationship for type II vehicles.



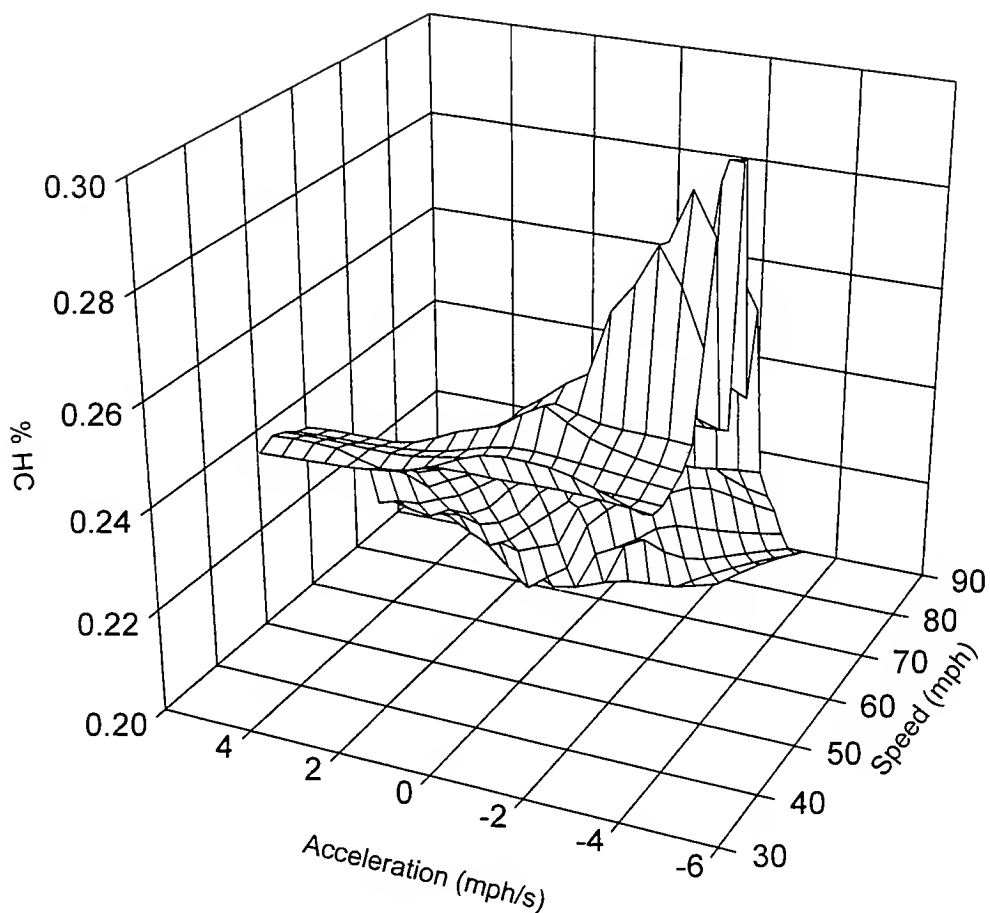


Figure C4.2.2. Three-dimensional plot of the mode-average HCs exhaust emission concentration obtained from the mathematical relationship for type II vehicles.



**APPENDIX D****PVEM-BEA Source Code**



```

program pvem1
*****
*The Purdue Micro-scale Real-time Vehicle Exhaust Emission Concentration Modal *
*Model version 1.0 (PVEM1.0): The Borman Expressway Application (PVEM-BEA 1.0).*
*Developed by Dr. Ouattara Fatogoma, Civil Engineering, Purdue University,      *
*****
c
c
c////MAIN PROGRAM//////////c
c
c----Subroutines definitions
c writer1,2: output description of the model and all the modeling data.
c reader1,2: read all the input variables and calculates the # of vehicles.
c calcaccel: calculates average speed and acceleration for each vehicle.
c calcemission: calculates average CO and HC emission concentrations for each vehicle
c and each vehicle type.
c decmaker: makes decisions about emission concentration levels per vehicles type.
c reseter: resets counters and variables for the next prediction time.
c opener: opens all the necessary files.
c closer: closes all the opened files.
c initializer: initializes and sets all constants and counters.
c
c----Variables definitions
c sp = average vehicle speed(mph) within averaging time.
c msp = measured vehicle speed(mph).
c ac = average vehicle acceleration(mph/s) within averaging time.
c vt = vehicle type(typeI(1),typeII(2),typeIII(3)).
c em = average exhaust CO and HC emission concentrations(%) from each vehicle.
c aem = average CO,HC emission concentrations(%) per vehicle type.
c asp,aac = average speed(mph) and acceleration(mph/s) by vehicle type.
c eth = CO and HC emission concentration thresholds(%).
c flg = CO and HC emission concentration threshold flags.
c eofg = end of file flag.
c nv = number of vehicle by type.
c frq = frequency of vehicles by type (#veh/s).
c nl = number of traffic lanes
c dl = distance between speed-reading points or between loops(ft)
c nvat = number of vehicles emitting more than the thresholds.
c ts = time(hhmmss) of simulation.
c sss,mms,hhs = second, minute, hour of simulation.
c ds = date(mmddyy) of simulation.
c ti = time interval between two consecutive speed readings.
c eat = emission concentration averaging time (sec).
c loc = name of the emission prediction location.
c run = modeling run number.
c pef = product of emission concentration and frequency by vehicle type(%/sec)
c peft = product of emission concentration and frequency threshold(%/sec) by vehicle typ
e
c peffg = product of emission concentration and frequency flag
c d1 = array dimension representing number of vehicles accross speed detection points in
eat
c d2 = array dimension representing number of loops in eat
c x = array dimension representing number of pollutants
c y = array dimension representing of vehicle types
c ddm,tdm = date and time of decision making
c c0,1,2,3,4,5 = mode-average emission concentration regression parameters
c b0,1,2 = accel bin-average emission concentration regression parameters

```



```

c
c----Variables declarations
    integer d1,d2,x,y
    parameter(d1=100,d2=2,x=2,y=4)
    integer ds(d1,d2),ts(d1,d2),nl,msp(d1,d2),nv(y),run,nvat(x,y),
&vt(d1,d2),rvt(d1),ddm,tdm,tnv
    real eat,em(x,d1),aem(x,y),eth(x,y),ti(d1),asp(y),aac(y),dl,
&sp(d1),ac(d1),frq(y),pef(x,y),peft(x,y),c0(x,y),c1(x,y),c2(x,y),
&c3(x,y),c4(x,y),c5(x,y),b0(x,y),b1(x,y),b2(x,y)
    character flg(x,d1)*2,loc*50,eofg*y,peffg(x,y)*2,name*25
c
c----Include constants initialization file
c      print *, 'Simulation initialization filename: '
c      read(*,100) name
c 100 format(a25)
c      open(unit=9,file=name)
c      include name
      include 'c:\workpu\borman\programs\pvembeac.for'
c
c----Open files
      call opener
c
c----Input location name,number of lanes, and distance between loops
      call reader1(loc,nl,d1)
c
c----Output model description
      call writer1(loc,nl,d1,eth,peft)
c
c----Input vehicle and traffic parameters. Calculate numbers of vehicles and frequencies
      10 call reader2(ds,ts,msp,vt,rvr,ti,eat,nv,nl,tnv,frq,eofg,ddm,tdm)
c
c----Calculate average speed and acceleration for each vehicle and each vehicle type
      call calcaccel(tnv,msp,sp,ac,ti,rvr,asp,aac,nv)
c
c----Calculate average CO and HC emission concentrations for each vehicle and and each
c      vehicle type. Flags high emitters. Calculate products frequency and emission
      call calcemission(tnv,nv,vt,em,b0,b1,b2,c0,c1,c2,c3,c4,c5,eth,flg,
      &           nvat,sp,ac,aem,pef,frq,nl)
c
c      Make decission about vehicle type whose emission concentration exceed designed thre
sholds
      call decmaker(pef,peft,peffg,aem,ddm,tdm)
c
c----Output individual vehicle modeling data and total fleet modeling data
      call writer2(tnv,run,ds,ts,rvr,sp,ac,em,flg,nv,frq,nvat,
      &           asp,aac,aem,pef,peffg)
c
c----Reset counters for the next simulation time or end the simulation if end of file
      call reseter(run,eofg,*10)
c
c----End main program
      stop
      end
c
c
c///SUBROUTINES FOR FILE I/O///////////////////////////////
c

```



```

c----Files description
c pvembeai.dat = traffic and vehicle parameters input file
c pvembeao.dat = modeling output file
c pvembeac.dat = simulation constant initialization input file
c
c----Open all necessary files
      subroutine opener
c
c----Simulation input and output files
c      character namei*24,nameo*24
c      print *, 'Enter traffic data input filename: '
c      read(*,100) namei
c      print *, 'Enter modeling output filename: '
c      read(*,100) nameo
c 100 format(a24)
c      open(unit=10,file=namei)
c      open(unit=20,file=nameo)
      open(unit=10,file='c:\workpu\borman\programs\pvembeai.dat')
      open(unit=20,file='c:\workpu\borman\programs\pvembeao.dat')
c
c----Simulation constants file
c
c----Position all files to the beginning
      rewind 10
      rewind 20
c
      end
c
c
c----Close input and output files
c
      subroutine closer
      close(10)
      close(20)
      end
c
c
C///SUBROUTINE FOR VARIABLES RESET///////////////
c
      subroutine reseter(rr,reofg,*)
c
c----Variables definition
c rr = Run number counter
c reofg = end of file flag
c
c----variable declaration
      integer rr
      character ryon,reofg*4
c
c----Next modeling session w/o interuption
      if(reofg.eq.'fend') then
        call closer
      else
        rr=rr+1
        return 1
      endif
c
c----Next modeling session with pause

```



```

c 30 print *, 'Do you wish to run another simulation? (y or n): '
c   read(*,100) ryon
c   if(ryon.eq.'y') then
c     if(reofg.ne.'fend') return 1
c     call closer
c   elseif(ryon.eq.'n') then
c     call closer
c   else
c     print *, 'Enter y or n!'
c     goto 30
c   endif
c
c 100 format(a1)
c   end
c
c
c////SUBROUTINE FOR READING INPUT DATA/////////////////////////
c
c----Read location name, number of traffic lanes, distance between speed detection point
s
c
      subroutine reader1(rloc,rnl,rdl)
c
c----Variables definition
c rloc = modeling location
c rnl = number of traffic lanes
c rdl = distance between the 2 loops
c
c----Variables declaration
      integer rnl
      real rdl
      character rloc*50
c
c----List directed input
c      print *, 'Location name: '
c      read(*,110) rloc
c      print *, 'Number of traffic lanes: '
c      read(*,115), rnl
c      print *, 'Distance between the speed detection points: '
c      read(*,120), rdl
c
c----File input
      read(10,100) rloc,rnl,rdl
c
c 100 format(a50/i1/f6.2/)
c 110 format(a50)
c 115 format(i1)
c 120 format(f6.2)
c   end
c
c
c----Read all vehicle parameters: vehicle type, speeds at loops
c   Calculate number and frequency of vehicles by type
c
      subroutine reader2(rds,rts,rmsp,rvt,rrvt,rti,reat,rnv,rnl,rtnv,
&                   rfreq,reofg,rddm,rtdm)
c
c----Variables definition

```



```

c i,j = counters
c rts = time(hhmmss) of simulation.
c rsss,rmmms,rhhs = second, minute, hour of simulation.
c rds = date(mmddyy) of simulation.
c rd = array dimension = maximum number of vehicles
c rsp = vehicle speed(mph)
c rvt = vehicle type
c rnv = car,truck,car+truck,heavy trucks,combined fleet counts at loops
c ravg = averaging time(sec)
c rtsec = time in second
c rti = time interval for two consecutive readings(sec)
c reat = maximum averaging time interval(4.0 sec)
c reofg = end of file flag
c rfrq = vehicle frequency by type(#veh/sec)
c rddm,rtdm = date,time of decision making
c
c----Variables declaration
    integer rd1,rd2,ry
    parameter (rd1=100,rd2=2,ry=4)
    integer i,j,l,i1,i2,rn,rmfp(rd1,rd2),rnv(ry),rds(rd1,rd2),
    &rts(rd1,rd2),rsss(rd1,rd2),rmmms(rd1,rd2),rhhs(rd1,rd2),
    &rnl,rvt(rd1,rd2),rrvt(rd1),rddm,rtdm,rtnv
    real reat,rti(rd1),rtsec(rd1,rd2),rfrq(ry)
    character ryon,reofg*4
c
c----counter initialization and constants
    i=0
    j=0
    rtnv=0
    do 5 m=1,4
        rnv(m)=0
    5 continue
c
ccList directed input of real-time traffic data
c-----First loop data reading
c    20 j=j+1
c    30 i=i+1
c    print '(a\')','Date of vehicle, ',i,' at point ',j,' (mmddyy): '
c    read *,rds(i,j)
c    print '(a\')','Time of vehicle, ',i,' at point ',j,' (hhmmss): '
c    read *,rts(i,j)
c    print '(a\')','Vehicle, ',i,' speed at point ',j,' (mph): '
c    read *,rmfp(i,j)
c    print *,'Vehicle, ',i,' type at point ',j,' : '
c    print *,'1-type I, 2-type II, 3-type III'
c    read *,rvt(i,j)
c
c-----continue reading
c    18 print '(a\')','Another Vehicle? (y or n): '
c    read *,ryon
c    if(ryon.eq.'y') then
c        goto 30
c    elseif(ryon.eq.'n') then
c        print '(a\')','Reading over at loop ',j
c    else
c        print '(a\')','Enter y or n'
c        goto 18
c    endif

```



```

c
c-----Second loop data reading
c      if(j.lt.2) then
c          i=0
c          goto 20
c      endif
c
c
ccFile input of real-time traffic data
c
        40 j=j+1
        50 i=i+1
c
c-----Read data recorded at point j
       60 read(10,110) rds(i,j),rts(i,j),rmsp(i,j),rvt(i,j)
c
c-----Convert time in second
       rsss(i,j)=mod(rts(i,j),100)
       rmms(i,j)=mod((int(rts(i,j)/100)),100)
       rhhs(i,j)=int(rts(i,j)/10000)
       rtsec(i,j)=rhhs(i,j)*3600.0+rmms(i,j)*60.0+rsss(i,j)*1.0
c
c-----Next vehicle at that loop
       if(i.lt.rnl) goto 50
c       if((rtsec(i,j)-rtsec(1,j)).le.reat) then
c           goto 50
c       else
c           rds(1,2)=rds(i,j)
c           rts(1,2)=rts(i,j)
c           rmsp(1,2)=rmsp(i,j)
c           rvt(1,2)=rvt(i,j)
c           j=2
c           i=1
c           goto 50
c       endif
c
c-----Total number of vehicles at point j
       if(j.eq.1) i1=i
       if(j.eq.2) i2=i
c
c-----Read data recorded at point j+1
       if(j.lt.2) then
           i=0
           goto 40
       endif
c
c-----Check for data consistency in vehicle type,number and licence plate number,
c      and time and calculate time interval and real vehicle counts
c-----Case I&III: no change in lanes
       if(i2.eq.i1) rn=i1
c-----Case II: convergence; eliminate far end vehicle
       if(i2.lt.i1) rn=i2
c-----Case IV: divergence; speed 1 of the added veh=speed of the closest veh
       if(i2.gt.i1) rn=i2
c
       do 70 i=1,rn
c           if(rlpn(i,2).eq.rlpn(i,1)) then
c               if(rv(i,2).eq.rv(i,1)) then

```



```

rrvt(i)=rvt(i,1)
rti(i)=rtsec(i,2)-rtsec(i,1)
c-----Calculate number of vehicles by type at loop j. l=1(type1),l=2(type2),l=3(type
3)
c      l=4(combined 1+4 fleet)
c      if (rti(i).le.reat) then
        if(rrvt(i).eq.1) l=1
        if(rrvt(i).eq.2) l=2
        if(rrvt(i).eq.3) l=3
        rnv(l)=rnv(l)+1
        if((l.eq.1).or.(l.eq.2)) rnv(4)=rnv(4)+1
        rtnv=rtnv+1
c      endif
c      endif
70 continue

c
c-----End of file clause
if(eof(10)) then
  reofg='fend'
endif
c
c-----Vehicle flow rate (# vehicle within the maximum averaging time per lane)
do 80 i=1,4
  rfrq(i)=(rnv(i)/reat)/real(rnl)
80 continue
c
  rddm=rds(1,1)
  rtdm=rts(1,1)
c
110 format(2(i6,1x),i2,1x,i1)
99 end
c
c
C///SUBROUTINE FOR THE CALCULATION OF VEHICLE AVERAGE SPEED AND ACCELERATION//  

c calculates the average speed and acceleration for each vehicle and each  

c vehicle type within the time interval
c
  subroutine calcaccel(ctnv,cmsp,csp,cac,cti,cvt,casp,caac,cnv)
c
c----Variables definitions
c cd = arrays dimension
c cmsp = measured vehicle speed(mph)
c cvt = vehicle type
c csp = average vehicle speed within time interval(mph)
c cac = average vehicle acceleration within time interval(mph/sec)
c cssp = sum of speed by vehicle type(mph)
c casp = average speed by vehicle type(mph)
c csac = sum of acceleration by vehicle type(mph/sec)
c caap = average acceleration by vehicle type(mph)
c cti = time interval(sec)
c ctnv = total number of vehicles
c cnv = number of vehicles by type
c
c----Variable declaration
  integer cd1,cd2,cy
  parameter(cd1=100,cd2=2,cy=4)
  integer cmsp(cd1,cd2),i,j,l,k,cnv(cy),cvt(cd1),ctnv

```



```

real csp(cdl),cac(cdl),cti(cdl),cssp(cy),csac(cy),casp(cy),
&caac(cy)
c
c----Initialization
do 5 l=1,4
  cssp(l)=0.0
  csac(l)=0.0
5 continue
c
c----Calculate average speed and acceleration within time interval
do 10 i=1,ctnv
  csp(i)=real(cmsp(i,2)+cmsp(i,1))/2.0
  cac(i)=real(cmsp(i,2)-cmsp(i,1))/cti(i)
c
c-----Range acceleration values
if(cac(i).le.-3.75) cac(i)=-4.0
if((cac(i).gt.-3.75).and.(cac(i).le.-3.25)) cac(i)=-3.5
if((cac(i).gt.-3.25).and.(cac(i).le.-2.75)) cac(i)=-3.0
if((cac(i).gt.-2.75).and.(cac(i).le.-2.25)) cac(i)=-2.5
if((cac(i).gt.-2.25).and.(cac(i).le.-1.75)) cac(i)=-2.0
if((cac(i).gt.-1.75).and.(cac(i).le.-1.25)) cac(i)=-1.5
if((cac(i).gt.-1.25).and.(cac(i).le.-0.75)) cac(i)=-1.0
if((cac(i).gt.-0.75).and.(cac(i).le.-0.25)) cac(i)=-0.5
if((cac(i).gt.-0.25).and.(cac(i).lt.0.25)) cac(i)=0.0
if((cac(i).ge.0.25).and.(cac(i).lt.0.75)) cac(i)=0.5
if((cac(i).ge.0.75).and.(cac(i).lt.1.25)) cac(i)=1.0
if((cac(i).ge.1.25).and.(cac(i).lt.1.75)) cac(i)=1.5
if((cac(i).ge.1.75).and.(cac(i).lt.2.25)) cac(i)=2.0
if((cac(i).ge.2.25).and.(cac(i).lt.2.75)) cac(i)=2.5
if((cac(i).ge.2.75).and.(cac(i).lt.3.25)) cac(i)=3.0
if((cac(i).ge.3.25).and.(cac(i).lt.3.75)) cac(i)=3.5
if(cac(i).ge.3.75) cac(i)=4.0
c
c-----Sum of speeds and accelerations by vehicle type
if(cvt(i).eq.1) j=1
if(cvt(i).eq.2) j=2
if(cvt(i).eq.3) j=3
cssp(j)=cssp(j)+csp(i)
csac(j)=csac(j)+cac(i)
if((j.eq.1).or.(j.eq.2)) then
  cssp(4)=cssp(4)+csp(i)
  csac(4)=csac(4)+cac(i)
endif
10 continue
c
c----Calculate average speed and acceleration by vehicle type
do 15 k=1,4
  if(cnv(k).eq.0) then
    casp(k)=0.0
    caac(k)=0.0
  else
    casp(k)=cssp(k)/real(cnv(k))
    caac(k)=csac(k)/real(cnv(k))
  endif
15 continue
end
c
c

```



```

C///SUBROUTINE FOR THE CALCULATION OF VEHICLE MODE-AVERAGE EMISSION CONCENTRATIONS/
c Calculates the average co and hc emission concentrations for each vehicle and
c each vehicle type as well as the product of concentration and frequency. Flags
c all the high emitters
c
subroutine calcemission(ctnv,cnv,cvt,cem,cb0,cb1,cb2,cc0,cc1,cc2,
&                               cc3,cc4,cc5,ceth,cflg,cnvat,csp,cac,caem,
&                               cpef,cfrq,cnl)
c
c----Variables definitions
c cd,cx,cy = arrays dimensions
c i,j,k,l,m,n = counters
c cn = number of vehicles by type for emission averaging purpose
c cnvat = number of vehicles by type above thresholds
c csp = vehicle speed(mph)
c cac = vehicle acceleration(mph/s)
c cvt = vehicle type
c cem = CO and HC average emission concentrations within time interval(%)
c ceth = CO and HC emission concentration thresholds(%)
c csem = sum of emission concentrations by vehicle type w/i time interval(%)
c caem = average emission concentrations by vehicle type w/i time interval(%)
c cflg = emission concentration threshold flags
c cpef = product of emission concentration and vehicle frequency by type(%/s)
c cfrq = vehicle frequency(#veh/s)
c cc0,1,2,3,4,5 = mode-average emission concentration regression parameters
c cb0,1,2 = accel bin-average emission concentration regression parameters
c
c----Variables declaration
integer cd1,cx,cy,i,k,l,m,n
parameter(cd1=100,cx=2,cy=4)
integer cn(cx,cy),cnvat(cx,cy),cvt(cd1),cnv(cy),cnl,ctnv
real csp(cd1),cac(cd1),cem(cx,cd1),ceth(cx,cy),csem(cx,cy),
&caem(cx,cy),cpef(cx,cy),cfrq(cy),cc0(cx,cy),cc1(cx,cy),cc2(cx,cy),
&cc3(cx,cy),cc4(cx,cy),cc5(cx,cy),cb0(cx,cy),cb1(cx,cy),cb2(cx,cy)
character cflg(cx,cd1)*2
c
c----Constants initializations
k=0
c
c----Emission summation,number,high emitter flags initialization
do 10 m=1,2
  do 15 n=1,4
    csem(m,n)=0.0
    cn(m,n)=0
    cnvat(m,n)=0
15  continue
10 continue
c
c----Calculate emission concentrations
c   k=1 for CO emission concentration, k=2 for HC emission concentration
c   l=1 for type 1,l=2 for type 2,l=3 for type 3,l=4 for combined fleet
c
20 k=k+1
  do 30 i=1,ctnv
    if(cvt(i).eq.1) l=1
    if(cvt(i).eq.2) l=2
    if(cvt(i).eq.3) l=3
c----Vehicle numbers for emission averaging

```



```

cn(k,l)=cn(k,l)+1
if((l.eq.1).or.(l.eq.2)) cn(k,4)=cn(k,4)+1
c
c-----Emission calculation formula
  if(csp(i).lt.35.0) then
    cem(k,i)=cb0(k,l) +
&      cb1(k,l)*((cac(i)-0.0)/4.0) +
&      cb2(k,l)*((cac(i)-0.0)/4.0)**2.0
  else
    cem(k,i)=cc0(k,l) +
&      cc1(k,l)*((csp(i)-55.0)/30.0) +
&      cc2(k,l)*((csp(i)-55.0)/30.0)**2.0 +
&      cc3(k,l)*((cac(i)-0.0)/4.0) +
&      cc4(k,l)*((cac(i)-0.0)/4.0)**2.0 +
&      cc5(k,l)*((csp(i)-55.0)/30.0)*((cac(i)-0.0)/4.0)
  endif
c
c-----High emitters. at=above emission concentration threshold, bt=below.
  if(cem(k,i).gt.ceth(k,l)) then
    cflg(k,i)='at'
    cnvat(k,l)=cnvat(k,l)+1
  else
    cflg(k,i)='bt'
  endif
c
c-----Sum of emission concentrations
  csem(k,l)=csem(k,l)+cem(k,i)
  if((l.eq.1).or.(l.eq.2)) csem(k,4)=csem(k,4)+cem(k,i)
c
  30 continue
c
c-----Next pollutant
  if(k.ne.2) goto 20
c
c-----Average emission concentration and product of (average emission/number of vehicle)
  and
c    flow rate and number of lane per vehicle type
  do 40 m=1,2
    do 50 n=1,4
      if(cn(m,n).eq.0) then
        caem(m,n)=0.0
      else
        caem(m,n)=csem(m,n)/real(cn(m,n))
      endif
      cpef(m,n)=caem(m,n)*cfreq(n)*cnl
  50  continue
  40 continue
  end
c
c
c////SUBROUTINE FOR DECISION MAKING///////////////
c Flags the vehicle types which average emission concentrations by frequency
c products are greater than the designed Thresholds
c
  subroutine decmaker(dpef,dpefft,dpeffg,daem,dtdm,dddm)
c
c----Variables definitions
c dpef = product of emission concentration and vehicle frequency(%/sec)

```



```

c dpeft =product of emission concentration and vehicle frequency threshold(%/sec)
c dpeffg = product of emission concentration and vehicle frequency flag
c daem = average emission concentration by vehicle type
c
c----Variables declaration
  integer i,j,dx,dy,dtdm,dddm
  parameter(dx=2,dy=4)
  real dpef(dx,dy),dpeft(dx,dy),daem(dx,dy)
  character dpeffg(dx,dy)*2
c
do 10 i=1,2
  do 20 j=1,4
    dpeffg(i,j)='bt'
    if(dpef(i,j).gt.dpeft(i,j)) then
      dpeffg(i,j)='at'
      write(*,*) dtdm,dddm,i,j,daem(i,j)
      call beepqq(1000,150)
    endif
 20  continue
10 continue
end

c
c
c///SUBROUTINES FOR MODELING RESULTS AND MODEL DESCRIPTION OUTPUT///////////
c
c
c----Ouput aknowledgements and descriptions, and simulation constants
c
  subroutine writer1(wloc,wnl,wdl,weth,wpeft)
c
c----Variables definition
c wloc = location name
c wnl = number of traffic lanes
c wdl = distance between traffic lanes(ft)
c weth = individual vehicle emission concentration threshold(%)
c wpeft = product of emission concentration and vehicle frequency threshold(%/sec)
c
c----Variable declaration
  integer wx,wy,j,wnl
  parameter (wx=2,wy=4)
  real wdl,weth(wx,wy),wpeft(wx,wy)
  character wloc*50
c
  write(20,95)
  write(20,210)
  write(20,97)
  write(20,101)
  do 5 j=1,4
    write(20,103) j,weth(1,j),weth(2,j)
 5  continue
  write(20,102)
  do 10 j=1,4
    write(20,103) j,wpeft(1,j),wpeft(2,j)
 10 continue
  write(20,200)
  write(20,100) wloc,wnl,wdl
  write(20,210)
c

```



```

95 format(' ****',
     &'*****',
     &' * Purdue Real-Time Vehicle Exhaust Emission Modal Model V 1.0',
     &'1x,'(PVERM1.0)',4x,'*'/' * Developed by Dr. Ouattara Fatogoma. ',
     &'Civil Engineering, Purdue University */',
     &' * Copyright (C) 1998. All Rights Reserved.',33x,'*'/
     &' *****',
     &'*****')//)
97 format('NOTES'/'====')
100 format(/'Modeling location: 'a50 /'Number of lanes: 'i1/
     &'Distance between 2 speed detection points (ft): 'f6.2)
101 format('CO and HCs instantaneous exhaust'/
     &'emission concentration thresholds(%)'/
     &'VT',4x,'CO',6x,'HCs')
102 format(/'Designed CO and HC threshold limit values'/
     &'by vehicle type(%/sec)'/
     &'VT',4x,'CO',6x,'HCs')
103 format(i1,2x,f7.4,2x,f7.4)
200 format(/'Notes: bt = below threshold, at = above threshold'/
     &'1=type 1 vehicles (LDV), 2=type 2 vehicles (MDV),',1x,
     &'3=type 3 vehicles (HDV)', '4=Combined 1&2')
210 format('=====',
     &'=====')/
end

c
c
c----Output vehicle, traffic, and emission data subroutine
  subroutine writer2(wtnv,wrun,wds,wts,wvt,wsp,wac,wem,wflg,wnv,
    &           wfrq,wnvat,wasp,waac,waem,wpeff,wpeffg)
c
c----Variables definition
c wrun = simulation run number
c wds = date of simulation(mmddyy)
c wts = time of simulation(hhmmss)
c wvt = vehicle type
c wsp = vehicle speed(mph)
c wac = vehicle acceleration(mph/s)
c wem = average emission concentration(%)
c wflg = emission threshold flag
c wnv = vehicle count by type
c wfrq = vehicle frequency(%/s)
c wnvat = number of vehicles above threshold
c wasp = average vehicle speed by type(mph)
c waac = average vehicle acceleration by type(mph/s)
c waem = average emission concentration by type(%)
c wpeff =
c wpeffg =
c
c----Variable declaration
  integer wd1,wd2,wx,wy,i
  parameter (wd1=100,wd2=2,wx=2,wy=4)
  integer wts(wd1,wd2),wds(wd1,wd2),wrun,wnv(wy),wnvat(wx,wy),
  &wvt(wd1),wtnv
  real wsp(wd1),wac(wd1),wem(wx,wd1),wasp(wy),waac(wy),
  &waem(wx,wy),wfrq(wy),wpeff(wx,wy)
  character wflg(wx,wd1)*2,wpeffg(wx,wy)*2
c
c----Write

```



```

write(20,100) wrun
write(20,105)
do 10 i=1,wtnv
    Write(20,110) wds(i,1),wts(i,1),wvt(i),wsp(i),wac(i),wem(1,i),
    & wflg(1,i),wem(2,i),wflg(2,i)
10 continue
c-----Output header
    write(20,120)
    write(20,121)
c-----Average data output per type
    write(20,130) wnv(1),wnv(2),wnv(3),wnv(4)
    write(20,132) wfrq(1),wfrq(2),wfrq(3),wfrq(4)
    write(20,135) wasp(1),wasp(2),wasp(3),wasp(4)
    write(20,140) waac(1),waac(2),waac(3),waac(4)
    write(20,145) waem(1,1),waem(1,2),waem(1,3),waem(1,4)
    write(20,150) waem(2,1),waem(2,2),waem(2,3),waem(2,4)
    write(20,155) wnvat(1,1),wnvat(1,2),wnvat(1,3),wnvat(1,4)
    write(20,160) wnvat(2,1),wnvat(2,2),wnvat(2,3),wnvat(2,4)
    write(20,165) wpef(1,1),wpef(1,2),wpef(1,3),wpef(1,4)
    write(20,170) wpef(2,1),wpef(2,2),wpef(2,3),wpef(2,4)
    write(20,175) wpeffg(1,1),wpeffg(1,2),wpeffg(1,3),wpeffg(1,4)
    write(20,180) wpeffg(2,1),wpeffg(2,2),wpeffg(2,3),wpeffg(2,4)
    write(20,210)
c-----Formats
100 format('Run#: ',i6.6)
105 format('SIMULATION DATA'/'=====',' Date',5x,'Time',4x,
  &'Vt',3x,'Spd',4x,'Acc',7x,'CO',4x,'COfg',3x,'HC',4x,
  &'HCfg'/(mmddyy)',(hhmmss)',6x,(mph)',1x,(mph/s)',5x,(%)',
  &10x,(%)')
110 format(2(i6.6,3x),i1,3x,2(f5.2,3x),f7.4,2x,a2,2x,f7.4,2x,a2)
120 format(//SUMMARY DATA'/'=====')
121 format(44x,'Type_1',4x,'Type_2',4x,'Type_3',4x,'CF_1&2')
130 format('Number of vehicles: ',t44,4(i3,7x))
132 format('Vehicle Flow rate(#veh/sec/lane): ',t45,4(f5.2,5x))
135 format('Average speed(mph): ',t45,4(f5.2,5x))
140 format('Average acceleration(mph/sec): ',t45,4(f5.2,5x))
145 format('Average CO emission concentration(%): ',t45,4(f7.4,3x))
150 format('Average HC emission concentration(%): ',t45,4(f7.4,3x))
155 format('Number of vehicles exceeding CO threshold: ',t44,4(i3,7x))
160 format('Number of vehicles exceeding HC threshold: ',t44,4(i3,7x))
165 format('CO PCFNL(%/sec): ',t45,4(f7.4,3x))
170 format('HCs PCFNL(%/sec): ',t45,4(f7.4,3x))
175 format('CO PCFNL flag: ',t46,4(a2,8x))
180 format('HCs PCFNL flag: ',t46,4(a2,8x))
210 format('=====',
  &'=====','/')
end
c///////////

```





